

1

The Basics

1.1

General Introduction and Historical Perspective

This chapter covers the basic definitions, main features and engineering and design of ceramic membranes. We give a brief history of the development of ceramic membranes, define key terms in membrane science, outline the popular separation processes (ultrafiltration (UF), nanofiltration (NF), pervaporation and gas separation) and explain the main module designs (plate-and-frame, spiral-wound, tubular, honeycomb and hollow fibres). The historical overview shows how membranes started, when the big breakthrough occurred, where membranes are now and how the near future will look like. The actual making of ceramic membranes is in itself an interesting story, and a good part of the chapter is devoted to the synthesis of various layers of the membrane. We give an overview of the main methods and materials used for preparing such membranes and characterizing them, as well as their key advantages and limitations. The discussion covers both isotropic and anisotropic membranes, prepared from a range of materials (zirconia, titania, alumina, hafnia, tin oxide, mixed oxides, zeolite membranes, silica, hybrid organic–ceramic membranes and metallo-organic frameworks). We analyse in detail the formation of support layer and list some rules of thumb collected by many researchers in numerous trials. A key aspect here is the gradual transition from the support layer through the intermediate layers and ultimately to the top layer. The development of top layer is reviewed through the basics of chemical vapour deposition (CVD), sol–gel technology and zeolite modifications. The chapter concludes with a list of books for further reading, qualitative and quantitative exercises and references.

A membrane is a semipermeable active or passive barrier that permits the passage of one or more components in the initial mix and limits the passage of others. Although Graham in 1848 used a sort of membrane in the development of diffusion law, and although the first membranes were synthesized more than a century ago, the development and implementation of membranes really turned into a scientific discipline in the second half of the twentieth century.

Today's membranes, with their modest energy demands and small footprint, have become even more attractive and are often compared favourably with conventional separation processes such as distillation, adsorption, absorption, extraction and crystallization. There are many books on the development, characterization and implementation of polymer membranes. Ceramic membranes are much less in the focus, and this book will hopefully rectify this a little, by shedding light on this important subfield of membrane science.

By the layman's definition, ceramics are materials made of pottery (*κέραμοζ* in Greek) that is then hardened by heat. A more scientific definition (from the *Ceramic Tile Institute of America*) describes ceramic material as an inorganic, non-metallic solid prepared by the action of heat and subsequent cooling [1]. This definition explores an older Sanskrit meaning of the Greek *keramos* – to be burned (unlike glass that is amorphous, ceramics are crystalline materials). Ceramics are compounds of metallic and non-metallic elements such as aluminium and oxygen (Al_2O_3), zirconium and oxygen (ZrO_2) or silicon and carbon (SiC). These compounds occur naturally in clays and other minerals and are processed in supported forms. With such available ingredients, simple recipes and long-term robustness, no wonder that archaeologists have found man-made ceramics that date back to at least 24,000 BC [2]. The durability of ceramic artefacts has given them prominence in archaeology [3]. Ceramics were one of the remarkable keystones that marked the transition from Stone to Bronze Age when humans first started using man-made tools instead of sharpened stones. In this sense, ceramics are the oldest of three large classes of solid materials (ceramics, metals and polymers) on the main development route of industrial products. The first ceramics, found in former Czechoslovakia, were made of animal fat and bone mixed with bone ash and clays [4]. The initial mix was hardened at kilns dug in the ground at temperatures between 500 and 800 °C. We do not know how these ceramics were then used. The first use of ceramics as containers for holding and storing grains and other food dates back to 9000 BC. Heating the sand that contained calcium oxide combined with soda resulted in a coloured glaze on ceramic containers in Upper Egypt about 8000 BC [5]. One of the earliest civilizations, the Sumerians who lived in Southern Mesopotamia (modern Iraq) more than 5000 years ago, wrote on ceramic stone plaques. The ceramic amphora, which was invented in Greece, became a standard for the transport and storage of liquids (mostly wine and olive oil) in the Roman Empire. The need to purify the water transported in air-open aqueducts [6] expanded the use of ceramics in the Empire. Figure 1.1 shows one of the first ceramic filters, which dates back to Israel Iron Age II – 800 BC (an artefact from the Israeli National Museum).

So ceramics have been with us for thousands of years, but ceramic technology has really developed only in the last century. Today's ceramics are no longer just dinnerware, bricks and toilets. Technical ceramics are used in space shuttles, engines, artificial bones and teeth, computers and other electronic devices and of course membranes. The first modern industrial application of ceramic membranes was in the separation of U-238 and U-235 isotopes for making nuclear



Figure 1.1 One of the first ceramic filters dated back to the second Iron Age, circa 800 BC. A clay vessel that is probably used for serving beer. (<https://www.pinterest.com/pearsonaf/pottery-of-the-past/>.)

weapons and fuels in the 1940s and 1950s [7]. This separation was performed at high temperatures by forcing highly corrosive UF_6 through semipermeable membranes. The only membrane materials that could withstand such harsh environments were oxides such as Al_2O_3 , TiO_2 and ZrO_2 . Many aspects of that work, carried out by the Western Bloc during the Second World War (the so-called *Manhattan Project*), are still classified [8]. The only information on these comes from several patents filed in the 1970s. Trials using the same membranes in purification of liquids met with limited success, mainly due to low separation efficiency and low flux. The idea of dividing a membrane into a skin and a porous substructure, proposed by Loeb and Sourirajan [9] in 1962 for polymer membranes, boosted the development of a new generation of ceramic membranes. It appeared that ceramic membranes could also be made in a number of layers like onions. In this new anisotropic membrane, the skin layer determines the separation and the support layer gives the mechanical strength and uninterrupted flux. Technical questions on fusion of layers made from different materials were significantly facilitated by Burggraaf and Cot [10] who developed in the 1980s a concept and procedures for intermediate membrane layers. This opened the door to applications in food and beverage industries [11,12], gas separation [13,14] and biotechnology [15], albeit in small installations.

In the past two decades, ceramic membranes have become a valuable component of fuel cells and play a central part in the hydrogen economy. Full-scale installations for water and wastewater purification started in Japan in 1998, and have recently started spreading to Europe and the United States. The separation of uranium isotopes, that started more than half a century ago, reached its maximum in the 1970s when nuclear energy was considered a valuable replacement of fossil fuels. However, after the Chernobyl disaster in 1986, reassessment of true amount of

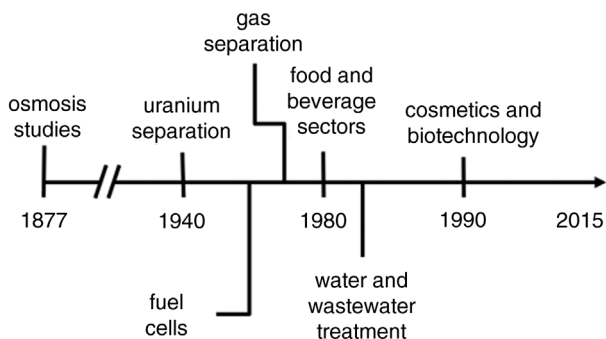


Figure 1.2 A timeline of ceramic membrane applications.

fossil fuels available, and development of more cost-effective uranium enrichment techniques such as centrifuge and laser, the use of ceramic membranes for uranium enrichment halted. Companies such as Atech Innovations, Orelis, Veolia Water, Hyflux, Kubota, TAMI Industries, Inoceramic GmbH, Metawater, Mitsui, Meidensha, Jiangsu Jiuwu, Pervatech and Ceraver [16,17] [acquired by Alcoa in 1986, then Societe des Ceramiques Techniques as USFilter in 1992, and (since April 2002) Pall Corporation] now advance ceramic membranes in new fields such as the water and wastewater treatment, food and beverages, chemical, pharmaceutical, electronic, petrochemical and energy sectors. Figure 1.2 sketches a brief of ceramic membrane history and their entry into various industrial sectors.

Today, ceramic membranes are established in modern separation techniques. As we will show in this book, in the future ceramic membranes with their clear advantages in chemical and thermal stability, longer lifetime, higher flux and higher recoveries will be employed in more applications. This is supported by recent reports on large-scale piloting with ceramic membranes and several full-scale installations. Here we will introduce the main developments in ceramic membranes, starting with a brief introduction into the general field of membranes that will help us to discuss technical details of membrane preparation and operation.

1.2

The Basics of Membrane Separation

Here we give a very brief introduction to the general membrane field emphasizing the difference between ceramic and other membranes, where appropriate. For readers wishing to delve deeper into the principles of membrane separations, there are several books that give a good introduction to the subject [16–18]. Other books with a special emphasis on the ceramic membranes are also briefly discussed in the ‘Further Reading’ section at the end of this chapter (Section 1.10).

Ceramic membranes, as any other membranes, are used for separating suspensions, aerosols and mixtures. They leave particles, organic molecules, dissolved salts or even gases and liquids on one side and transfer purified gases and liquids to the other. Thus, the ceramic membrane is a semipermeable barrier that separates purified and concentrated streams out of a mixture. Figure 1.3 depicts the essentials of membrane separation where the initial feed is separated into *permeate* and *retentate* streams. If the separation is performed for purification purposes, the permeate stream is the final product and the retentate stream is the by-product. If the separation is performed to concentrate a component in the mixture, the retentate stream is the product and the permeate is the by-product.

Mathematically, we express the above definition as the feed flow that approaches the membrane splits into permeate and retentate flows:

$$Q_f = Q_r + Q_p \quad (1.1)$$

where Q_f , Q_r and Q_p are the feed, the retentate and the permeate flows.

The efficiency of separation is evaluated using two parameters: the quantity of purified gas–liquid on the permeate side and the degree of purification. With different membrane areas and measurement periods, the quantity is unified by the transmembrane flux defined as the volume of gas–liquid passing through a unit of membrane area per a period of time:

$$J = \frac{Q_p}{A_m} \quad (1.2)$$

where J is the volume flux, Q_p is the flow of the fluid that passes through a membrane, and A_m is the membrane surface area. Fluxes in liquid–liquid separations are typically reported in litres per square metre of the membrane surface per hour ($l/(m^2 \text{ h})$) or gallons per square foot per day ($\text{gallons}/(\text{ft}^2 \text{ day})$). Fluxes in

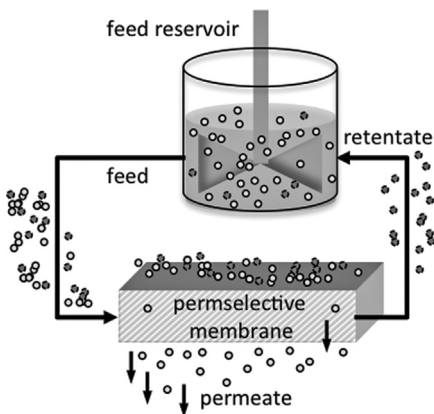


Figure 1.3 The basic membrane separation set-up showing the feed tank, the permeable membrane and the feed, permeate and retentate flows.

gas and vapour separation are reported in cubic centimetres of gas per second per square centimetre of membrane area ($\text{cm}^3/(\text{cm}^2 \text{ s})$). Transmembrane pressure and temperature significantly change gas fluxes and reported gas flux values assume standard conditions of 0°C and 1 atm. The volume flux J can be converted into mass flux or molar flux by using the density and the molecular weight of the feed, respectively. Some processes, for example DNA or protein purification, require high separation efficiency [19]. In others, the membranes must provide a predetermined flux (e.g. in dialysis or controlled drug release). Membranes used in controlled drug delivery need to provide a certain flux of a drug from a reservoir to the body. The ratio of permeate to the feed flux/flow is called the recovery ratio, RR, and defined as

$$\text{RR} = \frac{Q_p}{Q_f} \quad (1.3)$$

A fluid passes through a membrane by the shortest path. Intuitively, the fluid should be forced through a membrane perpendicularly to its surface following this general concept of *dead-end filtration*. The concept of filtration perpendicular to the filter surface was developed for granular filters in France in the middle of the eighteenth century. An additional tangential or a *cross-flow filtration* (CFF), also known as *tangential flow filtration* (TFF), was developed in the middle of the twentieth century. In this mode, a fluid flows in parallel to the membrane surface. A pressure difference across the membrane drives the fluid through the membrane. Figure 1.4 shows the dead-end and cross-flow filtration modes.

The *transmembrane pressure* (TMP) in dead-end filtration is calculated as

$$\text{TMP} = P_f - P_p \quad (1.4)$$

The TMP in cross-flow filtration is an average between the pressure on permeate and retentate sides:

$$\text{TMP} = \frac{1}{2}(P_f + P_r) - P_p \quad (1.5)$$

Here P_f , P_r and P_p are the feed, retentate and permeate pressures, respectively. In a single-stage installation, the permeate pipe is open to the air and, therefore, P_p

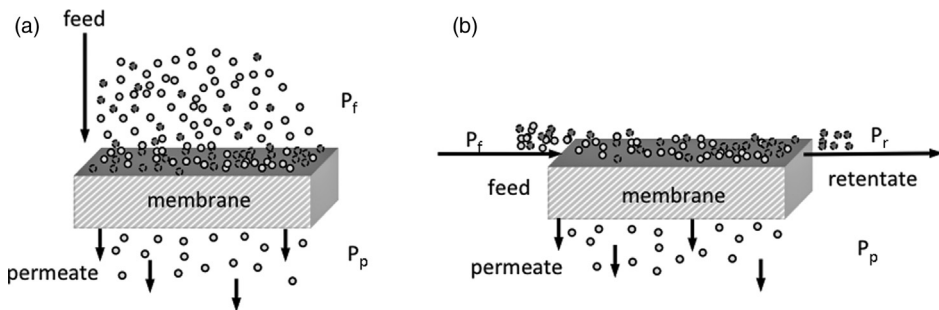


Figure 1.4 Schematics of dead-end (a) and cross-flow (b) filtration modes.

equals 1 bar. The TMP thus is the additional pressure (above the atmospheric pressure) needed to pass a fluid through a membrane. Dead-end filtration is more suitable for treating dilute suspensions. Conversely, cross-flow filtration is used for more concentrated suspensions when the deposits are swept away from the membrane surface by the shear stress that is exerted by the flow.

A fluid passes through the membrane overcoming its resistance. This resistance has two components: the intrinsic resistance of the membrane itself, and the resistance of materials accumulated within the membrane during the filtration operation:

$$R_t = R_m + R_o \quad (1.6)$$

where R_m , R_o and R_t are the membrane resistance, the operational resistance and the total resistance, respectively. The increase in the total resistance is the result of changes in the operational resistance when the membrane resistance remains constant.

A flux J (Eq. (1.2)) through the membrane system is related to the TMP (Eq. (1.4)) through the total resistance R_t (see Eq. (1.6)) as

$$J = \frac{\text{TMP}}{R_t \mu} \quad (1.7)$$

where μ is the viscosity of the fluid at a given temperature. A ratio of flux to TMP for a given membrane depends on the total membrane resistance and the viscosity but not on the operational parameters. The *membrane permeability* M (Eq. (1.8)) is independent of the applied pressure and permits the comparison of the performances of different membranes operating under various conditions:

$$M = \frac{J}{\text{TMP}} \quad (1.8)$$

A permeability coefficient through a gas separation membrane takes into account the membrane thickness:

$$P^* = \frac{J \Delta l}{\Delta P} \quad (1.9)$$

Here P^* is the permeance through a membrane of thickness Δl and ΔP is the partial pressure difference of a gas across the membrane. A transmembrane gas flux J depends on the membrane thickness but does not depend on fluid viscosity as in Eq. (1.7).

The degree of purification or the membrane selectivity is often evaluated using its retention ratio R or the separation factor α . In dilute solutions, it is more convenient to report the selectivity by R assuming that the solute is partially retained by the membrane when the solvent passes freely through the membrane:

$$R = 1 - \frac{C_p}{C_f} \quad (1.10)$$

where C_p and C_f are the concentrations of the separable compound in the permeate and in the feed, respectively. The retention ratio is dimensionless and

does not depend on the units in which concentration is expressed. Its value ranges from 0 for a free penetration up to 1 for complete retention. The membrane selectivity in separation of gases and organic liquids, α_{AB} , is expressed by the ratio of pure gas permeabilities for the individual components A and B:

$$\alpha_{AB} = \frac{P_A}{P_B} \quad (1.11)$$

Permeation through membranes occurs in two stages. A sorption of gas molecules onto and into membrane surface is followed by the diffusion of a gas through the membrane. Thus, the permeability P can be expressed as a multiplication of a thermodynamic component K related to sorption and kinetic component related to diffusion D :

$$\alpha_{AB} = \frac{P_A}{P_B} = \left(\frac{K_A}{K_B} \right) \left(\frac{D_A}{D_B} \right) \quad (1.12)$$

In this equation, the diffusion coefficients D_A and D_B reflect mobilities of individual molecules in the membrane material, while the gas sorption coefficients K_A and K_B (cm^3 of component in cm^3 of membrane) express the number of molecules A and B adsorbed or dissolved in the membrane material. The K_A/K_B ratio can be viewed as the sorption or solubility selectivity of gases A and B [18]. As defined in Eqs. (1.11) and (1.12), α_{AB} is the ideal coefficient that does not account for mutual interactions of gases as they pass through a membrane. In binary mixtures with significant concentrations of A and B, the coefficient is calculated as the molar retention ratio, α_{AB} :

$$\alpha_{AB} = \frac{y_A/y_B}{x_A/x_B} \quad (1.13)$$

where $[y_A, y_B]$ are concentrations of gases A and B in the permeate, and $[x_A, x_B]$ are their concentrations in the feed.

The selectivity is always ≥ 1 . If the concentration of A in the permeate is higher than the concentration of B, the separation is denoted as α_{AB} . If the concentration of B in the permeate is higher than that of A, the separation is denoted as α_{BA} . If $\alpha_{AB} = \alpha_{BA}$, no separation is achieved [16].

1.3

Membrane Separation Processes

Membrane separation is a field that embraces many processes. These are subdivided by the origin of the applied driving force, phases of feed and permeate and pore size. The division by the driving force describes the origin of the force needed to transfer the fluid from the feed to the permeate side. Pressure, temperature, concentration or electrical potential are the driving forces available. Table 1.1 lists some common membrane processes, separation phases, driving forces, sizes of retained compounds and their types.

Table 1.1 Common membrane separation processes.

Membrane process	Feed phase – permeate phase	Driving force	Size of retained compounds	Type of retained compounds
Microfiltration (MF)	L → L	ΔP	0.1–100 μm	Bacteria, fine solids
Ultrafiltration (UF)	L → L	ΔP	5 nm to 100 μm	Viruses, total suspended solids, natural organic matter
Nanofiltration (NF)	L → L	ΔP	1 nm to 100 μm	Inorganics, sugars, dyes, surfactants
Reverse osmosis (RO)	L → L	ΔP	0.1 nm to 100 μm	Salts, metal ions, minerals
Gas separation	G → G	ΔP	0.5 nm to 100 μm	Gases
Vapour permeation	G → G	ΔP	0.5 nm to 100 μm	Liquids
Pervaporation	L → G	ΔP	0.5 nm to 100 μm	Liquids
Electrodialysis	L → L	$\Delta\Phi$		Ions
Dialysis	L → L	ΔC		
Membrane distillation	L → L	ΔT		Liquids

Note: G and L stand for gas and liquid phases, respectively, ΔP is the pressure difference, $\Delta\Phi$ is the electrical potential difference, ΔC is the concentration difference and ΔT is the temperature difference.

Except for membrane distillation (see Section 4.4.5) that uses a temperature difference as the driving force, ceramic membrane separations use pressure. The level of applied pressure varies as a function of size of solutes separated by a membrane. For the same flux J , small pores require high pressure and offer a retention of small solutes. A relation between pore size, solute size, flux and applied pressure resulted in an additional subclassification of pressure-driven membrane processes mostly applicable in particle–liquid separation. Particles in liquids can be quite big and reach the maximum size of 100 μm . Membranes are generally not applied for the retention of particles larger than 100 μm . These separations are typically done using either sedimentation or filtration. Membranes separate particles using pressure as the driving force and micro-, ultra-, nano- and subnanopores incorporated in microfiltration (MF), ultrafiltration, nanofiltration and reverse osmosis (RO) membranes. Table 1.1 details proper implementation of pressure-driven membranes in particle–liquid separation. *Reverse osmosis* and *nanofiltration* are processes used for separating solute and solvent components on the nanoscale. Water desalination is the most famous example of RO technology. The separation is so sensitive that while water molecules with a radius of 1.3 Å diffuse through the membrane, electrolytes and organic solutes with several hydrophilic groups cannot pass. Nanofiltration is similar to RO, and uses the same principles. The pores of NF membranes are slightly larger than in RO membranes and they can separate multivalent ions.

Two main advantages of NF over RO membranes are the lower operational costs due to a lower required TMP and a wider choice of membrane materials. Both processes are commercially performed with polymer membranes, where the dense polymer layer needed for separation of monovalent ions can be synthesized from cellulose acetate (CA) or polyamide (PA). Similarly, NF membranes are made from cellulose acetate blends or polyamide composites but can also be synthesized from more stable polymers such as polysulfone or polypiperazine. Ceramic NF membranes are prepared from alumina, titania, hafnia, silica-zirconia and zeolites, although higher cost and lower mechanical strength are currently limiting their wide commercialization.

Ultrafiltration and *microfiltration* are another popular subclass of membrane separation processes. Although RO, NF, UF and MF processes are all pressure-driven, a significant difference in the pore size determines different applications and features of these membranes. The UF/MF membranes are used in the food and beverage industries, in water and wastewater purification, in pharmacology and in medicine. A typical size of separable colloidal particles and high-molecular-weight solutes ranges from single nanometre to micrometres, so UF/MF membranes cannot be used in desalination. On the positive side, the bigger pore size means that a much lower TMP is needed to achieve a reasonable flux. Polymeric MF/UF membranes are synthesized from polyacrylonitrile (PAN), polysulfone (PS), polyethersulfone (PES) and polyvinylidene fluoride (PVDF). These polymers are more mechanically, thermally and chemically stable than cellulose acetate and polyamide and the resulting UF/MF membranes are employed under harsh conditions. There is no clear distinction between UF and MF (basically, the same particles can be retained by both membranes with the same applied TMP and with higher separation efficiency of UF membranes). The recent trend is therefore to use more UF membranes with a smaller pore size and a wider range of separated materials. Ceramic UF membranes synthesized from alumina, titania and zirconia are used in separations performed at high temperatures or with non-aqueous solvents such as benzene or toluene.

Gas separation, pervaporation and membrane distillation membranes deal with small molecules. The separation of gas molecules on the basis of their size requires small pores that can be described as low NF pores. The subdivision into MF, UF or NF membranes is therefore not applicable here and it is not implemented. Unsurprisingly, gas separation is performed with gas separation membranes. The basic role in the implementation of a certain type of membranes is rather simple – a preset degree of purification is to be achieved at a lowest possible cost. Larger membrane pores produce less resistance to the transmembrane flow and demand less pump energy. Thus, the membrane operational costs increase in the order MF → UF → NF → RO but so does the retention. This subdivision is somewhat arbitrary and the same membrane may be described as UF, MF or NF (although RO membranes are rarely mixed with others). We will get back to definitions and methods of detection of membrane pores in Chapter 3.

1.4

The Morphology of Membranes

From a morphological point of view, membranes are divided into two large groups. *Porous membranes* transport the solutes in a continuous fluid phase through the voids within the membrane structure. *Dense membranes* transport solutes by dissolution and diffusion across the membrane. Most ceramic membranes are porous. The examples of non-porous ones include Pd membranes for hydrogen separation and mixed (electronic, ionic) conducting oxides for oxygen separation [20]. Both porous and dense membranes can be prepared from polymers, ceramics, paper, glass and metals. The polymer membranes are also called 'organic' ones, while ceramic, glass and metal membranes are called 'inorganic'. Polymer membranes are synthesized from different polymers, including cellulose, polyacrylonitrile, polyamide, polysulfone, polyethersulfone, polycarbonate, polyethylene, polypropylene and polyvinylidene fluoride. In addition, many polymers are grafted, custom-tailored, blended or used in a form of copolymers [21,22]. These modifications are made to increase the flux and retention of certain compounds or to avoid the flux drop due to accumulation of compounds on the membrane surface. Metal membranes are manufactured from palladium, nickel, silver, zirconium and their alloys, while ceramic membranes are made from metal oxides (alumina, titanium, zirconia), silica, zeolites and other mixed oxides.

There are various membrane preparation techniques, each with its own pros and cons. Typically, polymer membranes are prepared by phase inversion [9], track etching [23] and stretching [24]. Inorganic membranes are prepared by calcination and sintering and coated using sol-gel processes, chemical vapour deposition or hydrothermal methods. A detailed discussion on preparation techniques of ceramic membranes is given in Section 1.9.

The morphology of ceramic membranes is closely related to the membranes' pores. Pore size and size distribution, structure and tortuosity, interconnectivity and density (i.e. the number of pores per unit area) are the physical parameters that affect flux and separation efficiency. Membrane pore sizes are subdivided into *macropores* (diameter >50 nm), *mesopores* (between 50 and 2 nm) and *micropores* (<2 nm). The International Union of Pure and Applied Chemistry (IUPAC) also distinguishes between *supermicropores* (<2 nm) and *ultramicro-pores* (<0.7 nm) [25]. Pore size distribution indicates the presence of pores of different sizes within the membrane. Pore density is described by the *porosity* – the membrane surface or the membrane volume occupied by pores versus the total membrane surface or volume, respectively. Detailed definition of pore densities and their definitions are given in Chapter 3. Less porous structures are stronger, but also more resistant to flow, so the optimal porosity is a trade-off between the stability and the flux. There is no one-to-one relation between the porosity and the separation efficiency. After the initial packing of particles, the colloidal or polymer soils are heated at high temperatures. The sintering that occurs during the heating results in changes in porosity and pore size. Yet, the higher packing density of smaller initial grains, that is a low initial porosity,

embeds more uniform distribution of grains during the sintering and will result in denser membranes with smaller pores [26].

Membrane structures are divided according to the type of their pores. Membranes with finger-like pores are called *isotropic* (having symmetrical pores going from one to another membrane side with the same width). Membranes with sponge-like pores are called *anisotropic* (having asymmetrical pores, see Figure 1.5).

The synthesis of membranes with symmetric pores is relatively simple, and symmetric nitrocellulose MF and UF membranes were successfully prepared in Germany a century ago [27]. These membranes were later commercialized by Sartorius and used by the German army during the Second World War for bacteriological water quality tests in cities where the water supply system was destroyed. A symmetric membrane has a rigid void structure with randomly distributed interconnected pores. Such a membrane acts as a molecular sieve, retaining solutes that are larger than its pore size and transferring those having similar or smaller dimensions. The pore size itself, however, can vary significantly from $100\ \mu\text{m}$ all the way down to $3\text{--}5\ \text{\AA}$. It can be so small that these membranes are sometimes described as non-porous [17]. The transition through such pores is by diffusion, driven by either concentration or electrical potential gradient. Porous membranes can be electrically charged when the pore walls carry either a positive charge (anion exchange membranes) or a negative one (cation exchange membranes). The main problem of symmetric membranes is their inherent high resistance to the flow due to the pore width uniformity. Moreover, the selectivity of symmetric membranes is determined already at the skin membrane part and does not change through the pore.

In 1962, Loeb and Sourirajan solved the problem of unnecessary resistance to the flow, inventing asymmetric polymeric membranes [9]. Here, the separation is determined by the upper membrane layer, and the mechanical strength and support are provided by the lower layers. The upper separation layer has the smallest pores within the membrane structure, while the supporting system has larger

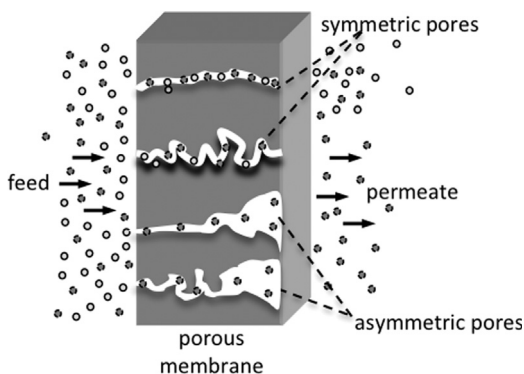


Figure 1.5 Symmetric and asymmetric membrane pores.

pores with lower hydraulic resistance to the permeate flow. The surface and support layers can be prepared simultaneously or sequentially. The membrane can be *homogeneous*, that is made from one material, or a *composite* made from different materials. In the latter case, the pore size and structures are conveniently determined by each constituent. Most ceramic membranes are asymmetric composites made from four or even five different layers. The composite structure of ceramic membranes is depicted in Figure 1.6, together with a cross-sectional scanning electron micrograph of a γ -alumina thin top layer of small pore sizes on top of an α -alumina support layer with gradually increasing pores towards the permeate side.

The membrane support layer D, often called simply 'the support', has to provide the maximum mechanical strength at the minimum membrane resistance. The support is therefore often over 1 mm thick and macroporous. Such thick supports are very stable but are also resistant to transmembrane flow. An intrinsic deficiency of membrane supports is their high average pore size, high surface roughness and high void defect density. The ideal membrane support layer should be strong, homogeneous, stable and possess minimum flow resistance but not the separation ability [29]. It must also be chemically compatible with the intermediate and filtration layers, and mechanically and thermally stable.

The intermediate layers B and C must provide good chemical and thermal stability, and must have a narrow pore size distribution and a smooth homogeneous surface. While the former is a general requirement for the entire ceramic membrane, the smooth surface relates to the main function of intermediate layers. It is almost impossible to coat the separation layer A on top of the support layer D with macroporous voids. Therefore, the intermediate layers B and C are used to gradually decrease the pore size of the support, thus preventing the penetration of the very fine particles used for the formation of top layer. Typical intermediate layers are thick enough to increase the mechanical strength of a ceramic membrane. The thickness of a single intermediate layer is usually a few

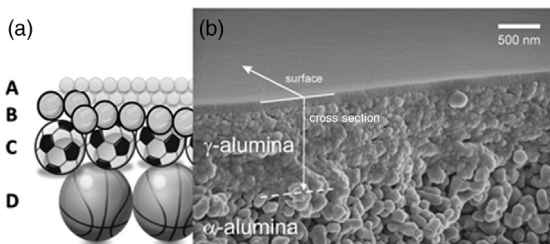


Figure 1.6 (a) Pictorial representation of an asymmetric composite ceramic membrane that consists of a nanofiltration-modified separation layer of 50 nm depth with pores less than 2 nm wide (A), an ultrafiltration layer of 100–500 nm depth with 10 nm pores (B), a

1–10 μm microfiltration intermediate layer with pores 100–200 nm wide (C) and a porous support of 1–1.5 mm width (D). (b) Scanning electron micrograph of a cross section of a ceramic composite membrane: γ -alumina on top of an α -alumina support [28].

hundred micrometres. Pore widths are in a mesoporous range of 2–50 nm in diameter. The number of intermediate layers varies, depending upon the difference in grain sizes between layers A and D, and the intended membrane use. Membranes for water and wastewater treatment might possess a support and maybe one intermediate layer. Gas separation membranes will contain four to five layers with macropores in the support and ultramicropores in the top layer. Generally, the bigger the difference in the pore widths between the support and the top layer, the higher the number of layers. An insufficient number of intermediate layers will result in penetration of small particles into the next-layer pores, leading to an increase of flow resistance and low mechanical stability of the sintered membranes [20].

The actual separation is performed in the top layer A. This layer is typically coated last on top of an existing membrane from different materials. It is responsible for the separation and therefore contains the smallest pores in the membrane structure. Note that this layer is not responsible for the mechanical strength of the membrane and thus it is relatively thin. A typical thickness of the separation layer is between 10 and 20 μm , and the intermediate and support layer are of 1–2 mm in total. Similar to layers B and C, the top layer A should be chemically and thermally stable and must possess a narrow pore size distribution and a smooth homogeneous surface. Importantly, the top layer may not have any large pores – even a few macropores will render the membrane useless as the entire flux will be directed through those pores. In fact, a good top layer should also compensate for any structural defects of the intermediate layers.

Together, this multilayer configuration provides the membrane its separation and flux properties. Every membrane layer is functional and purposeful, yet the total number of membrane layers varies depending upon the separation processes. For a precise separation such as gas separation or water desalination, the membrane will contain all A + B + C + D layers. Conversely, the concentration of proteins in food and dairy industries or sterilization of beverages does not require the microporous separation and can be performed with layers C and D only. Table 1.2 shows the link between a number of layers in a ceramic membrane and its designated separation process [30].

Table 1.2 The layer structure of composite ceramic membranes.

Separation process	Number of layers	Average pore size
Microfiltration (MF)	1	5 μm
	2	0.25 μm
Ultrafiltration (UF)	3	100 nm
Nanofiltration (NF)	4	2 nm
Reverse osmosis (RO), gas separation, pervaporation, vapour permeation	5	10 Å

Source: After Bonekamp [30].

Layer A is sintered; layers B, C and D are produced by sequential calcination at high temperatures making the manufacturing of ceramic membranes a complicated procedure. Layer A is often produced by CVD or by sol-gel techniques [31] and requires a high variability to suit the separation needs.

1.5

Membrane Modules

Laboratory-scale ceramic membranes are typically produced in a plain form, often as small discs suitable for cylindrical benchscale filtration units. This geometry reduces production expenses and makes further examination of the membrane surface easier. Small solid ceramic discs are also fun to play with. Typical available membrane surface ranges from a few to a few dozen square centimetres. Practical, real-life industrial membrane applications require hundreds or even thousands of square metres of membrane surface, raising the question of packing density. The *membrane packing density* is defined as the total membrane surface available per a module volume. Each module needs space and the packing density is an expression of membrane footprint. Commercial membranes are produced in plate or tubular form. The membranes are packaged in modules that represent the 'smallest discrete separation unit in a membrane system' [32]. Each module contains at least several square metres of the membrane surface potted or sealed into an assembly. Modules are assembled in larger production units, also called *skids*, *racks* or *trains*. A production unit shares feed, retentate and filtrate valves, and allows the isolation of single modules. Plate membranes are assembled in plate-and-frame and spiral-wound modules, and tubular membranes are assembled in tubular and hollow fibre modules. Plate-and-frame and spiral-wound modules are often employed in cross-flow mode (see Figure 1.4). Tubular and hollow fibres are often used in dead-end and semi-dead end installations. Plate ceramic membranes cannot be bent, and therefore relevant ceramic membrane skid geometries are plate-and-frame, tubular (also called honeycomb) and hollow fibres.

The development of membrane modules started soon after the membranes entered large-scale industrial processes. *Plate-and-frame modules* developed in the 1960s are probably the oldest configurations used in commercial applications [33]. The design of modules was inspired by the filtration technology and is similar to a simple filter press. A module consists of multiple flat sheet units packed together as a multilayered sandwich. Each unit includes a support plate, a flat membrane sheet and feed and permeate spacers. A flat sheet placed on the permeate spacer is bent over the support plate, forming an envelope open to the feed from both sides. The edges of the membrane are sealed to the support. Many of these units, called cassettes, are stacked in parallel to form the module. Figure 1.7 shows an example of industrial tubular membranes made of alumina, the essence of the module. The feed fills the entire empty volume and is either released through a central permeate channel as the permeate or collected at the

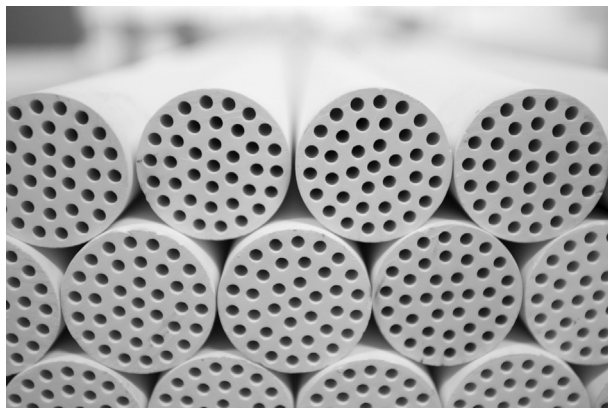


Figure 1.7 Stacks of tubular alumina membranes after the sintering stage. (Photo courtesy of Atech Innovations GmbH.)

exit as the retentate. Two main advantages of plate-and-frame modules are the ease of cleaning and replacement of defective membranes and the ability to handle viscous feeds. A low packing density is the main disadvantage of plate-and-frame modules. The packing density of plate-and-frame modules can be increased with alumina multichannel monolithic elements [34] or by stacking many membrane sheets together [35].

The packing density of flat sheets was increased in *spiral-wound modules* invented at the end of 1960s [36,37], a few years after the plate-and-frame modules. The module is arranged exactly as you would expect – several pairs of membrane sheets are placed back-to-back and then wound up. The edges of each pair of sheets are sealed to each other on three sides. On the fourth side, they are attached to a central perforated permeate channel of a pressure vessel. The sheets in a pair are separated by a fabric spacer that allows a permeate flow. A single spiral-wound module may consist of up to 20 pairs of sheets, each separated by a plastic mesh called a *feed spacer*. Viewed from the side, the path of a fluid on either feed or permeate side looks like an Archimedean spiral. The feed is usually pumped into the space outside the envelope through the feed spacers. Similarly, the permeate flows through a permeate spacer to the permeate channel. The advantages of the spiral-wound module are the high packing density and relatively low manufacturing cost. Its disadvantages are the difficulties in cleaning and repair of damaged membranes.

A parallel approach for increasing the packing density is to synthesize narrow hollow tubes, each only a few millimetres in diameter [38]. Although the diameter of each hollow fibre is small, a bundle of fibres packed inside a pressure vessel will have several square metres in total membrane surface. A typical commercial hollow fibre module consists of a few hundred to several thousand fibres. The fibres are often glued with a resin on the end that is far from the

pump, so the feed must pass through the membrane. In this case, the hollow-fibre module works in a dead-end mode, having only two streams: one for the feed and one for the permeate. The retentate is held inside the fibres and released only during washing. If the feed can go through the membrane and be released as the retentate, the membrane works in a cross-flow mode. The modules are typically mounted vertically (although the option of a horizontal mounting does exist). If the skin membrane layer A (Figure 1.6) is synthesized near the lumen part of the fibre (the inside), the separation is performed in *inside-out mode*. If the skin layer is on the outer part of the fibre, the separation is performed in *outside-in mode*. The advantages of a hollow-fibre module include high packing density, a relative ease of cleaning and replacement/shutting down of single fibres and low dead volumes. Reported packing densities calculated as surface area to volume ratios are 30–250 m²/m³ for tubes, 130–500 m²/m³ for plate and frame and up to 9000 m²/m³ for hollow fibres [39]. The main disadvantage is the fragility of single fibres.

Hollow tubes can be small in diameter and thus fragile, or larger and more robust. Originally, *tubular modules* consisted of several single tubes with large inside diameters between 0.3 and 2.5 cm [40]. The wall thickness of a single element was about 2 mm. The tubes are bundled together similarly to hollow fibres and placed inside a plastic or stainless steel vessel to form a cartridge. These tubular membranes can have either circular or elliptic cross sections. Such membranes are usually cast in place within a support tube made of fibreglass, ceramic, plastic or stainless steel. Higher mechanical strength and relative ease of cleaning and replacement of single tubes are the advantages of tubular modules. The tubes are also less prone to clogging than fibres and spirals [41]. Low packing density, high capital cost and high dead end volume are the main disadvantages. A high internal hold-up volume of each tube allows creating turbulent flow regimes with intensive pumping and indeed tubular membranes are used in feeds with high solid content. Although there are some suppliers that still produce those elements, majority of them have switched to *multichannel* or *honeycomb* configurations. The channels of millimetres have become a part of one large element. The elements were produced commercially by SCT-Exekia and Orelis and called Membralox[®] and Kerasep[®] membrane modules, respectively. Further development of the elements changed the cylindrical shape of the channels for non-cylindrical flower-like geometries [42]. These elements with cross-sectional diameters of 10 or 25 mm and excellent packing density were developed by Metawater (Japan) and Tami Industries (France). The total dimensions of a single element can be up to 0.2 m in diameter and 1.5 m in length, and their total available membrane area is above 10 m². The typical membrane element size cannot be increased any further due to limited hydraulic resistance of top layer and a chance for peeling off the top layer. Table 1.3 compares the relative advantages of each configuration, emphasizing the exploitation advantages of each module.

Here the *hold-up volume* is defined as the volume of the fluid retained inside the filter during the filtration process. An additional parameter significant in the

Table 1.3 Advantages and disadvantages of tubular and plate-and-frame modules.

	Hollow fibre	Plate-and-frame	Tubular
Cost/area	Low	High	Low
Membrane replacement cost	Moderate	Low	Moderate/low
Flux (l/(m ² h))	Good	Low	Low
Packing density (m ² /m ³)	Excellent	Good/fair	Good
Hold-up volume	Low	Medium	Medium
Cleaning in place	Good	Fair/poor	Fair/poor

Source: Modified after Ref. [43].

selection of a membrane module is the feed channel height. Selecting the correct height can prevent channel blockage. A rule of thumb in the industry is that the channel height should be at least 10 times larger than the diameter of the largest particle that can ever enter the channel. That ratio increases up to 25:1 in spiral-wound modules [44]. Companies resort to the lowest possible ratio to prevent intensive pumping. Larger pump capacities are needed in filtration with modules with high channel heights.

The above analysis of relative advantages and disadvantages of different modules has been known to membrane manufacturers for a long time. Still, companies use all types of modules when the exact design is a proprietary of the membrane manufacturer. For example, Asahi Kasei (Japan), GE Healthcare (United Kingdom) and Inge AG (Germany) use hollow fibres. Pall Corporation (USA), Sartorius (Germany), GE Healthcare (UK) and Microdyn-Nadire (Germany) use plate-and-frame modules. Pall Corporation (USA), NovaSep Process (France), Tami Industries (France) and IBMEM (Germany) are using tubular modules. Koch membrane systems (USA) uses all types of modules.

1.6

Fouling and Cleaning

1.6.1

Fouling

A membrane module can be operated in either constant flux or constant pressure mode. In a constant flux mode, the flux through the membrane remains constant, but the TMP rises as the operation continues. Conversely, in a constant pressure mode, the pressure remains constant, but the flux decreases. In both cases, we understand that the main operational parameters change during the operation and membrane performance deteriorates. This happens because of fouling, defined as ‘The process resulting in loss of performance of a membrane

due to the deposition of suspended or dissolved substances on its external surfaces, at its pore openings, or within its pores' [45]. The deterioration is so severe that the membrane operation must be stopped periodically for cleaning. Both fouling and cleaning are two integral parts of the membrane operation that now can be properly described as a sequence of four stages: normal operation – fouling – cleaning – integrity test. Many books and thousands of research papers have been written on fouling and cleaning. Here we provide only a brief overview. Readers who are especially interested in fouling are referred to 'Fundamentals of fouling' by Field [46], 'Fouling and cleaning of ultrafiltration membranes: a review' by Shi *et al.* [47] or 'Membrane chemical cleaning: from art to science' by Liu *et al.* [48].

The loss of membrane performance can be due to two separate phenomena, but only one of them is called fouling. The other is the pre-concentration of solutes near the membrane surface due to a preferential passage of a solvent through the membrane. These solutes, however, are located near the membrane surface but not attached to the membrane in any way. They reduce the solvent activity and the flow. This is known as *concentration–polarization*, a natural phenomenon that can be mitigated by TMP and flux. Conversely, fouling is a phenomenon of attachment of solutes to the membrane surface that reduces the available membrane surface or blocks membrane pores. Two other forms of fouling are *cake formation* and *gel formation*. A 'cake' is formed when the fouling layers are built up on each other. In this case, the main fouling cause is the solute–solute attachment. In a case of the extreme concentration–polarization, certain macromolecules such as proteins can form a gel layer near the membrane surface.

Fouling is subdivided into four categories – inorganic, colloidal, organic and biofouling [49]. *Inorganic fouling* or *scaling* is caused by the accumulation of inorganic precipitates on membrane surface or within pore structure. Precipitates are formed when the concentration of chemical species exceeds their solubility limit. For example, if a reverse osmosis plant is operated at 0.75 recovery ratio (RR), the concentration of sparingly soluble salts in the retentate will be four times larger than their concentration in the feed. Some salts such as CaSO_4 , CaCO_3 and silica are only slightly soluble and that pre-concentration level could be enough to cause scaling. Other salts such as CaF_2 , BaSO_4 and SrSO_4 have a scaling potential and their concentration should be carefully inspected not to exceed the solubility limits. The inorganic fouling due to concentration polarization in MF and UF membranes is much less common, but can occur due to chemical interactions between ions and other fouling materials, such as organic polymers.

Colloidal fouling can occur with different kinds of particles. Algae, bacteria and certain natural organic matters fall in the size range of particle and colloids. However, they are different from inert particles and colloids such as silts and clays. In most cases, particles and colloids do not really foul the membrane. This is because the flux decline caused by their accumulation on the membrane surface is largely reversible by hydraulic cleaning measures such as backwash and air scrubbing. A

rare case of irreversible fouling by particles and colloids happens when they are small relative to the membrane's pores. Such particles and colloids can enter and get trapped within the pores. Removing these by hydraulic cleaning is difficult.

Organic fouling is caused by organic solutes with molecular weights ranging between few thousands and 1 million Da. For example, proteins present the main challenge in biopurification and food industry. The fouling is caused by complex solute–solvent–membrane interactions such as electrostatic, lyophilic/lyophobic, steric and covalent bonding effects. Many factors can affect organic fouling: the properties of the feed constituents such as size, hydrophobicity, charge density and isoelectric point; the properties of the membrane (hydrophobicity, charge density, surface roughness and porosity) and the properties of the solution phase, such as pH, ionic strength, and concentration of metals. Other factors of importance are the hydrodynamics of the membrane system (characterized by the solution flux) and surface shear.

Microbial fouling is a result of formation of biofilms on membrane surfaces. Once bacteria attach to the membrane, they start to multiply and produce extracellular polymeric substances (EPS) to form a viscous, slimy, hydrated gel. The EPS typically consists of heteropolysaccharides which have a high negative charge density. This gel structure protects bacterial cells from both hydraulic shearing and chemical attacks of biocides such as chlorine.

In gas separations, membrane fouling has often been neglected, mainly because feeds are protected by upstream filtration and are therefore relatively clean. The remaining foulants can damage the membrane or the seals but cannot cause fouling. There are a few reports on the organic fouling in vapour permeation [50]. We will discuss some typical fouling models in detail in Chapter 2.

1.6.2

Cleaning

Membrane cleaning can be defined as ‘a process whereby material is relieved of a substance that is not an integral part of that material’ [51]. An efficient cleaning should leave the membrane physically, chemically and microbiologically clean. The cleaned membrane should display adequate flux and separation efficiency, close to the features of a virgin (pristine) membrane. Cleaning of membranes is performed by physical and chemical methods, and really depends on the type of fouling. In general, physical cleaning is preferred over chemical cleaning, for two reasons. First, a physical cleaning is faster and cheaper. Second, the chance to damage a membrane by an adequate physical cleaning is much lower. However, despite all these advantages, chemical cleaning is an integral part of many membrane operations. The main reason is that not all foulants can be removed by physical cleaning. Ideally, after cleaning, the membrane surface should contain no foulants. Without dismantling the module after each cleaning, the degree of cleaning is assessed by the flux ratios through virgin and cleaned membranes. If the flux after physical cleaning is as high as the flux through a virgin membrane, the fouling is considered reversible and no chemical cleaning is needed. That

said, some foulants will deposit on the membrane surface irreversibly and their cleaning will require chemicals. A fouling that can be cured by physical cleaning is called *reversible fouling*, while one that requires a chemical intervention is called *irreversible fouling*. Figure 1.8 schematically depicts the TMP development over time in reversible and irreversible fouling.

Physical cleaning of ceramic membranes can be done by relaxation, flushing, mechanical scouring and electrical cleaning. Membrane relaxation (i.e. discontinuous operation) allows reversibly attached foulants to diffuse away from the membrane surface under the influence of a concentration gradient [52]. Flushing the membrane surface (surface wash) or membrane pores if they exist (backwash) is done with a slight overpressure, forcing the fluid to move from the permeate side to the feed side. Similarly, air scouring is employed to enhance foulant removal, especially at a relatively high TMP values. Different methods such as air backwash, air sparging and air scrubbing are employed to inject the air into the module. This is done either intermittently or continuously through either the retentate side or the permeate side of the membrane.

Chemical cleaning is done following the *similia similibus curantur* or 'like cures like' principle. In general, there are six groups of cleaning chemicals (acids, caustic, oxidants, chelating agents, surfactants and enzymes), and each group is used for treating different foulants. Caustic agents such as NaOH, for example, are typically used for cleaning membranes fouled by organic and microbial foulants by hydrolysis and solubilization. Acids such as citric acid ($\text{HOOCCH}_2\text{C}(\text{COOH})(\text{OH})\text{CH}_2\text{COOH}$) and nitric acid (HNO_3) are used primarily for

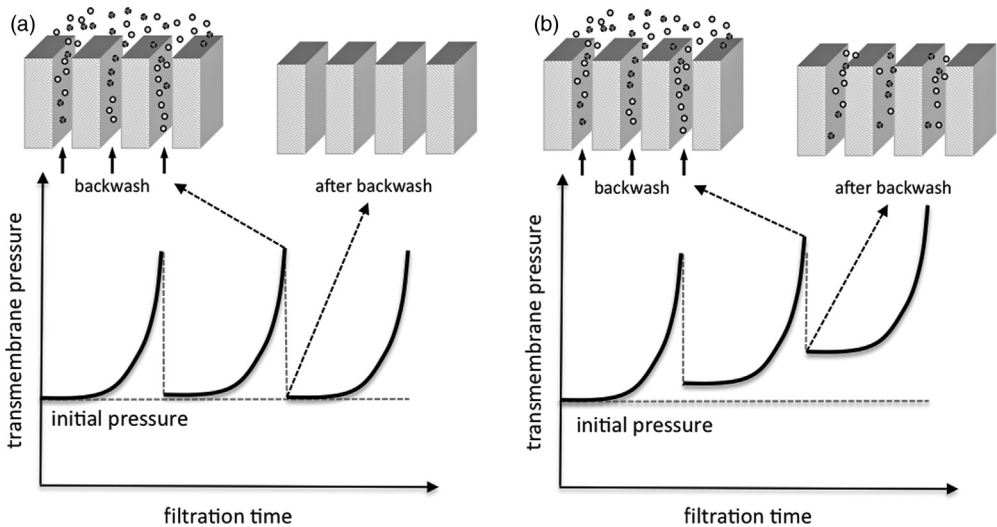


Figure 1.8 Development of reversible fouling (a) and irreversible fouling (b) in UF membranes working under a constant flux regime.

removing scales and metal oxides from fouling layers. Oxidants such as chlorine, HOCl and H₂O₂ partially decompose the foulant, forming more soluble compounds that contain ketone, aldehyde and carboxylic functional groups. Chelating agents such as ethylenediaminetetraacetic acid (EDTA) lock and remove divalent cations, thus significantly reducing the strength of a fouling layer [53]. Surfactants solubilize the foulants to dislocate them from the membrane surface and to enclose them in micelles [54]. Finally, enzymes are especially useful in cleaning membranes fouled by proteins when both a complete cleaning and the integrity of the cleaned membrane are important.

A chemical cleaning process has six stages: (i) dissolution and reaction of the cleaning agents, (ii) transport of these agents to the membrane surface, (iii) penetration through the fouled layers, (iv) cleaning reactions, (v) transporting the reaction products back to the interface, and (vi) transporting the products back to the bulk solution. The entire process can be done without dismantling the membrane module, simply by introducing the cleaning agents through the feed or the permeate openings. This kind of chemical cleaning mode is called *cleaning-in-place* (CIP) and it is run as long as it can successfully revamp the membrane to its initial flux level. When a more specific cleaning is needed, the module is dismantled from a rack and treated by *cleaning-out-of-place* (COP). Both CIP and COP can be performed by a combination of chemical and physical cleaning methods, depending on the fouling problem at hand [54].

Both physical and chemical cleaning processes can affect the membrane in different ways, including altering its integrity [55,56]. Therefore, the checking of membrane integrity after each cleaning is now a standard part of any membrane operation. There are several different methods for doing this. We will discuss these methods in detail in Chapter 3.

1.7

Ceramic versus Polymer Membranes

Although ceramic membranes have been known for centuries while polymer ones are relative newcomers, the latter are dominating the market. There are three good reasons for this, namely money, money and money (typically, ceramic membranes cost three to five times as much as polymer ones). Rough estimates are considering the material cost of US\$2000/m² of ceramic membrane versus US\$400/m² of a polymer one [57]. Accounting for higher fluxes and longer lifetimes of ceramic membranes, the difference becomes less dramatic: \$60 versus \$20 per unit of permeate volume, but still significant. Polymer membranes are much cheaper than ceramic ones and are therefore preferred in new installations. Ceramic membranes require more expensive starting materials, their fabrication process is complex and consists of multiple stages and their packing density in each membrane module is low. All that said, ceramic membranes also have many advantages and unique features that are helping them gradually enter the industrial market. The question of cost that is now central to the future of ceramic membranes is gradually being

resolved by industrial R&D. Historically, the same happened with polymer membranes. Some 50 years ago polymer membranes were so expensive that they were predicted to be used in laboratory installations only. A prediction made in 1949 says that *For the purpose of thermodynamic demonstrations, it is accepted that films exist, that are selective to one given component. In practice, it has been possible to prepare only a few of the membranes postulated in theory* [58]. Some 30 years ago, using RO polymer membranes was a more expensive option for desalination and new installations used the distillation process. Now polymer membranes are not the only option for the new RO desalination plants, and old plants are being revamped to use the membranes. Polymer membranes have put out of business other filtration technologies with a stable growth rate of 6–7% per year. All this time, membrane manufacturers improved their membranes in a strong competition for ever-growing markets. As a result of last 30 years of development, water flux has doubled and the salt passage has dropped sevenfold [17]. In the two decades from 1980 to 1999, the cost of RO membrane operation has dropped by over 80% [59].

We believe that the same will happen with ceramic membranes. A growing consensus regarding the positive features of ceramic membranes currently results in a massive piloting in the last decade for several full-scale installations in water and wastewater sector (mainly in Japan, with two new installations in the United States). Ceramic membranes are an established technology in food and beverage industry, and play an integral part in reshaping the energy strategy through the hydrogen economy and fuel cells. Tailor-made ceramic membranes serve as ultimate solutions in several gas separation processes and gradually enter the water and wastewater treatment market. Due to their robustness, ceramic membranes are one of the fastest developing membrane applications for the treatment of liquid wastes. The ability to perform CIP at high temperatures with any chemical cleaning agents, or to apply steam sterilization for sanitizing membrane plants is unique feature of ceramic membranes. Several companies such as SCT (Societe des Ceramique Techniques), thereafter Alcoa and now Pall Corp. (USA), Atech Innovations GmbH (Germany), LiquiTech (Denmark), CeraMem (now Corning, USA), TAMI Industries (France), Rhodia Orelis (NovaSep/Orelis, France), Filtrox (Switzerland) and Jiangsu Jiuwu Hitech Co. (China) realized the potential of ceramic membranes and currently offer full-time installations. Soon other companies will join. Applications of ceramic membranes constantly increase by field, by the total number of the installed plants and by the sales. Current sales of ceramic membrane modules are estimated between \$650–\$850 million with a forecast CAGR of 10–15% a year [42]. We believe that in a decade, numbers and relations between polymer and ceramic membranes will become irrelevant. We therefore give here the current price ratios, as this is the data available, yet realizing that the price will not determine the future of ceramic membranes. A detailed discussion of the economics of ceramic membrane manufacturing and application is given in Chapter 5.

The main advantages of ceramic membranes over polymer ones are their higher flux and longer lifetime. Reported fluxes of up to 360 l/(m² h) through ceramic membranes are on average double that of polymer membranes [60].

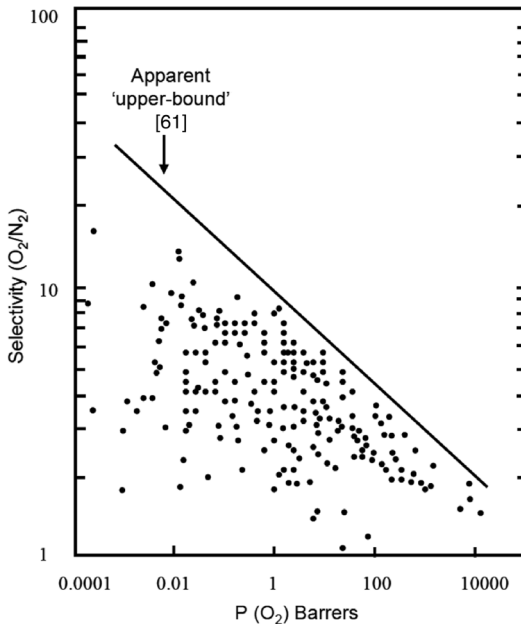


Figure 1.9 A typical Robeson diagram, showing a plot of the O_2/N_2 upper limit selectivity-permeability trade-off [61]. The dots denote the data points of various polymer

membranes investigated and the line is the upper limit of selectivity/permeability. The oxygen permeability is expressed in Barrers (1 Barrer = $10^{-10} \text{ cm}^3 \text{ (STP) cm}/(\text{cm}^2 \text{ s cmHg})$).

Moreover, unlike polymer membranes which show deteriorated selectivity at higher flux, the selectivity of ceramic membranes does not change as a function of TMP. One of more powerful examples is the so-called *Robeson diagram* for polymer and ceramic membranes shown in Figure 1.9. The analysis in the paper clearly shows that in O_2/N_2 gas separation, the combined (flux + separation) efficiency of ceramic membranes is far above the efficiency of polymer ones.

However, the higher flux is accomplished by application of membranes with bigger pores or operation at higher TMPs. In the latter case, the average permeability of 1.3 ± 0.1 and $0.87 \pm 0.08 \text{ l}/(\text{h m}^2 \text{ Pa})$ through ceramic and polymer membranes, respectively, are almost equal [57]. The average 15–20 years lifespan of ceramic membranes is roughly double than the 7–10 years of current polymeric membranes [57]. Curiously, this fact actually creates problems for ceramic membrane manufacturers. In comparison to polymeric membranes, ceramic membranes are mechanically, thermally and chemically stable. Uhlhorn *et al.* [62] also mentioned long-term durability of ceramic membranes, although the polymer membranes had also improved tremendously since their report. Table 1.4 compares the advantages and disadvantages of ceramic membranes and lists some applications where these advantages are important. Below, we survey the raw materials used for making ceramic membranes. In the next section, we explain and discuss the fabrication

Table 1.4 Advantages, limitations and current applications of ceramic membranes.^{a)}

Advantages	Disadvantages	Current status	Applications
Thermal stability (>200 °C)	Low hydrothermal stability of composite membranes with a silica top layer. Complicated sealing at high temperatures	Surface modification to improve hydrothermal stability	Reactions at high temperature, pervaporation, gas separation
Resistance to organic solvents	Expensive source materials, complex processing; relatively high capital installation costs		Separation of organic liquids and oils, wastewater treatment
Chemical stability over a wide pH range	Difficult sealing and module construction		Chemical cleaning, separation at extreme pH, recovery of acids/bases
Long-time operational stability, no ageing, potentially lower life cycle cost	Low packing density		Small-scale applications
Mechanical stability under large pressure gradients	Brittleness incurs special configurations and supporting systems		Operation at high flux (up to 500 l/(m ² h)), backwashing at high flux
High structural integrity	Relatively high installation and modification costs in case of defects	Depends on the separation process	
Uniform pore size distribution	Difficulty to achieve high selectivity on a large scale		Precise size-based separations in pharma and bio applications
(Electro)catalytic and electrochemical activity easily realizable	Low permeability of high-selectivity (dense) membranes at medium temperatures		Solid oxide and other dense electrolyte fuel cells

a) The advantages of ceramic membranes depend strongly on the type of ceramics used in their preparation.

of different layers (Section 1.4) in ceramic membranes. Indeed, improving the price/performance ratio of ceramic membranes depends on both the raw materials and the production process.

1.8

Raw Materials for Ceramic Membranes

Ceramic membranes can be made from many materials. A strict definition of ceramics as inorganic non-metallic material prescribes the use of metal oxides or zeolites, and indeed alumina and silica are among the most common membrane

precursors [10]. The limited stability of these membranes and the ongoing optimization led to the use of more stable (but also more expensive) titania and zirconia. Recent reports on membranes made of tin and hafnium oxides or mixtures of different oxides show that the search continues. Meanwhile, the definition of ceramic membranes has broadened. Today, a composite ceramic membrane is defined as a membrane that has at least one of its layers made of a ceramic material. This definition includes inorganic membranes on a metal or glass support [63], as well as hybrid ones with an organic-templated top layer [57]. Here we describe several typical materials used in the preparation of ceramic membranes, and explain their inherent advantages and drawbacks. A detailed description of the different membrane synthesis procedures is given in Chapter 2.

1.8.1

Alumina

The most known material associated with the ceramic membrane is aluminium oxide (alumina, Al_2O_3) [64]. Alumina is abundant, has good chemical and thermal stability, relatively good strength and thermal and electrical insulation properties. It has several allotropes, including the α - and γ -alumina, the two forms used in the preparation of ceramic membranes. The internal crystal structure of α -alumina is a hexagonal close-packed array of O^{2-} anions. The Al^{3+} cations fill two-thirds of the octahedral interstices and form close-packed planes inserted between the oxygen layers. Each Al^{3+} centre is octahedral. The structure of γ -alumina is often described as a defect cubic spinel, with vacancies on part of the cation positions. Each γ -alumina unit cell contains 32 oxide and $64/3$ aluminium ions to fulfil stoichiometry. The aluminium ions occupy both octahedral and tetrahedral positions, but the relative partial occupancy in each position is still a matter of dispute, since the structure in practice is highly complex [65]. Alumina ceramic membranes are usually made by sintering α -alumina and γ -alumina powders at high temperatures ($>1300^\circ\text{C}$). Figure 1.10 depicts the stability of various forms of alumina as a function of temperature [1,66].

The main source of aluminium in nature is the ore bauxite (named after the French village *Les Baux*, where its high aluminium content was discovered in the 1820s). Bauxite is a mixture of gibbsite $\text{Al}(\text{OH})_3$, boehmite $\gamma\text{-AlO}(\text{OH})$, diaspore $\alpha\text{-AlO}(\text{OH})$ minerals, two iron oxides, kaolinite clay and small amounts of TiO_2 . Heating the ore results in a formation of allotropic forms such as α -, γ -, δ -, η -, θ -, and χ -alumina. However, sintering above 1000°C transforms all these forms to $\alpha\text{-Al}_2\text{O}_3$, which is the most thermodynamically stable allotrope. The melting point of $\alpha\text{-Al}_2\text{O}_3$ is about 2047°C , but the impurities and alloying elements will melt at significantly lower temperatures. Typical pore sizes of α -alumina membranes are dozens to hundreds of nanometres, making them suitable as support layers for composite membranes. Subsequently, γ -alumina, which has much smaller pores (down to single nanometre), is coated on these using sol-gel methods. The coating step is followed by firing (calcination) at 500°C to avoid the gamma-

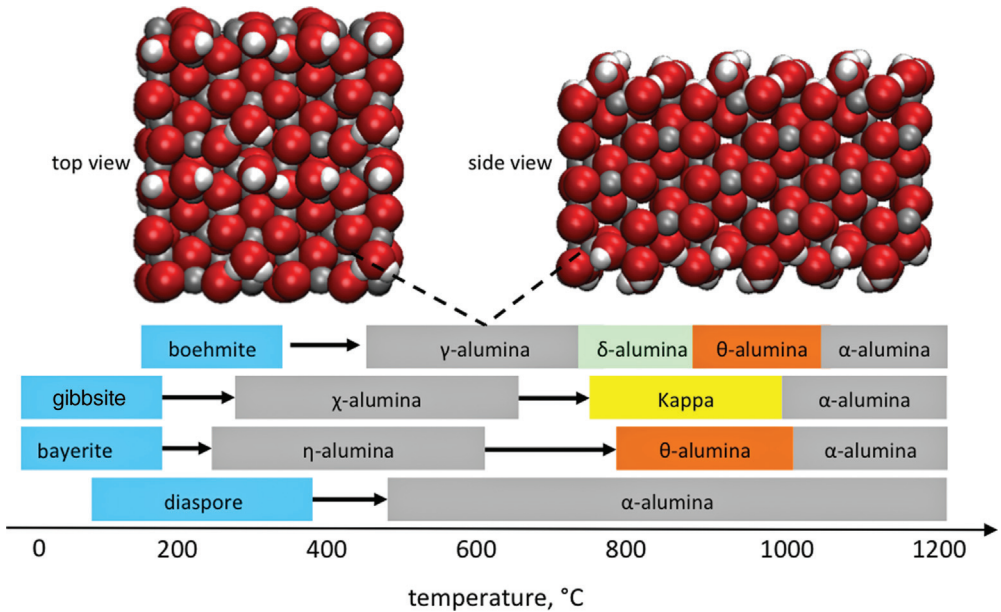


Figure 1.10 Simulated structures of a repeating γ -alumina unit cell (front and side view; simulation courtesy of Dr. Manuel Louwerse) and a diagram showing the phase transitions of alumina at different temperatures starting from different mineral ores. (Data redrawn from Ref. [1].)

to- α transition. This protocol was developed in the 1980s by the groups of Burggraaf, at the University of Twente, and Cot, at University of Montpellier [10]. The aluminium metal powder is subdivided into first-grade (A1–A5) that contains at least 99% of pure aluminium powder and second-grade that contains between 80 and 95% α - Al_2O_3 . Ceramic membranes are usually prepared from the second-grade powder that is cheaper but also contains many impurities. These hamper the sintering, resulting in weakened membranes that can crack at relatively low stress values.

1.8.2

Silica

Silicon dioxide (SiO_2 , commonly referred to as silica, from the Latin *silex*) is another inorganic material often used in ceramic membranes. Silica has a tetrahedral structure where each Si atom is surrounded by four oxygen atoms. A part of the Si electron density is transferred to its neighbouring oxygen atoms that in turn share their electronegativity with their neighbour silicon atoms in a polymeric structure that has SiO_2 as its net chemical formula. This endless network of covalently bonded ' SiO_4 ' units gives rise to a large number of different amorphous and crystallized forms, including mineral quartz, cristobalite and tridymite. The lengths of the Si–O bonds fluctuate around 1.6 Å, and the Si–O–Si

angles vary between 140° in α -tridymite and up to 180° in β -tridymite [67]. Similarly, the Si—O—Si flexibility and almost free rotation of the bond around the axis give to amorphous silica (no long-range order) its unique properties often used in preparation of thin (down to 30 nm) coating layers used for molecular sieving applications. This coating is done by CVD and sol-gel methods. The CVD results in a formation of ultra-micropores (less than 0.7 nm) that have superior separation properties but low fluxes. A sol-gel coating typically produces super-micropores (between 0.7 and 2.0 nm) that are less selective but permit higher fluxes. Some authors claim that pores of sizes 3–4 Å can be achieved by the sol-gel method [29]. Silica is the only available truly microporous material that can be employed in molecular sieving. The sol-gel membranes are much easier to prepare, but their low reproducibility precludes many industrial applications.

Silica-coated membranes are highly popular in a variety of separation processes, from gas separation [68] to water desalination [69]. The major drawback of amorphous silica is its hydrothermal instability. Typical lifetimes of silica-based microporous membranes are just a few days at moderate temperatures ($<100^\circ\text{C}$) [31]. Humidity and heat, even under mild conditions of 200°C [60], cause a substantial shrinkage of pore volume due to physisorption of water molecules on the surface silanol Si—OH groups followed by a reaction with nearby siloxane Si—O—Si bonds. Scission of these bonds releases silica ‘molecules’ (small oligomers) that migrate to small pores, recondense there and block them. The low hydrolytic stability of siloxane sets a natural limit to use of pure inorganic silica membranes, restricting full applications to water-free atmospheres only. Currently, on industrial scale, the silica-coated membranes are mainly used in gas separations. Interestingly, the water sensitivity problem can be solved using *hybrid silica*, a combination of SiO_2 and organic linkers, invented by Castricum *et al.* [70].

1.8.3

Titania

Titanium dioxide (titania, TiO_2) is another popular material used for coating ceramic membranes, sought after for its excellent chemical resistance at both acidic and alkali pH. Titania occurs in nature mainly in a form of ilmenite, a $\text{FeO}\cdot\text{TiO}_2$ ore that contains between 15 and 40% of iron, and rutile that contains up to 15% iron and other impurities (and therefore 85% TiO_2). The other main impurities are magnesium and manganese. Two of the three crystalline forms of titania, anatase and brookite, are metastable and convert into the stable rutile form upon heating. The rutile form is the only one used commercially. Its crystalline structure has a tetragonal unit cell, wherein each Ti^{4+} cation is surrounded by an octahedron of six oxide ions. These O^{2-} anions are in turn surrounded by titanium cations in a trigonal planar coordination. The TiO_6 octahedra are linked by their edges, form chains parallel to the z -axis. The structure of ilmenite is a hexagonal close-packed anion lattice. Here, Fe and Ti

cations occupy two-thirds of the available octahedral interstices in a way that cation–oxygen octahedra share edges in a honeycomb arrangement in one plane and octahedral faces between adjacent planes [71]. Titania particles and colloids are widely used in paints and varnishes as well as in paper and plastics, thanks to two features – white pigmentation and photocatalysis under ultraviolet (UV) light. Chemical companies use the photocatalytic feature of TiO_2 to either degrade organic pollutants or to perform transformation of organic compounds in gas and liquid phases. The melting point of rutile TiO_2 is about 1800 °C.

In ceramic membranes, titania can be applied as both self-standing and coating layers. The self-standing titania membranes are produced as tubes of nanometric diameter and micrometric length. These are obtained from titania nanoparticles either by synthesis of titanium alkoxide compounds under alkali conditions or by a direct hydrothermal attack on TiO_2 nanoparticles under alkali conditions. In the latter case, the nanotubes are made of pure anatase that shows a greater photocatalytic activity than rutile [72]. The prepared titanium nanofibres, rods and surfaces fall under the definition of membranes mainly because these structures are porous and a fluid can pass through them. Conversely, the self-standing titania membranes suffer from poor structural stability [73]. They cannot be assembled into a module. When they are used, for example in catalytic reactions, they are suspended as particles in the reactor.

The coating of supports with a titania layer is mainly performed via the sol–gel method, similar to silica coating. Ti-based organometallic precursors are hydrolyzed in the presence of excess water and dip coated or spin coated on the support surface, followed by firing at relatively low temperatures. A transition from amorphous titania to anatase occurs at 300–400 °C, and from anatase to rutile between 400 and 600 °C. The anatase-to-rutile phase transformation is generally undesirable [72] due to a brittle structure and low photocatalytic activity of rutile TiO_2 . Sol–gel coating is usually done using either amorphous titania or anatase titania having smaller pore sizes than the rutile. The resulting membranes have pore sizes below 2 nm. Other methods include a direct deposition of titania from an aqueous solution of titanium tetrafluoride on an α -alumina support [74] or photografting and photopolymerisation of a blend that contains photocatalyst particles and suitable polymers [75]. Part of these methods, including the physical deposition of TiO_2 particles entrapped within the pores of a UF membranes, intend to ensure the presence of TiO_2 particles on the membrane surface rather than forming a solid separation layer. Research and implementation of titania-encapsulated membranes mainly use the photocatalytic feature of TiO_2 for catalysis [76].

1.8.4

Zirconia

Zirconium dioxide (zirconia, ZrO_2) is one of the most popular ceramic coating materials. This popularity reflects its chemical stability, especially in alkali solutions [3]. Zirconia occurs in nature mainly as baddeleyite, a rather rare ore that

comes in a variety of monoclinic prismatic crystal forms. Baddeleyite is a refractory mineral that melts at 2700 °C. Hafnium is a substituting impurity and may be present in quantities ranging from 0.1% to several percent. Zirconia exists in three crystalline forms – monoclinic, tetragonal and cubic. Unlike titania, which features six-coordinate Ti in all phases, monoclinic zirconia consists of seven-coordinate Zr centres (this difference is attributed to the larger size of Zr ions). The transition from one crystalline form to another is triggered by heating, where the higher cubic symmetry forms at temperatures above 2370 °C. A transition from a monoclinic to tetragonal zirconia occurs at 1173 °C, so zirconia membranes can crack after sintering at high temperatures. This cracking, which is a known problem of zirconia membranes, is due to a large volume change (about 9%) in the transition from tetragonal to monoclinic phases. To avoid it, zirconia used in coating top layers is fired at 500–600 °C, or doped with yttria (Y₂O₃) in its cubic polymorph, which increases its thermal stability. The thermal stability of zirconias can also be improved by adding 12–13 mol% CaO, 8–9 mol% Y₂O₃ and Sc₂O₃ or 8–12 mol% of other rare-earth oxides (Yb₂O₃, Dy₂O₃, Gd₂O₃, Nd₂O₃, Sm₂O₃) [8]. Yttria-substituted zirconia is currently the state of the art in solid electrolyte membrane materials for high-temperature fuel cells (see details in Chapter 4).

1.8.5

Zeolites

Another common membrane material group is the crystalline-hydrated aluminosilicate minerals called *zeolites*. These crystalline materials are made of tetrahedral cations of Al and/or Si surrounded by four oxide anions. The units are linked to each other by sharing the oxygen ions in a three-dimensional polyhedral (cubes), hexagonal prisms or cubo–octahedral arrangements. These superstructures contain intracrystalline channels or interconnected voids and can be extended infinitely. The channels are partially filled with water that can be removed by heating (hence the name ζέω, meaning ‘to boil’ and λίθος, ‘stone’). The negative charges of the AlO₄ tetrahedra (SiO₄ is neutral) are counterbalanced by mobile cations (e.g. Na⁺, K⁺, Mg²⁺ or Ca²⁺) from nearby channels. Chemically, zeolites can be represented by an empirical formula M_{2/n}O·Al₂O₃·aSiO₂·bH₂O where *a* is between 2 and 200, *b* is the water trapped in voids and *n* is the valence of the metal cation M [77].

Zeolites were discovered in 1756, and for the first 200 years were used mainly in adsorbent applications. Some zeolites possess exceptional chemical and thermal stability, in addition to their catalytic activity and natural nanometric pore dimensions [78]. Starting from the mid-twentieth century, zeolites were synthesized in several industrial laboratories. Today, over 200 different families of zeolite frameworks are known [79]. These new compounds are used in numerous technological processes, including catalysis, adsorption, ion exchange and, of course, separation. That said, only a few zeolites and zeolite-like structures are useful in membrane separations (here we shall focus only on the applications of

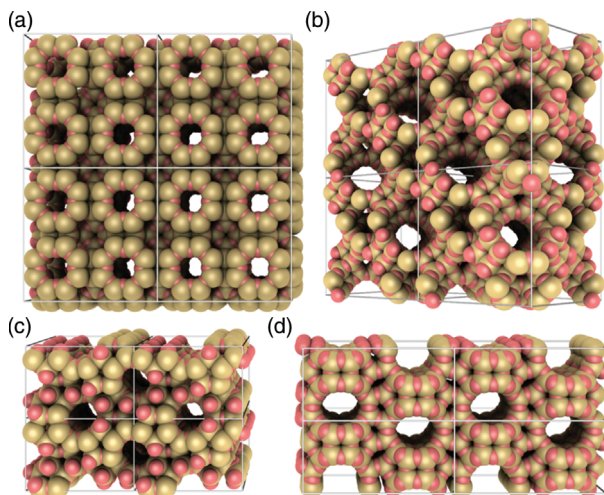


Figure 1.11 Three-dimensional simulations of four different zeolite structures (courtesy of Dr. David Dubbeldam): (a) Linde Type A (LTA). (b) Faujasite (FAU). (c) Zeolite SOCONY Mobil 5 (ZSM-5, MFI). (d) Zeolite beta (BEA).

zeolites as ceramic membrane components). Four of the most popular ones are Linde Type A (zeolite A, eight-ring pores of 0.30–0.45 nm), ZSM-5 (10-ring pores of 0.45–0.60 nm), zeolite Y (faujasite, 12-ring pores of 0.6–0.8 nm) and zeolite beta (see structures in Figure 1.11).

Zeolite membranes can be prepared as self-standing materials, as well as top layers for composite membranes. A recent trend is growing zeolite crystals during the synthesis of polymer membranes for a formation of metal-organic frameworks (MOFs) with tunable separation properties and permeability [80]. The self-standing zeolite crystals are typically first grown on a support such as Teflon that is removed after the synthesis. Membranes of this type are of interest in model studies of an ideal zeolite layer, but their practical applications are limited. This is because growing zeolite layers larger than few square centimetres is difficult, and the fragility of the structures prevents their industrial implementation. Usually, zeolite membranes are used as the top layers in a composite arrangement. They are prepared by crystallization followed by a substantial growth on the support. The crystallization is done on the surface and/or in pores without seeds for nucleation (the so-called *in situ* nucleation), or with seeds deposited on the support or in the vapour phase. This method gives structures that are reasonably defect-free (and the defects, even when they exist, are not much larger than the zeolite pores), so the only transport of fluids occurs through the zeolite pores. The inherent deficiency of zeolite membranes is the main transport mechanism. Compounds pass through pores by adsorption, making it difficult to maintain a steady-state operation as the zeolite becomes saturated with adsorbate. That said, the retention by adsorption can also be viewed as advantageous, as large-pore zeolites can combine high permeate fluxes with high

selectivity. Thermal stability up to 400–500 °C and resistance to organic solvents are additional advantages of zeolites over polymer membranes with same pore widths, facilitating their implementation. Zeolite membranes are often used in gas separation and catalytic membrane reactors at elevated temperatures. More details on these applications are given in Chapter 4.

1.9

Preparation of Ceramic Membranes

There are numerous methods for preparing ceramic membranes. These include structural leaching or sublimation of one component of a mixture, slipcasting, tape casting, extrusion, pressing, pyrolysis, sintering of suspensions that contain ceramic powders and various additives, sol–gel synthesis, hydrothermal treatment, anodic oxidation and chemical vapour deposition. This variety reflects the different raw materials that often dictate the method of choice. In many cases, different membrane layers are prepared from various materials using methods suitable for that specific material. The support layer is often made of α -alumina by extrusion, slipcasting or tape casting. This gives a ceramic membrane support with micrometre-size pores and millimetre-depth thickness. Then, intermediate layers are typically prepared from γ -alumina by dip coating the support layer followed by calcination. The number of intermediate layers depends on the grain size of the initial slurry and the degree of separation required (the intermediate layer is 300–400 μm thick and contains nanometric pores). Above these, the top layer, which determines the membrane's separation abilities, can be made from many materials using different methods. These include sol–gel synthesis of silica, titania and zirconia, chemical vapour deposition of silica, pyrolysis of carbon, SiC or Si_3N_4 , hydrothermal treatment of zeolites such as NaA and NaY, anodic oxidation of amorphous alumina and structural leaching of silica. In the following sections, we will outline the main methods of preparing ceramic membrane supports. Further discussion on the preparation of composite membranes for specific applications is given in Section 1.10.

1.9.1

Support Your Local Membrane

A membrane support has two seemingly controversial functions. It must make the membrane stronger without interrupting the transmembrane flow. The two are sometimes incompatible, because thick supports are stronger, but also more flow-resistant. Therefore, the support must be sufficiently thick, but also porous. The typical thickness of a membrane support is 1–2 mm and its typical pore size is on the order of micrometres. Support layers were mainly investigated back in the 1990s, and the current shortlist of widely used supports contains ceramics, ceramic composites and stainless steel. One of the main demands from supports

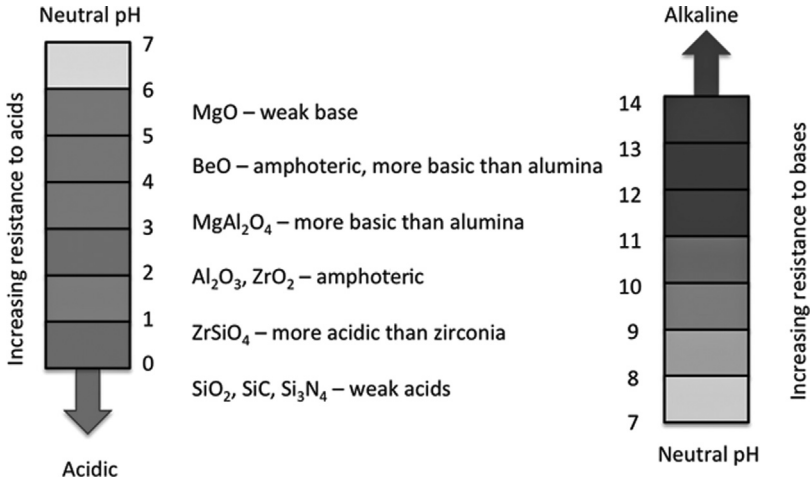


Figure 1.12 Relative resistance of various ceramic materials to acids and bases. (Drawn after Ref. [85].)

is good chemical and thermal stability. Alumina and silica are considered more thermally stable [82,83], whereas anatase titania and zirconia have a limited thermal stability due to their relatively low phase transition temperature [84]. Figure 1.12 shows the relative resistance of various ceramic materials to acids and bases.

Generally, the more acidic a ceramic is, the greater is its resistance towards acids, and vice versa with bases. If the ceramic material is more base resistant, it is more prone to acidic attacks. For example, silica, which is slightly acidic, has poor alkaline resistance. The chemical resistance may vary between allotropes. For example, α -alumina is very stable against strong acids and bases, but γ -alumina decomposes at $\text{pH} \leq 4$ and $\text{pH} \geq 9$ [86]. Titania and zirconia are considered very chemically resistant membrane materials, and yet enjoy only a limited success in manufacturing due to a highly sensitive (and therefore costly) synthesis procedure [87].

The majority of supports are prepared from α -alumina, which is cheap, commercially available, chemically inert, durable and withstands high pressures and temperatures [88]. Its two main disadvantages are its wide pore size distribution and the tortuosity of synthesized supports. As defect-free coating is not possible on surfaces with the average roughness of $1 \mu\text{m}$ and higher [30], α -alumina supports must be covered by intermediate layers that smooth the surface. Often, these intermediate layers are prepared from γ -alumina. They are less inert and increase the flow resistance, negating the advantages of α - Al_2O_3 support. Nevertheless, α -alumina is preferred over supports made from TiO_2 , ZrO_2 , CeO_2 , because the latter give higher flow resistance and might crack at high pressures. Stainless steel supports have some mechanical and manufacturing advantages, but they are even rougher than ceramic ones, and have a low compatibility with

coating ceramic layers. Their high thermal expansion coefficient can promote cracking at sintering or problems with adhesion of layers of the sintered support.

Ceramic supports are prepared by several sequential steps. The first is the formation and mixing of the initial slurry that consists of powder grains, solvent and chemical additives. At the second stage, the slurry is shaped by dry pressing, extrusion of ceramic paste or slipcasting or tape casting into the desired shape. These are typically disks, tubes, hollow fibres and honeycomb monoliths (see Section 1.4). Dehydration to evaporate water and drying at low temperatures to decompose volatile organics is the third stage of preparation. At the fourth stage, the consolidated slurry called the *green body* (GB) is sintered at high temperatures. Finally, the support is cooled and polished. Figure 1.13 shows the five stages in the preparation of a ceramic support. Details and highlights of each stage in the preparation are discussed below.

1.9.1.1 Forming the Initial Slurry

The formation of a ceramic slurry starts from a powder of inorganic particles such as Al_2O_3 . Other oxides such as TiO_2 and ZrO_2 can also be used, although their small sintered pores often cause a large flow resistance. The conventional method for preparing an α -alumina powder from bauxite by hydrothermal attack with NaOH was invented by Karl Josef Bayer in 1892 [89]. This method is highly efficient and the final powder contains 99.4–99.9% pure alumina. The remaining impurities, mostly SiO_2 and Fe_2O_3 , precipitate during sintering, thus increasing cavities within the ceramic construct and reducing its mechanical strength. The concentration of impurities can be reduced below 0.1% or even 0.01% using a modified Bayer process, but that has additional stages (and increased costs) [89]. Alumina powders can differ in their grain size, shape and size distribution. The differences in size and shape have more influence on the permeability and the mechanical strength of the sintered support [30]. Since a wide grain size distribution will result in undesirable large pore size distribution, the slurry is preferably made from monodispersed particles. When such a powder is not available or

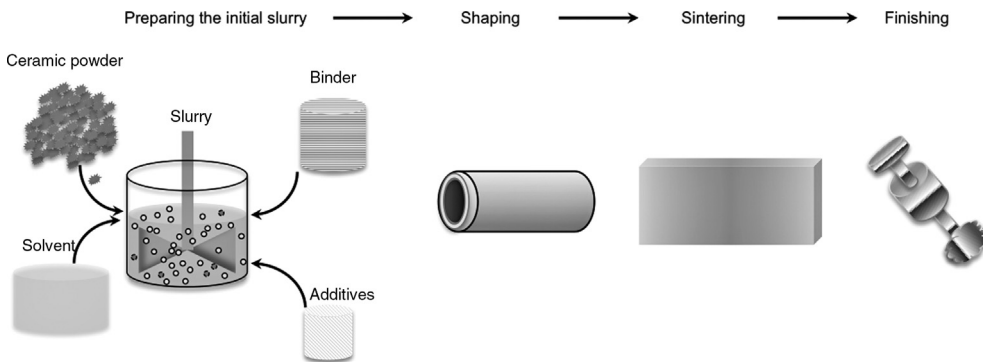


Figure 1.13 The five stages in the preparation of a ceramic membrane support layer.

prohibitively expensive, the fraction of particles with largest diameters is removed by sedimentation or by centrifuging. Small grains decrease the support's porosity and fluid permeability but increase the mechanical strength of the final sintered membranes. Several equations suggest the same empirical correlation between the tensile strength of a support σ_t and a grain size d_g in the form $\sigma_t \sim 1/\sqrt{d_g}$ [29]. A correlation between the pore size d_p and grain size d_g varies between 2:5 and 2:3. Thus, if the mean grain diameter is 1 μm , the pores will typically have a mean diameter of 400–660 nm [8]. This ratio, however, is influenced strongly by the shape of the grains [90]. Grains of 1–2 μm are the largest that can still ensure the formation of hard and dense membranes (using larger grains gives low-density macroparticle membranes). The 0.5 μm grains are the lower limit of the grain size, ensuring that the support permeability will be at least 10 times higher than that of the top layer.

Dense packing of particles in the initial slurry increases mechanical strength and decreases membrane permeability. A paste with higher density is less likely to shrink during sintering. The *packing density* is defined as a dimensionless ratio of particle fraction to the total slurry. An ordered packing with equal spherical particles can reach a packing density value of 0.74. The densest packing is achieved by an ordered (crystalline) stack of particles in parallel hexagonal layers forming the so-called Barlow packing (the highest coordination number of 12, theoretically predicted by Newton in 1694) at density $\rho = \pi/\sqrt{18} \approx 0.74$ [91]. Here the *coordination number* of a central particle is defined as the number of its nearest neighbours. Usual packing densities range between 0.58 (cubic packing type, coordination number 6) and 0.62 (orthorhombic packing type, coordination number 8). In ceramic supports, packing densities typically range 0.3–0.7 based on dry solid loading.

Ancient sellers sold dry grains (such as barley, oats and wheat) by volume and not by weight. And why did it matter? They increased their profit by an old trick. Pouring grains into a container with a stick inserted inside and slowly removing the stick can result in loose packing density of 0.55, increasing the seller's profit by approximately 10% [91].

Packing densities higher than 0.74 can be achieved by preparing the initial slurry from a powder that intentionally contains more than one grain size [74]. Figure 1.14 illustrates how, in this approach, the small grains fill the voids between the large ones, 'glueing' the large particles together without increasing the overall slurry volume.

The optimal size ratio determined through studies of various large/small grain arrangements is 0.155, wherein the small particle touches three neighbouring large particles (coordination number 3) [92,93]. There is no similar simple rule regarding the quantity ratio of large/small grains. Li reported that exceeding the optimal quantity of small particles forces large grains apart and no longer improves packing density [26]. In our experience [75], the dual-size grain approach has a small negative effect on the flux and a significant positive effect

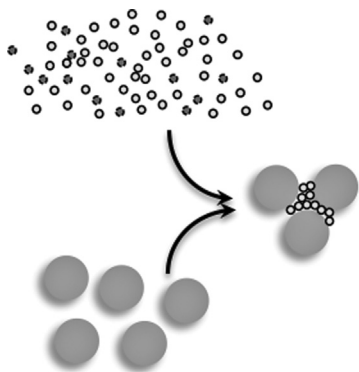


Figure 1.14 The increased packing density of slurry that intentionally contains particles of two different sizes.

on the mechanical strength. Adding 1 wt% of 13 nm particles into a powder of 0.85–1.0 μm $\alpha\text{-Al}_2\text{O}_3$ increases the mechanical strength by 16% and decreases the flux by 3% only, and adding 3 wt% increases the mechanical strength by 44% and decreases the flux by 6% [75].

The powder should be equally dispersed in a liquid before it can be consolidated into the so-called *green body* (sometimes also called a *green cast*; this term refers to an unfinished membrane before sintering that has its final form but not the ceramic properties, just like unripe fruit). A solvent is added to suspend the ceramic powder and dissolve additives and binders that form the initial slurry. The solvent should evaporate with no traces during the heating stage resulting in the formation of the GB. Water is the cheapest solvent. Using water, however, significantly increases evaporation time and may result in agglomeration due to hydrogen bonding [94]. Organic solvents such as toluene [95] and ethanol [96] dry faster than water, yielding GBs with a high density. The advantage of another popular non-aqueous solvent, trichloroethane, is its non-flammability, although it is also a VOC with adverse environmental effects [97].

The initial slurry of a powder and a solvent is milled or ultrasonically dispersed for uniformity. The exact homogenizing process depends on the viscosity of the slip, the time span allocated for the process, and the quantity of additives. During the homogenizing, grains constantly bump into each other. This bumping should not result in agglomeration. If the grains are already clustered, the homogenization should promote deagglomeration. Adding a deflocculant (sometimes also called a dispersant) increases the electrostatic repulsion or the steric hindrance of two particles in aqueous and non-aqueous suspensions, respectively, thus preventing agglomeration. Deflocculants coat ceramic particles and prevent a direct contact between them. The positive influence of a deflocculant increases as the size of powder particles decreases. Popular deflocculants for aqueous suspensions are relatively inexpensive soda ash, polyacrylates [94] and sodium silicates [95]. The advantage of polyacrylates is their relatively low

molecular weight that affects the stability and rheology of aqueous slurries. Polyethyleneimines [96], menhaden fish oil, phosphate ester and glyceryl trioleate [10] are popular dispersants for non-aqueous mixtures. Li lists 27 dispersants for use in organic solvents, mostly fatty acids and esters [26]. There is an optimum in the concentration of the dispersant in the slurry. For example, Sarraf and Havrda [98] report an optimal 0.5 wt% of a dispersant to stabilize the alpha alumina ($\alpha\text{-Al}_2\text{O}_3$) slurry.

Solvent evaporation during the drying should not affect the plasticity nor the mechanical resistance of the GB. Binders and plasticizers are added to maintain GB shapes before drying, and to prevent cracking at sintering. These are typically long-chain polymers with a backbone of covalently bonded carbon–carbon linkages with different side chains. They either physically wet the powder grains or chemically adsorb organic functional groups on the grain surfaces [99]. A good binder should strengthen the GB, improve lubrication, be inexpensive, non-toxic and decompose completely at 300–500 °C leaving no ashes. Onoda [100] indicated three possible locations of binder in GBs that are redrawn here in Figure 1.15. Poor wettability (Figure 1.15a) results in no glue between grains. Too viscous a binder completely covers the grains (Figure 1.15c) preventing the attracting interactions between near grains that are crucial at the end of drying and beginning of thermolysis. A wetting (pendular) state (Figure 1.15b) where the binder is located at the neck intercept (a junction of few grains) is the desirable one, promoting formation of particle clusters linked by ‘liquid necks’ [101]. Thanks to the repulsion between near clusters, the pore structure remains open and the pores become smoother and rounder. The exact structure depends on the binder used and its quantity, particle size and shape and the number of particle interactions.

In a sense, the perfect binder is ‘the last line of defence’ that decomposes later than any other additive, leaving voids that change their form and dimensions during sintering [102]. The open voids are the membrane pores in the final support structure. Pore sizes can be governed by the molecular weight of binder molecules [103] and the pore density by the binder concentration. The optimal concentration should be as low as needed to prevent cracking, and at the same time reduce pore size distribution (a narrow pore size distribution is more valuable in separation). Adding more than 10 wt% binder increases the pore size distribution [104], promotes particle agglomeration in the slurry and results in the formation of closed pores [105]. But burning out green bodies that contain more than 10 wt% binder is more difficult. Many polymers can be used as binders. Examples

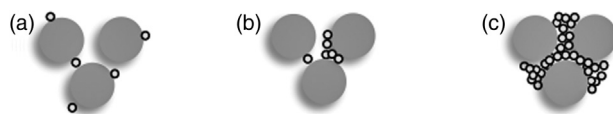


Figure 1.15 Location of a binder between slurry grains: non-wetting liquid (a), good wetting, perfect binder position (b) and viscous liquid (c). (Drawn after Ref. [90].)

of non-aqueous suspensions include polyvinyl butyral (PVB) [97], polyvinyl acetate (PVAc), poly(propylene carbonate) (PPC), poly(butyl methacrylate) (PBMA) and poly(methyl methacrylate) (PMMA). For aqueous suspensions, the commonly used binders are poly(ethylene oxide) (PEO)/poly(ethylene glycol) (PEG), starch [106], polyvinyl alcohol (PVA) and cellulose ethers (methyl cellulose, hydroxyethyl cellulose) [107]. Long-chain linear polymers in aqueous solutions ensure binder solubility. However, adding a binder is not the only method for creating porosity during sintering. The idea of sacrificing molecules or particles for the generation of voids can be realized with the addition of sawdust, coal, spongy polymers such as cellular plastic, latex [108] or foamed polyurethane [109].

Plasticizers are low-molecular-weight polymers that are typically added with the binder to the initial slurry. A plasticizer penetrates into the binder, improving its distribution in the slurry. This softens the binder, increasing flexibility and lowering the glass transition temperature [99]. The plasticizer also lubricates, allowing a slide movement of neighbour binder molecules, thus increasing the flexibility of green body and reducing cracking [110]. Adding a plasticizer might increase the surface area, the pore volume and the pore diameter of the final ceramic membrane [111]. Plasticizers are more common in tape casting where the flexibility of the tape is important. Popular plasticizers in aqueous suspensions are ethylene glycols and glycerol [112]. Polyethylene glycols [113] and dibutyl-*o*-phthalates [94] are often used in non-aqueous suspensions.

Lubricants are sometimes used in addition to the plasticizers to help withdraw green bodies from their moulds during slipcasting [114]. Wax emulsions [95] and ammonium stearates [115] are often used in aqueous suspensions, while stearic acids are used in non-aqueous suspensions.

The addition of dispersants plus mechanical stirring can give foam that can cause cracks or abnormal pores in the green body and/or later in the membrane. Antifoam agents may either prevent or destroy the foam by forming a monomolecular hydrophobic layer over the slurry surface and reducing the surface tension [116]. Interestingly, sometimes the foaming itself is used as for producing highly porous ceramics with very large pores (50 μm to 5 mm) [117].

Magnesium oxide (MgO) or yttrium oxide (Y_2O_3) are sometimes added as a material that will melt before the matrix phase in liquid-phase sintering, or to obtain dense membranes with low pore size distribution in solid-state sintering. The former is used to help sinter materials such as Si_3N_4 , WC and SiC. According to Dörre and Hübner [118], MgO prevents the discontinuous growth of the grains as the pore will become part of the grain, the diffusion distance between the grains will significantly increase and the pore will not shrink. Other relatively rare additives that impart specific ceramic membrane properties promote porosity, water retention and antistatic properties or act as fungicides/bactericides [26]. Figure 1.16 summarizes different studies and shows the percentage of each ingredient in the initial slurry [119]. The majority of green bodies were prepared with 60–80 wt% ceramic powder, 20–40 wt% water and 0–20 wt% organics (mainly binder or plasticizer). Table 1.5 summarizes and clarifies main functions of each additive in the initial slurry.

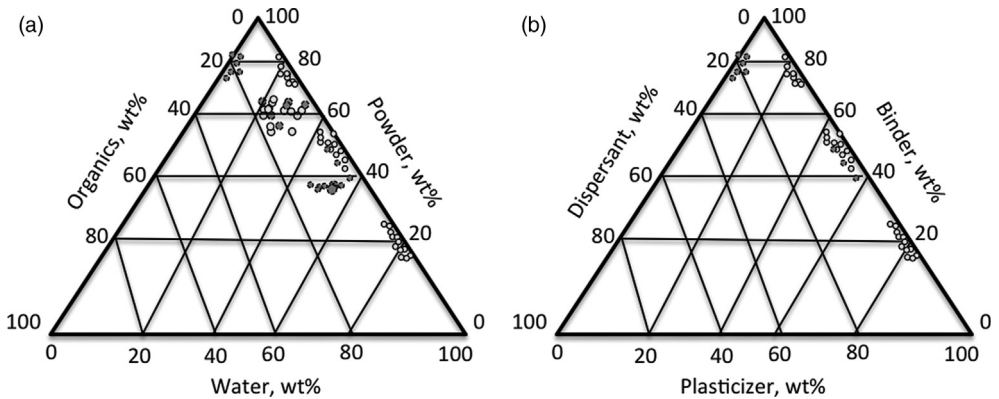


Figure 1.16 Ceramic slurry content [119]. (a) The diagram presents wt% of solvent, organics and ceramic powder in ceramic slurry summon from different studies. (b) The diagram presents the wt% of organic content (binder, plasticizer and dispersant).

1.9.1.2 Mixing and Pugging

Using the right grains and additives is important, but composition is not the whole story. The order on which the ingredients are added, mixed and pugged is essential to prevent voids that might lead to membrane cracking at later stages. Here (unfortunately) there are no hard-and-fast rules. Obtaining a good homogeneous paste is an empirical process, closer to art than to science. Indeed, in our research for this book, we were amused to learn that practically all

Table 1.5 A summary of the functions of additives in ceramic processing.

Additive	Function
Common	
Solvent	Suspends the ceramic powder and dissolves additives and binders that form the initial slurry
Deflocculant/dispersant	Increases the electrostatic repulsion or the steric hindrance of grains in aqueous and non-aqueous suspensions, respectively, and prevents aggregation
Binder	Maintains green body features and prevents cracking at sintering
Less common	
Plasticizer	Penetrates into the binder to structurally expand it and improve its distribution in the slurry
Antifoam	Prevents or destroys foam
Lubricant	Helps in releasing the green body from its mold
Chelating agent ^{a)}	Inactivates undesirable ions
Fungicide/bactericide ^{a)}	Stabilizes against degradation with ageing

a) From Ref. [120].

companies that make ceramic membranes have a few experienced employees who are the only ones who can determine the correct conditions for the paste. Typical protocols start from a dissolution of a known quantity of a dispersant in a certain volume of solvent by stirring or by rolling [26]. The percentage of grains added at the next stage depends on grain size and the ability of the dispersant to keep the final mixture deagglomerated – more grains can be added when an efficient dispersant is used. If several grain types are used, they are mixed first. Adjustments to the solid loading are often a question of experience. Organic additives are added after the grains starting from a most hygroscopic one [90]. Usually it is first plasticizer and then binder. The slurry is then well mixed, and the mixing efficiency depends on the viscosity, amount of deflocculants and time [90]. Insufficient mixing results in the formation of aggregates and cracking at later stages. Table 1.6 compares the three popular mixing techniques.

During the mixing, the slurry can trap air bubbles that must then be removed, usually by partial vacuum and a gentle stirring. Air bubbles can lead to cracking at the sintering step.

In tape casting and slipcasting, the paste is shaped quickly to avoid premature drying and ageing that can result in phase separation, formation of agglomerates and cracking at sintering. In extrusion, the order of addition can change and organic additives sometimes are added before a solvent [90]. The quantity of added solvent is optimized empirically. Too little solvent will not give good extrusion. Too much solvent will result in soft suspensions unsuitable for shaping. Adding a solvent gives a viscous slurry that is kneaded into a plastic consistency. This is called *pugging* and is done for a short period with high intensity. The resulting paste is aged for several days prior to extrusion.

Table 1.6 Slurry mixing techniques.

	Description	Mixing time (h)	Advantages	Disadvantages
Ball milling	A rotating container that hosts the slurry mixed by inert parts (e.g. metal balls) moving inside it	6 [121], 12 [122], 20 [123], 24 [124], 48 [125]	Applicable on large scale and at different stages, cheap	Noisy, long mixing time
Ultrasonic milling	The sonication results in high- and low-pressure cycles, promoting cavitation	0.25 [126], 0.16 [127]	Very short mixing time, high homogeneity	Very strong – can break the grains, harmful noise
Magnetic stirring	A rotating magnetic field turns a bar that quickly mixes the slurry	24 [128–130]	No noise, immersed magnets are inert and easily cleaned	Inapplicable on large scale, used in non-viscous suspensions only

1.9.1.3 Shaping the Slurry

Now the paste is ready to be shaped into one of four membrane geometries. The choice between plates, tubes, hollow fibres and honeycomb monoliths will determine if the slurry will be shaped by dry pressing, extrusion or slip/tape casting. Dry pressing is done in a special press. Typical pressures exceed 100 MPa and give a dense layer approximately 0.5 mm thick. This method is limited by the size of the press and is often used in fundamental research for optimizing ceramic membranes. Typically, one studies the effects of particle size, binder quantity, applied pressure and sintering temperature on pore size distribution of ceramic supports [129–131]. Small discs, a few centimetres in diameter, are the most common membranes made by dry pressing.

Extrusion is done by forcing the paste through a small opening (an extruder) with the help of an endless screw (in industry) or a piston (in the laboratory). The speed of extrusion and extrusion pressure vary and should ensure the formation of homogeneous tubes [90]. Typical extrusion rates range between 10 and 60 rpm of a screw barrel [132], at 10–15 bar. To avoid paste separation and excessive drying of the solvent, the extrusion is performed at room temperature and high partial pressure of the solvent (up to 80% relative humidity [132]). The geometry of extrusion nozzle (number of channels and their diameter) may vary and result in the generation of mono- and multichannel tubes. Tubular geometries are suitable for large industrial installations. Extrusion in ceramic membranes is similar to spinning in polymer ones, except for the presence of coagulation bath and one-step process in the latter [26].

Tape casting and *slipcasting* are used for preparing flat membranes and discs. Figure 1.17 depicts a tape casting process (the so-called *doctor blade*) for large-scale fabrication of ceramic supports and multilayered structures.

The paste is poured into a reservoir behind a casting knife and cast onto a stationary or moving surface passing through a blade [119]. In laboratory applications, the surface is fixed and the doctor blade moves at a controlled speed to ensure the uniform thickness of the tape. This gives tapes of up to 0.5 m width, 2 m length and 1–2 mm thickness [90]. Industrial ceramic supports are based on the moving surface, such as endless stainless steel, glass coated with silicon oil or polymer film belt (e.g. polyethylene) and a fixed doctor blade. The thickness of the slurry is controlled by adjusting the gap between the blade and the surface. Other important parameters include the reservoir depth, paste viscosity and carrier speed [26]. The usual casting speed is 0.1–1.5 m/min, depending upon the surface length, drying time and tape thickness. The typical thickness is a few millimetres, although membranes a few micrometres thick were also reported. The length can reach 40 m [90]. The tape is then dried by passing through a tunnel, peeled from the moving surface and rolled for storage. Supports prepared by tape casting are usually smoother, with fewer defects. Tape casting is a favourable method for preparing multilayer membrane structures where the intermediate and top layers are easily coated on a flat support.

Slipcasting is much simpler. Here, neither a doctor blade nor a moving tape is used. Instead, the slurry is poured directly into porous moulds of a desired

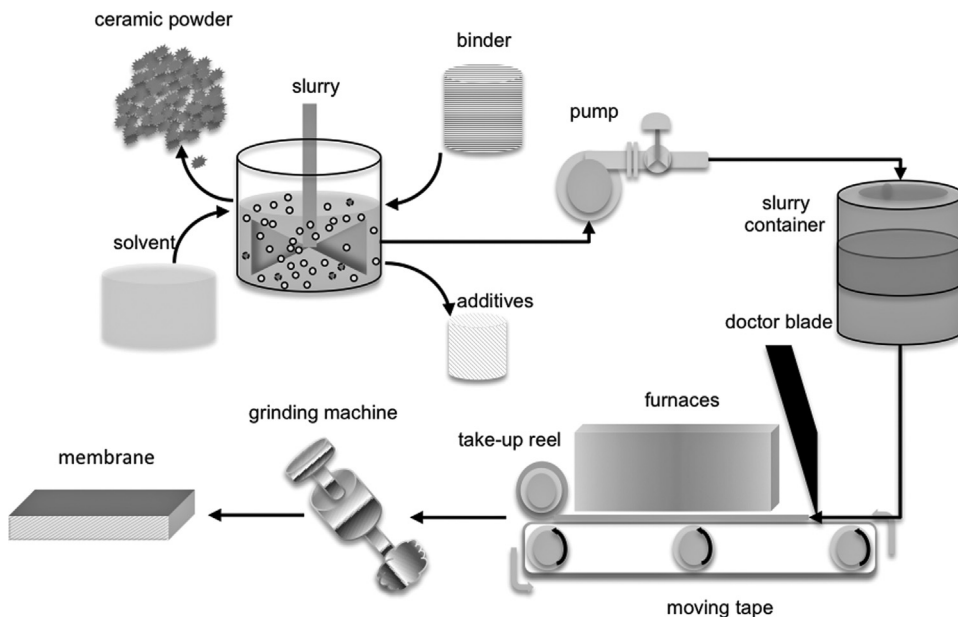


Figure 1.17 A tape casting process for large-scale fabrication of ceramic supports and multi-layered structures.

shape. The paste is sucked into the mould by a capillary action and fills all available space within the mould structure. The depth of penetration of a paste into the mould structure increases with time. Figure 1.18 shows that the shape of the final membrane is limited only by the mold shape. The disadvantage of slipcasting is the large number of intermediate steps, including pouring the slurry into a mould and peeling a green body when the desired shape is achieved. In addition, the casting time is usually long and the membrane thickness is usually high and more difficult to control.

1.9.2

Drying and Thermolysis

Drying, thermolysis and sintering are the three stages of heating that give the membrane its final properties. All three procedures are performed at different temperatures and with various heating ramps, as can be seen in Figure 1.19.

Drying is the initial heating stage that evaporates the solvent while keeping the grain network in order. It can be done at room temperature or at elevated temperatures. Drying at room temperature requires no energy for heating but takes significant time (up to few days). Industrial membrane producers usually dry at higher temperatures. The drying should remove the solvent, and yet keep organic additives, such as binders and plasticizers, in the bulk. These will be

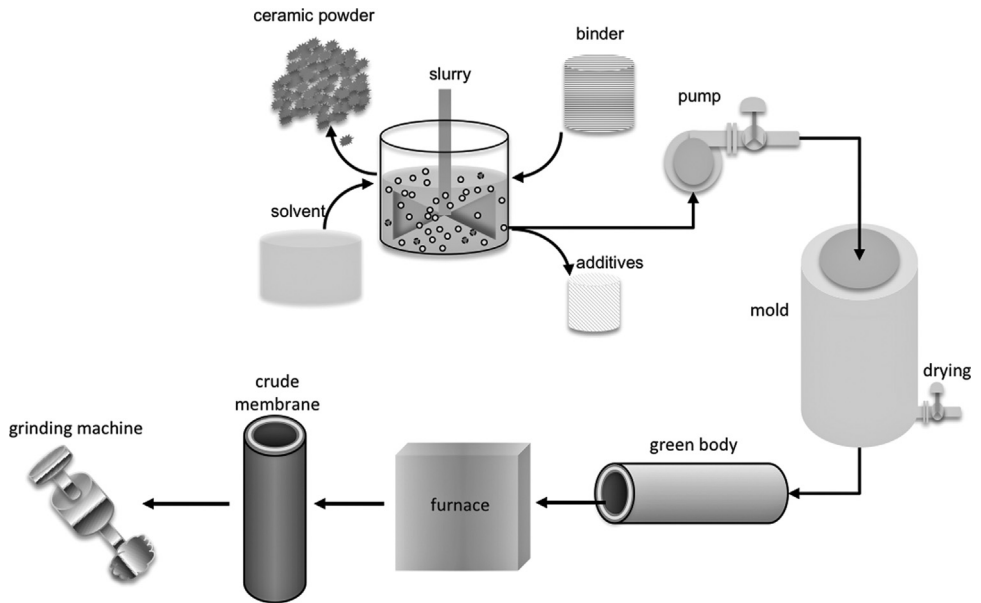


Figure 1.18 Various stages of ceramic membrane preparation by slipcasting.

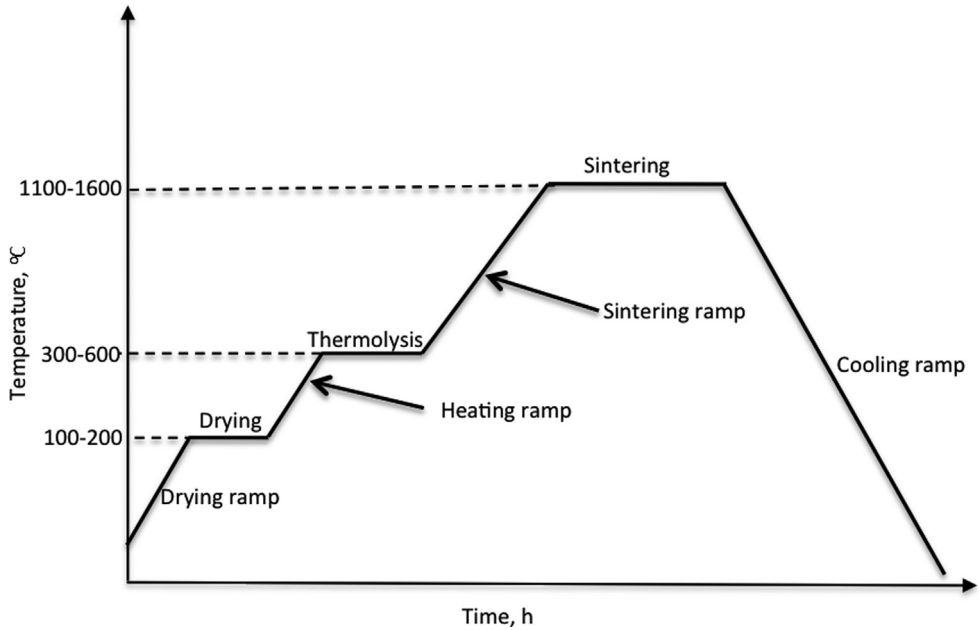


Figure 1.19 The three stages of heating – drying, thermolysis, sintering – in the preparation of ceramic membranes from the green body.

evaporated at the thermolysis stage, when no significant changes in the grain spatial arrangement are expected.

Concurrently, grains are moving closer to each other until they come into direct contact. The ceramic body shrinks to what will become the final membrane structure. At the membrane–air interface, the solvent changes its form from a flat to a meniscus, minimizing the liquid–vapour contact area. The evaporation rate decreases since evaporation from a curved interface is lower than that from a flat surface. The first falling rate period continues until the solvent maintains its continuity. When the solvent becomes disconnected (slurry saturation less than 10%) and remains only at the ‘necks’ between grains, the second falling rate period begins [99]. The solvent attached to the grains (e.g. by hydrogen bonds if the solvent is water) is removed by decomposition at higher temperatures rather than by evaporation from the slurry surface. During the second falling rate period, the slurry can be heated as no additional shrinkage is expected. The heating only results in a weight loss [90]. At the end of the drying, the slurry obtains its initial shape including the pores. The resulting green body has the desired shape, but it is still weak. At this stage, the process is still reversible, and immersing the green body into the solvent will dissipate it back into the initial slurry.

Now we are ready to eliminate binders and plasticizers by thermolysis (degradation at high temperatures). Note that thermolysis has been identified as a separate stage only lately [26]. Previous reports describe thermolysis as a part of the firing or sintering stage [90]. The exact binder elimination is a complex process that combines chemical and mass transfer phenomena. It was and still is a subject of many fundamental and practical studies. Due to its complexity, the thermolysis scheme (temperature–time–heating rate–atmosphere) is based on one of two extreme hypothetical practices. One uses a slow heating ramp (the increase of heating temperature from drying to thermolysis), low temperature at heating plateau (the heating at the constant temperature) and a long heating period. The other is rapidly passing from drying to thermolysis that is performed at high temperatures for short time periods to achieve the maximum weight loss rate. The latter is determined using thermogravimetric analysis (TGA). The difference can be as significant as between 1 and 20 °C/min, 300 and 600 °C, hours and days [133,134]. Both approaches aim at complete removal of binders and plasticizers by decomposition into volatile organic compounds (VOCs) and carbon residues. Many mechanisms can initiate this decomposition, although thermal and oxygen-induced degradations are the most common ones [135]. The diffusion rate is higher in gases than in liquids and therefore keeping the interstitial pores open will likely result in uniform heating, fast decomposition and removal of VOCs with no residues. Still, the proper heating rate should balance between massive gas production and diffusion during the binder degradation. Sometimes this is impossible, and the thermolysis generates involatile carbon and bubbles that cause cracking at the sintering stage.

Thermolysis of thermoplastic binders can lead to bubble formation, while that of thermoset binders can cause cracks in the final membrane [134]. Polyvinyl

butyral [97], polyvinyl alcohol and polyvinyl acetate are eliminated by side group elimination (a scission of the pendant groups attached along the polymer chain backbone [99]). PPC, PBMA and PMMA are decomposed by depolymerization, giving monomeric volatile products. PEOs and PEGs are decomposed by random scission, producing a spectrum of molecular fragments [99]. Side group elimination and random scission, as well as the thermolysis of cellulose ethers (e.g. methyl cellulose and hydroxyethyl cellulose [107]), often incurs side reactions such as cyclization and cross-linking [136]. This gives highly branched, non-aromatic carbon residues that are involatile at elevated temperatures (up to 1000 °C) under oxygen-deficient conditions. These carbons stay inside the green body, and removal requires an oxidative atmosphere. The organic weight loss passes through regions of rapid elimination of 70–80 wt% at 200–350 °C and final weight loss (20–30%) of carbon residues due to the oxidation (basically, burning under air).

The formation of non-volatile compounds is more likely at higher binder concentrations, and these are linked to the shaping method used. Dry pressing and slipcasting require less plasticity and, therefore, use less binder (up to 10 wt%). Tape casting (3–17 wt% binder) and extrusion (7–20 wt% binder) are built on a continuous paste. These high concentrations are likely to leave the interstitial volume full with binder, even after drying. The VOCs must exit through pores completely filled with binder, unlike the quick escape of VOCs through open pores at low binder concentrations. Moreover, the moving heating front will not be planar, resulting in different heating regimes for different green bodies. The formation of non-volatile carbon residues over a broad temperature range is more likely. This uneven heating can lead to bubbles when local temperatures exceed the boiling point of the solvents and plasticizers yet remain under the binder's boiling point.

The thermolysis of green bodies with high binder content is problematic, and must be avoided. One simple solution is using less binder. Keeping the ratio of binder to particle volume below 0.08–0.15 will leave the pores open [137]. Alternatively, you can use more plasticizers that will evaporate at low temperatures, thus leaving interstitial pores open to the fast escape of VOCs, combining this with low-viscosity binders and high volatile diffusivity (which generally depends on molecular weight). You can also limit the formation of non-volatile carbon by making lighter green bodies. This can be done by using larger powder grains. Finally, minimizing the diffusion path by reducing the thickness of the green body may also help.

1.9.3

Sintering

We now approach the most important stage in the formation of ceramic membranes. Sintering is, in fact, one of the oldest technologies used by man to produce dishware, storage cans and iron tools. It is also the last process step where the microstructure of the final ceramic can be changed. The word 'sinter' comes

from the Middle High German *Sinter* and is similar to the English ‘cinder’. Technically, sintering is a process that uses thermal energy to produce consolidated materials from ceramic or metal powders. There are two consolidation types: *General consolidation* gives a dense polycrystalline solid (also called a *compact*). Conversely, *local consolidation* affects only a limited number of grains. Among the four categories of sintering (solid-state, liquid-phase, viscous sintering and vitrification), we will focus only on *solid-state sintering*, the most commonly applied method in membrane preparation. The solid-state pressure-less conventional sintering (we will call it simply sintering) is the heating of a green body to a temperature that is between 0.5 and 0.9 of the melting point of the grains in the absence of a liquid [26]. This sintering is different from liquid-phase and viscous sintering that are done in the presence of 3 and ~25% of liquid, respectively,¹⁾ and from glass vitrification which is performed at or above the softening temperature [138]. It is also performed without additional pressure, unlike pressure sintering that uses hot pressing. Solid-state sintering is the most attractive sintering method for making ceramic membranes, because it is effective, simple and cheap.

Kinetically, sintering is often divided into initial, intermediate and final stages. This division is arbitrary. Each stage is described by a simplified model, such as a two-particle model at the initial stage, the channel pore model at the intermediate stage and the isolated pore model at the final stage. According to the two-particle model, at the initial sintering stage, two neighbour grains develop a solid neck between them and become a new united cluster. This happens as soon as the heating temperature gives atoms, ions and atomic clusters within a grain some degree of mobility. Actually, some mobility exists at any temperature above absolute zero. However, there is a difference between an elementary jump process of an atom between two neighbour sites and the succession of steps that lead to a macroscopic diffusion. An elementary atomic jump takes $\sim 10^{-13}$ s [139] and it is much quicker than the mean residence time of an atom on a lattice site. This elementary jump is chaotic and cannot be described in terms of diffusion. Generally, nine consecutive moves in one direction are considered as a meaningful movement of atoms that result in their relocation. Atoms will hop from one to a nearby vacant site if vacancies (point defects) are available,²⁾ or will detach from a grain for a further attachment due to Brownian motion. The latter mechanism is called evaporation/condensation, and is different from diffusion, which occurs entirely within a discrete grain.

The consolidation of two grains during sintering covers three types of diffusion that differ in the start and end points of their path. If the start and end points and all vacant sites are on the grain surface, the diffusion is called a *surface diffusion*. If the start and end points are on the grain surface, but the vacant

- 1) The high percentage of liquid at viscous sintering results in the full densification of a compact in the grain–liquid mixture. The liquid-phase sintering is also called a transient sintering as the liquid is present only at the initial stages of sintering and disappears at advanced stages, so the densification is completed in the solid state.
- 2) The number of vacancies increases exponentially with an increase in the temperature.

sites are within the grain volume, the diffusion is called a *lattice diffusion*. Compressive stresses on the grain boundary were suggested as an alternative mechanism for the atom ordered movement, although they are still marked as lattice diffusion [140]. If atoms move from the grain volume to its surface, it is called a *plastic deformation* (in this case it is also irreversible). The latter is considered unimportant in pressure-less sintering [140].

Practically, sintering can be viewed as a rearrangement of atoms on surface grains. In all three diffusion types, the number of vacancies increases exponentially at higher temperatures. Other factors that influence the diffusion are the partial pressure, the impurity and the type of the diffusion path. The vacancy diffusion flux depends on sintering temperature and diffusion path (surface or lattice). Similarly, the impurity diffusion path will depend on the quantity and type of the impurity. The overall sintering rate will depend on the slower diffusing ion, due to both diffusion rate and availability of defects. In α -alumina, the sintering rate is determined by the aluminium while oxygen rapidly diffuses on grain surface [118]. Some studies also distinguish between surface and lattice diffusion on the grain and on the intercept of two grains [138] to forecast the speed of neck formation. Figure 1.20 shows the various atom transport mechanisms during the three sintering stages.

According to Ashby, at each moment there is only one dominant transport mechanism [141]. Although the so-called *Ashby diagrams* vary in terms of green body materials and sintering conditions, the general trend is that after a preliminary adhesion, the initial stage of sintering is mostly influenced by the grain boundary diffusion. If the sintering is done at the same temperature, the grain boundary diffusion is followed by surface diffusion. Conversely, if the sintering temperature is raised at intermediate and final stages, lattice diffusion will dominate. Many Ashby diagrams also predict the kinetics of neck growth as the function of the grain diameter. This prediction is based on previous laboratory

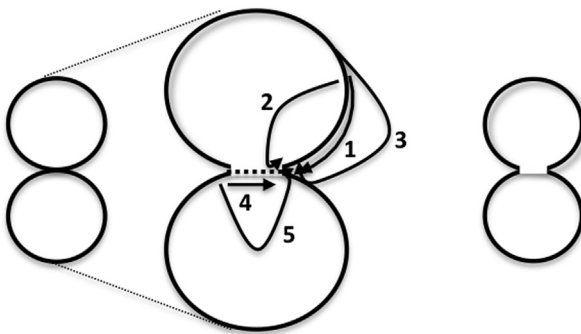


Figure 1.20 Three stages in sintering: (i) the initial neck contact; (ii) the subsequent growth; (iii) the final form formation. 1: surface diffusion; 2: lattice diffusion from the grain surface; 3: vapour transport; 4: grain boundary diffusion; 5: lattice diffusion from the grain boundary. (Drawn after Ref. [26].)

measurements and on *Herring's scaling law* that predicts the kinetics of diffusion as a function of the dominant diffusion mechanism. The relation is given by

$$\frac{t_2}{t_1} = \left(\frac{R_2}{R_1} \right)^m, \quad (1.14)$$

where R_2 and R_1 are sizes of powder grains with t_2 and t_1 sintering time periods, and m is an integer that corresponds to a transport mechanism ($m=2$ evaporation/condensation; $m=3$ lattice diffusion; and $m=4$ surface diffusion³⁾). According to this law, the transport by diffusion is much faster than by evaporation/condensation, and sintering of fine particles is much faster than of large ones.

An increased movement of atoms results in more frequent collisions. The driving force for sintering comes from the excess free energy that exists in powder compacts due to the annihilation of the solid–vapour interface. The enthalpy of the entire system decreases as the energy required for forming new solid–solid bonds at the neck between two grains is lower than the energy released at the annihilation of solid–vapour interface. A necessary condition for sintering is that the gain of the elimination will be larger than the loss of the generation. The formation of a neck decreases irregularities on grain surfaces, reshaping them into perfect spheres but not necessarily shrinking or compacting the entire matrix. The densification at this stage is small, around 2–3%. A considerable densification (up to 90% relative density) occurs at the intermediate stage. At the end of the intermediate stage, the compact contains only irregular isolated pores. These pores contribute up to 7% relative density and they are eliminated at the final stage. As a rule of thumb, the initial stage is said to continue until the distance between two opposite points on the concave neck curvature will reach 0.3 of a grain diameter.

At the *intermediate stage*, the neck continues to grow and evolve into a 3D structure of solid particles and continuous channel-like pores. This evolution can take two pathways: In the first, a grain or a cluster of two grains can grow as a separate unit when the surface diffusion and vapour transport lead to the rounding of particles and growth of necks. The migration of grain boundaries leads to increased grain and pore sizes, the latter due to pore coalescence. This process is called *coarsening*. It increases the diffusion path for atomic transport, thus reducing the sintering rate. The final compact will have an increased porosity along with lowered density. In the second pathway, clusters can evolve into 3D structures by developing necks with other grains by a process called *densification* immediately at the beginning of the intermediate stage. The dense membrane will have fewer open pores. As the intermediate stage occurs at high temperatures, there is no direct evidence of the exact evolution path. The exact pathway is discussed in a frame of one of two main theories. According to the first [142], the intermediate stage begins from coarsening that is a necessary step towards the densification. The theory is built on the Ashby diagram that states that the grain boundary diffusion is the ultimate initial stage. Following the

3) $m = 1$ corresponds to viscous flow in metals.

diagram, the sintering at constant temperature will lead to coarsening, but will not consolidate the compact [138]. Raising the temperature will lead to consolidation, shortening the required sintering time.

Alternatively, the second theory proposes that grain growth and densification are two parallel processes that are linearly related to each other [143], both eventually resulting in a compact. The two processes are necessary for the continuous densification during sintering. One weakness of this view is that experimental observations show unequal grain growth. While one assumes that all grains are grown by a simple and invariable increase of the grain size with time, the experiments report a quick formation of some exceptionally large grains in the matrix of fine grains with a very slow growth rate. The formation of the abnormal grains is explained by Ostwald ripening that postulates that in the event of uneven distribution of grains, there is a critical grain radii r^* . Grains with radii larger than r^* will grow and those with radii smaller than r^* will dissolve, 'feeding' the large particles with atoms and cluster building blocks. Such a bimodal grain size distribution is opposite to the unimodal distribution required for linking grain growth and densification. At the end of the intermediate stage, the channel-like pores break down into separated voids [138] that are eliminated at the *final stage* [26]. This stage, however, is not relevant to the ceramic membranes field and will not be discussed here. Figure 1.21 shows the sintering of a ceramic membrane showing the development stages of the final membrane structure.

The exact outcome of sintering is not known *a priori*, and the process is usually based on trial and error. However, certain variables have a proven effect on the final membrane. We divide these into two groups: green body parameters and operational variables. The first group includes, in addition to the grain size, shape and size distribution, the degree of agglomeration, the mixing of the slurry, the starting porosity, the chemical composition of the powder compact, the degree of homogeneity (presence of impurities) and the binder amount. These parameters will also determine the coarsening/densification competition at the intermediate sintering stage. The second group (operational variables) in

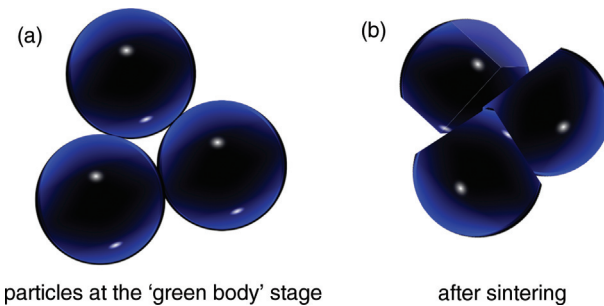


Figure 1.21 Development of a final membrane structure (b) from a green body (a) during sintering of a ceramic membrane.

pressure-less sintering includes temperature and time. We will describe the influence of some of these parameters in the next section, together with a few tested and proven recipes for sintering ceramic membranes.

1.9.3.1 Sintering Variables

Temperature is one of the most influential parameters. Historically, the lack of programmable furnaces has limited the flexibility in sintering. Today, however, any sintering temperature can be set, and any sintering regime programmed. The flexibility in controlling these two features gives endless variations of the sintering protocol. Here we describe general experimental observations regarding the temperature and the sintering regime (exact sintering protocols are often kept as a trade secret by manufacturers).

As a rule of thumb, the sintering temperature is set at 0.5–0.9 of the melting temperature (see above). This offers a wide range of sintering temperatures between 250 and 1700 °C. Table 1.7 gives the sintering temperatures of selected ceramics.

The exact sintering temperature depends on many factors, including the required target density and porosity, the presence of impurities, the sintering time and the intended service temperature. Short sintering times require high temperature and better furnaces, and the sintering temperature should be well above the service temperature. In general, sintering at high temperatures promotes densification and depresses coarsening but also increases the production cost. Sintering of α -alumina at 1550 and 1800 °C results in the formation of membranes with 4 and 2 μm average roughness (R_a), respectively [30]. A dense membrane has smaller grains and reduced porosity. This often results in superior mechanical strength and low transmembrane flux. Lowering the sintering temperature will generate membranes with high porosity and low mechanical strength. Since the ideal membrane should have both a high mechanical strength and a high flux, the sintering temperature must be optimized. This optimization, however, is not that simple. Using mid-sintering temperatures might result in the formation of a bimodal pore size distribution with a fraction of large pores. The presence of a transient stage has been reported in studies on the influence

Table 1.7 Recommended sintering temperatures of several ceramics.

Ceramic	Sintering temperature (°C)
Alumina porcelain	~1250
Quartz porcelain	~1300
Steatite	~1300
Cordierite	1250–1350
Aluminium oxide	1100–1600
Recrystallized silicon carbide	2300–2500
Sintered silicon carbide	~1900

of sintering temperature on pore size distribution in aluminium oxides [144]. A monomodal pore size distribution at 1000–1200 °C changes to a bimodal pore size distribution with a fraction of large pores at 1300–1400 °C and pore shrinkage at 1500–1600 °C. Microcracks were formed at temperatures of 1700 °C and above due to proximity of a melting point of aluminium oxide. The mechanical strength constantly increases in the entire sintering range until temperatures above 1700 °C, where the membrane loses its ceramic properties.

Many protocols recommend sintering with a gradual increase of temperature. This saves time and promotes densification instead of coarsening. The sintering temperature is usually increased by a constant increment over time, called the *sintering rate*. The final compact is cooled back to the room temperature with a certain *cooling rate*. Sintering and cooling rates are measured in degrees per minute, and can acquire values between 0.1 and 1000 °C/min. Typical heating rates are 2–15 °C/min. Steep sintering rates promote the formation of dense membranes due to a short time spent at low temperatures. The concept of fast sintering (also known as *fast-firing*) arose from adjustments to the sintering rate targeting the maximal densification at minimal coarsening [145]. In line with the rate-controlled approach, the green body is heated quickly to the sintering temperature, held at the constant sintering temperature plateau for a certain time period to allow consolidation and then cooled down with a certain cooling rate. A short processing time and reduced energy consumption are two economic benefits of steep sintering and cooling rates. The risk is the possibility of cracking of the final compact by a thermal shock caused by a fast temperature change. Slow sintering rate (the so-called *isothermal-stage sintering*) prevents the formation of temperature gradients that can lead to cracking and breaking, or to a differential densification (a formation of an outer dense layer with large internal voids). It is done by heating the green body for many hours up to the final sintering temperature and immediate cooling thereafter. This minimizes the holding time at the sintering temperature, giving membranes with high porosity (albeit with a lower mechanical strength). Definitions of high and low sintering rates are subjective, however, and depend on the grains used. According to Rahman [138], very high and very low sintering rates result in coarsening, while intermediate sintering rate favour densification. The cooling rate should be sufficiently high to save process time and reduce energy consumption, yet low enough to prevent thermal shock and breaking of already formed compact.

Regardless of whether you want dense or porous membranes, you must leave a certain degree of effective porosity to produce a transmembrane flux. The holding time is thus important. In general, long holding times result in significant densification and the entire process might enter the final sintering stage where transmembrane pores gradually disappear. Short holding times may result in the transition from coarsening to densification and in a production of large pores. The mechanical strength of the entire membrane will then be lower.

Grain size and grain size distribution also influence sintering. Basically, small grains give denser membranes. Current research focuses on the properties of ceramics made of nanosized grains. These studies are motivated by the

expectation that many ceramic properties will vary significantly with nanometric grains. However, the production of unisized nanosized powders is expensive, and benefits of such a membrane are moot. We will therefore focus on the typical micrometric grain sizes and their distribution. As already discussed, typical grains are of the sizes between 0.5 and 1.0 μm . This grain size is considered optimal for sintering a membrane of sufficient mechanical strength and low resistance. The ratio of the grain to the pore sizes was established before, and with the grains in the 0.5–1.0 μm range, the expected pores will be between 0.16 and 0.50 μm . These pores can be stable during sintering or may collapse to give the final compact with no pores. Note that the outcome of the sintering depends mainly on the initial sintering stage and is in general independent of the grain size. The only correlation reported by Chaim *et al.* [146] is that once the pore size exceeds the grain size, the pore elimination time is proportional to the fourth order of pore diameter. In practical terms, such pores cannot be eliminated.

Sintering protocols vary from one study to another, and, as already explained, industrial protocols are often kept as trade secrets. Therefore, we present here some of detailed sintering protocols found in the literature. Table 1.8 summarizes some known sintering protocols divided into drying, heating, sintering and cooling stages.

Table 1.8 Sintering protocols.

Raw materials	Drying and heating	Sintering	Cooling
Alumina (Alcoa Chemicals), magnesia (Merck), native potato starch (Portugal); TRECAMEX AET (Sweden), polyacrylic acid [106]	1 °C/min up to 500 °C; hold for 1 h at 200, 300 and 1000 °C	1600 °C for 2 h	
Alumina (Martinswerke); Zircosil 5, PVA [131]	20 °C/min to 1000 °C; rate of 5 °C/min up to sintering temperature	1200–1500 °C; 1 h soaking after sintering	
La(NO ₃) ₃ , SrCO ₃ , Co(NO ₃) ₂ ·6H ₂ O, Fe ₂ O ₃ , ZrO ₂ , isopropanol [147]	5 °C/h in 150–400 °C range; 60 °C/h to sinter- ing temperature	1200 °C for 5–10 h	
Ce _{0.8} Gd _{0.2} O _{2-x} (Rhodia), (Co(NO ₃) ₂ ·6H ₂ O, (Fluka), ethanol (Fluka) [148]	120 °C for 2 h; 1 °C/min to 450 °C; 3 °C/min to sintering temperature	900–1400 °C for 2 h	5 °C/min
Alumina, titanium tetraiso- propoxide (Aldrich), zirco- nium <i>n</i> -propoxide (Alfa), PVA, HPC [84]	100 °C/h to sintering temperature	500–1000 °C for 30 h	100 °C/h
Kaolin, quartz, calcium carbonate, sodium carbon- ate, boric acid and sodium metasilicate [149]	20 °C for 24 h; 100 °C for 12 h; 250 °C for 24 h; 2 °C/min to sintering temperature	850–1000 °C for 5 h	5 °C/min

1.9.4

Finishing

No matter how precisely we follow the manufacturing protocol, a ceramic membrane will never come out perfect. It could be a result of uneven drying or sintering, different shrinkage, gravity effects and a million other random factors. Membranes with major deviations in the form of cracks, curved surfaces, uneven support covering or cavities will be discarded. Figure 1.22 displays common failures in the preparation of membrane supports.

Conversely, minor deviations in the form of curved or rough ceramic surfaces can be fixed mechanically if the deviation from the linear average membrane thickness does not exceed 2%. Otherwise, the membrane is discarded. The definition of a bearable defect that can be fixed allowing further use of the membrane is unique for ceramic membranes. Polymer membranes have deviations of less than 1% that are regarded as their integral feature. If deviations exceed this value, the membranes are simply discarded with no attempts to prepare them for future use (unlike ceramic membranes). Similarly, metallic membranes are routinely machined to 25 μm tolerance with no difficulty or significant costs.

Finishing of ceramic membranes can be done by *grinding*, *lapping* and *polishing*. Grinding is a machining process, a subset of cutting that uses a grinding wheel as the cutting tool. Here, machining is a controlled alteration of a surface of a sintered membrane to achieve a desired degree of uniformity. Grinding is also implemented to alter membrane dimensions and shape, usually when the optimization of membrane preparation steps does not bring the desirable results. It is basically a very precise cutting technology that can reach single-micrometre

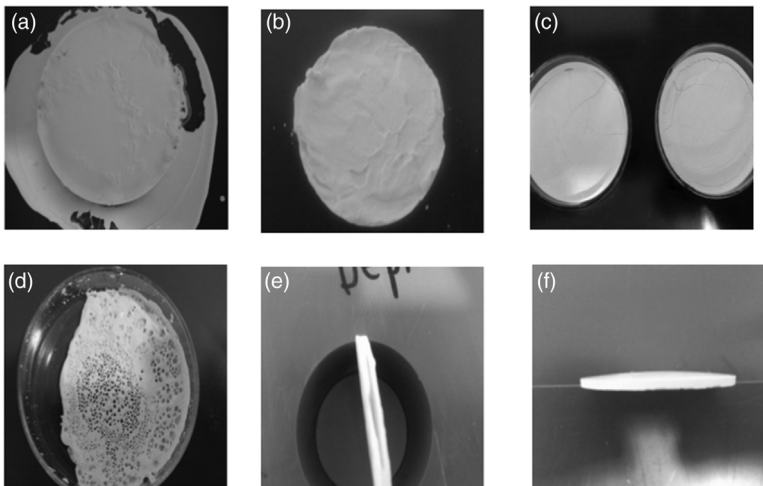


Figure 1.22 Examples of failures in preparation of $\alpha\text{-Al}_2\text{O}_3$ support membranes due to insufficient dispersant (a), high binder concentration (b), wrong drying regime (c and d), gypsum drying (e) and wrong sintering protocol (f). (Photographs by L. Tsapovsky.)

resolution. The preciseness of grinding is viewed different from cutting that is considered a macroscopic process. Abrasive grits (hard particles with sharp edges such as polycrystalline diamond (PCD) or cubic boron nitride CBN) are located on the edge of the grinding wheel that rotates at high speed. The geometry of surface grinding is variable and includes horizontal/vertical spindle, cylindrical grinding, internal grinding, centreless grinding and form (or plunge) grinding [150].

Lapping and polishing are finishing processes in which ceramic and abrasive surfaces slide parallel to each other. In this case, the finishing action is due to the presence of an abrasive pressed towards the membrane surface with either hand or a machine. *Coarse lapping* is performed with abrasives such as aluminium oxide, jeweller's rouge, optician's rouge, emery, silicon carbide or diamond, and can result in surfaces that bring the deviation down to 20 μm . The relative movement of the two surfaces removes material from both. *Gentle lapping* is performed with softer materials such as diamond or sand paper that are often wetted for easy sanding. Very intense and precise hand polishing may result in deviation of <1 μm . Lapping and polishing result in membranes with uniform thickness and decreased tortuosity of the membrane surface. The processes can also be used to fit the membrane to the required size of the support. This operation is often used in laboratory preparation of new membranes. The polished membranes are cleaned by ultrasonic rinsing in ethanol or by flushing water to clean the polished powder that can block the pores. In general, machining is considered as crude and expensive. Riedel and Chen [150] estimated the machining cost as 60–80% of the total manufacturing cost.

1.10

Intermediate and Top Layers

After all the hard work, many trials and a bit of luck, we have our first ceramic membrane. But is our membrane ready for industrial applications? Not really. At the moment we have a *membrane support*, a one-layered structure that is used in laboratory research and some low-cost industrial applications. For all other large industrial applications, the performance of membrane support is not sufficiently attractive to move from other separation technologies into ceramics. The performance of ceramic membranes should, therefore, be significantly improved in both separation efficiency and transmembrane flux. The ideal approach is to increase both the selectivity and the flux. As this is not possible, a wishful approach is to increase the flux without affecting selectivity or to increase the selectivity without affecting the flux. Is it possible? The answer is not that obvious. Although many industrial applications are built on sieving, improvements based on surface modifications are possible. The modification can target the membrane pore size compression that will definitely affect the selectivity. But this comes at the cost of a lower transmembrane flux. The other route is coating the membrane with molecules that give the membrane new and improved

features. Basically, both pore shrinkage and coating are processed through the attachment of additional layers to the membrane support, and the main difference between the two is in the retention mechanism. Whereas pore shrinkage aims at retaining molecules by physical restriction, coating can additionally adsorb desired molecules by designated end groups in the coating layer.

All ceramic membranes are modified to improve their performance. In many applications, only one type of ceramic material is suitable for the separation, such as dense perovskites for oxygen transport in fuel cells. Separations based on molecular sieving enjoy the possibility to choose from many ceramic membranes (as well as polymer and metallic ones). Those are room-temperature hydrogen and carbon dioxide separations, pervaporation, water and wastewater treatment, juice, beer and wine clarification and milk and cheese production. These applications are discussed in detail in Chapter 4. The implementation of dense membranes occurs through solution–diffusion and therefore requires a close match between the membrane material and the transferred compound. Convection is the driving force through porous membranes, and size restriction is the main separation mechanism. Many of the latter applications require a molecular sieving, that is a precise separation between two compounds with close dimensions, on the size base. The sieving mechanism requires a membrane with unified small size pores and minimal pore size distribution. Gas separations are usually performed with 0.3–0.4 nm pore size membranes. Liquid separation can be performed with 20–30 nm pores.

Homogeneous ceramic membranes with pore sizes $>1 \mu\text{m}$ can be used in microfiltration of liquids. All other applications require modifications by the addition of several intermediate layers and a top membrane layer. These modifications can be specific, targeting a single industrial application. Alternatively, they can be general, producing generic membranes suitable for many applications. Gas permeation membranes are not suitable in liquid applications due to their small pores and low flux. Similarly, liquid permeation membranes cannot separate gases, although they exhibit infinite fluxes.

Ultrafiltration ceramic membranes are formed from two- or three-layered structures. Typical pore sizes in UF membranes are between 2 and 50 nm; this structure can be obtained by sintering. Nanofiltration and gas and vapour separations are performed with microporous membranes with pore sizes between 0.7 and 2 nm. The pores can be obtained by either formation of a separate layer of nanoparticles or by a controlled development of the intrinsic structure of ceramic materials. The top layers can be prepared from ceramic oxide nanoparticles by a coating of these on the membrane intermediate layer. They can also be made by growing membrane materials such as zeolite crystals or by graphitization at high temperatures of organic carbons [42]. Ceramic oxide particles are incorporated on top of intermediate layers by different processes. The processes can be subdivided into physical vapour deposition (PVD), chemical vapour deposition, electrolytic deposition, sol–gel formation and hydrothermal treatment of zeolites.

PVD methods include thermal evaporation, physical sputtering, cathodic arc deposition and pulsed laser deposition. The reason why PVD techniques form a

separate category is that the film grows from a condensation of single atoms. In CVD techniques, molecular species react at the surface to form a film layer. The electrolytic deposition uses electrolyte where the atoms that form the film are present in as positively charged metal cations. Sol-gel is a general name for the process that converts a colloidal or polymeric 'solution' (sol) of silica, titania and zirconia to a gelatinous substance (gel). Here we will focus on three major modification methods, namely CVD, sol-gel and zeolite modifications. Both CVD and sol-gel can produce amorphous films with similar characteristics. The sol-gel route seems to offer more flexibility for tailoring the porosity and composition of separating layer. However, the final porosity depends drastically on various parameters and thus the reproducibility of sol-gel layers is challenging.

1.10.1

Preparing the Intermediate Layers

Our main message here is that the intermediate membrane layers cannot be prepared the same way as the support layer. A membrane structure can be sintered once and once only. This limits the choices of methods for forming intermediate layers. The most suitable method is called *dip coating* or *withdrawal coating*. Here the support layer is dipped into a ceramic dispersion and subsequently fired after withdrawal. Pressure filtration of a suspension through the support is an additional method to initiate the formation of intermediate layers, although this is limited to membranes with flat geometries.

The support layer has micrometre-sized pores and millimetre-depth thickness. It is suitable for separating compounds substantially larger than those typically affiliated with membrane processes. Examples of separable materials include bacteria and protozoa, coal dust, blood cells, milled flour and paint pigments. These are all micrometre-sized particles. Few applications require the separation of these materials by membranes. The application spectrum of ceramic membranes can be enlarged if the membrane pore size is reduced. As we saw above, the support layer is tuned by subsequent coating of intermediate and top layers. The number of intermediate layers may differ between one and three, depending on the pore size difference between the support and separation layers. A larger difference requires more layers. In each consecutive layer, the pore size decreases until at the very fine separation it drops from micrometres to single nanometre. This can be seen as the intentional compression of the pore size, but it is not the case. There is an empirical correlation between the pore size and the grain size (see Section 1.9.3). If the average grain size is 1 μm , then the mean pore width is between 400 and 660 nm. The grain size in the intermediate layer cannot be much smaller than the pore width. The first intermediate layer is expected to form from particles with 300–400 nm mean size, yielding a layer with 100–150 nm pores. Thus, the next layer will start with grains of 70–100 nm and yield pores of 30–40 nm. The third and final layer is likely to form from grains of 25–35 nm size and produce pores of 8–10 nm width. This pore size is sufficient for a smooth coating of separation layer that will contain 2–3 nm or

even 0.2–0.3 nm pores. The purpose of an intermediate layer is to successfully coat the membrane with a unified layer that will leave no uncovered places where the previous layer can be seen. This approach was proven effective in recent reports on defect-free surfaces obtained by the deposition of three intermediate γ -alumina layers. The layers were prepared by dip coating of boehmite ALOOH sols with 630, 200 and 40 nm particles. The top layer was made of silica [151,152] and silica–alumina [153]. One clear drawback of this approach is that making the interlayers is labour-intensive and time-consuming.

The thickness of the coating layer should be larger than the roughness of the support, so that it covers the support completely. With an estimated maximum roughness (R_{\max}) of 20–30 μm , a 30–40 μm thickness of the first intermediate layer is required [30]. This requirement will be reduced from layer to layer as each consecutive layer will be smoother. The average roughness (R_{av}) of the last intermediate layer should be below 1 μm as it is not possible to coat defect-free on support with an average roughness larger than 1 μm . In practice, the thickness of each layer is kept as low as possible to ensure a complete covering on the one hand and to avoid adding unnecessary membrane resistance on the other. A typical thickness of a coating layer is 100–1000 times the pore diameter [30]. This suggests that producing layers with smaller pores will at the same time reduce the thickness of each consecutive layer. For example, a typical thickness of a silica separation layer having pores of 2–3 nm is 200–300 nm [30]. The added membrane thickness of up to 0.1 mm can improve the mechanical strength, but thick intermediate layers lead to a higher resistance from the interlayers and reduce transmembrane flux.

Intermediate layers are built of ceramic particles. The coating particles should be chemically compatible with the support material to ensure a proper adhesion. Typically, the intermediate layers are made of same particles as the particles used in the preparation of the support, namely $\gamma\text{-Al}_2\text{O}_3$, SiO_2 , TiO_2 , ZrO_2 or their mixtures. This ensures not only decreased thickness and well-controlled pore size but also good thermal and chemical stability. Contrary to the support layer, the prepared suspension should remain stable during the coating process. Any aggregates or significant sedimentation can affect the drying process and result in non-uniform coating of the substrate. Hence, the average dry content of the suspension is approximately an order of magnitude lower than in preparation of substrate (3–5% for the intermediate layer versus 70% for the substrate).

When the support is withdrawn from a suspension, the dense dispersion layer of a defined thickness should not delaminate from it. Practically, this means that the support is wetted by the dispersion liquid. A consolidated coating is achieved after drying and calcination. Several intermediate layers can be obtained by the same routine, usually with a calcination step between each two consecutive coatings and by adapting the coating conditions.

An initial dispersion is either made of colloidal particles such as alumina or zirconia powders or prepared *in situ* from boehmite and titania sols using organometallic precursors. These particles are mixed in a polar solvent such as water or in an organic solvent such as ethanol or methanol. The suspension

should attach itself to the support so that it remains intact after being withdrawn from the suspension. There are two possible modes for this: *capillary colloidal filtration* and *film coating*. Capillary colloidal filtration occurs when the dry substrate contacts the suspension and the pore surface is wetted by the dispersion liquid. There are few research papers on the topic of intermediate layers. From what is available, Bayati *et al.* [154] found that decreasing the boehmite–titania content from 5 to 3 wt% results in the elimination of cracks and formation of more uniform intermediate layers on the support surface.

Any interactions between the support and the coating material should not lead to decreased permeability or defects in the membrane system such as micro-cracks. The thermal expansion behaviour of the coating should be comparable with that of the support. If the chemical compositions of support and filtration layers are sufficiently different, the intermediate layers need to buffer thermal expansion coefficients of various layers to minimize the number of defects formed during drying and calcination.

A membrane that has support and intermediate layers is suitable for MF and UF liquid separation processes, but not for those processes that require thermal, chemical and mechanical robustness. Such applications require a further coating of the ceramic membranes by a top layer. There are many methods for making such coatings. Here we will describe the two main ones: chemical vapour deposition and sol–gel. A zeolite coating is a different topic that is unique to zeolite-type structures.

1.10.2

Fundamentals of Chemical Vapour Deposition

Chemical vapour deposition is defined as a condensation of precursor compounds onto membrane support surface. Carrier gases such as hydrogen, nitrogen or argon deliver volatile precursor compounds such as metal halides, carbonyls or alkoxides into the reaction chamber [155]. The gas mixture in the reaction chamber flows over a membrane surface heated to a temperature needed to execute a chemical reaction such as oxidation, hydrolysis, thermal decomposition or compound formation. These reactions can occur in the vapour phase over a heated surface or by adsorption of reaction intermediates on the membrane followed by a surface reaction. This single-step operation gives a solid deposit layer. Heating can have a form of membrane heating, thermal radiation and photoradiation heating. Historically, the first experiments were run in the vapour phase using oxidation under atmospheric pressure and were named atmospheric pressure chemical vapour deposition (APCVD) or simply CVD. The deposition temperature ranges from 600 to 1500 °C depending on the reaction system. For many compounds, however, the heating temperature was high and CVD was considered an energy-intensive operation that can also damage the membrane surface. Further experiments aimed at reducing heating temperature by implementing plasma-assisted chemical vapour deposition (PACVD) or plasma-enhanced chemical vapour deposition (PECVD) [156]. PACVD and PECVD require temperatures below 500 °C and

sometimes as low as ambient temperatures. This is because electrical discharges in the gaseous phase are used for initiating the chemical reaction rather than thermal energy. Both methods give coating layers with high selectivity and a narrow pore size distribution. The deposition at low temperatures in PACVD and PECVD is suitable for temperature-sensitive compounds. The thickness of deposition layer is largely determined by the deposition time [157]. That said, the plasma bombardment of membrane surface can damage both the membrane and the coating film. In general, the efficiency of PACVD and PECVD depends strongly on the radio frequency, gas pressure, reagent flow rate and reactor geometry.

Photochemical vapour deposition (PCVD) uses high-energy photons that interact with the precursors either in the gas phase or on the growth surface. It is usually done with UV radiation due to the higher energy input and the absorption bands of simple organic precursors (that are often located in the UV range). It can also be performed at low or even ambient temperature and target a specific deposition area. PCVD enjoys the freedom of film thickness control due to the independency of bulk and membrane temperatures. However, it is limited to the precursor compounds that absorb photons and response in a predictable manner, with no or minimum side reactions and by-products.

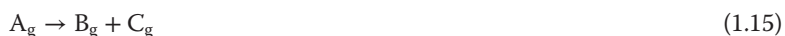
In atomic layer deposition (ALD) the precursors are introduced to the reaction chamber such that they reach the saturated adsorption level on the membrane surface. The deposition is due to a sequence of adsorption–chemical reactions steps. Here, the introduction of the precursors is controlled by an inert gas purge. This removes any excess precursor molecules and by-products from the reaction chamber preventing gas-phase reactions [158]. ALD has a superior control over the coating layer thickness due to a controlled step coverage. It is typically carried out at 250–300 °C, below the thermal decomposition threshold of most precursors. This thermal regime minimizes bulk reactions and avoids side reactions.

There are additional options such as laser chemical vapour deposition (LCVD), low-pressure chemical vapour deposition (LPCVD), metal–organic chemical vapour deposition (MOCVD) and chemical vapour infiltration (CVI). All together, the CVD processes form a family of chemical deposition processes with a common ground: Precursors are brought into reaction chamber in a vapour phase and turned into thin solid film on membrane surface after a chemical reaction of vapour-phase precursors. The reaction occurs either in the gas phase or on the membrane surface.

Due to the variety of precursors and possible gas-phase and surface reactions, CVD processes are extremely complex. Figure 1.23 presents an overall reaction scheme that includes both mass transfer and chemical reaction steps.

A classical CVD includes seven stages [158]:

- 1) Evaporation and transport of precursors into the reactor chamber
- 2) Gas-phase reaction of precursors in the reaction zone to produce reactive intermediates:



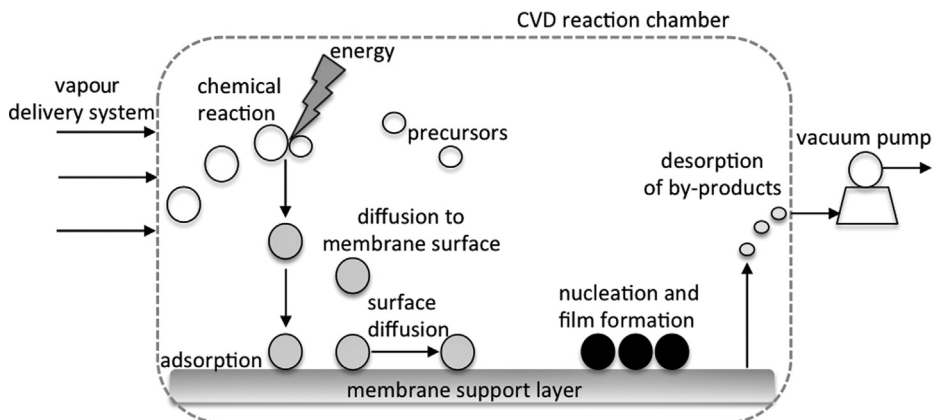


Figure 1.23 Precursor transport and reaction processes in CVD.

- 3) Diffusional transport of the intermediates to the membrane surface
- 4) Adsorption of the intermediates on the surface



- 5) Surface diffusion to growth sites, nucleation and surface chemical reactions that form the deposition film:



- 6) Desorption of by-products from the membrane surface and transport away of by-products from the membrane and from the bulk
- 7) Forced expel of by-products and carrier gases from the reaction chamber.

In the list above, A is a precursor compound, B is the reaction intermediate and S is an adsorbed B that contacts with other intermediates on the membrane surface. In parallel schemes, B can react and form oligomers in the gas phase. Thus, the oligomers land on the membrane surface and coalesce to form a porous network [159]. Some CVD processes might not have bulk reactions. In others, the film is already formed in the bulk and just lands as is on the membrane surface.

The formation of dense membranes requires that the vapour reactions be depressed and the film formation occur on the membrane surface only. This mode of film formation requires a smooth membrane surface, and is appropriate for growing films on mesoporous supports with 2–10 nm pores. The membrane pore size and structure here depend on the size and shape of precursors, as well as on the heating and drying conditions. The precursors are either decomposed in the vapour or land on the membrane support unconverted for further reactions. Growing a layer on the membrane support with pores larger than

10 nm requires a more sophisticated approach. The initial small nucleation centres are typically created in the bulk and land on the membrane support in the form of small clusters. The clusters are then grown on the support to form a film. Parallel heterogeneous reactions are needed to close the interparticle voids [159]. Growing a layer on the support with large pores results in a coating of not only the membrane surface but also the internal pore surface.

In traditional thermal CVD, the film growth rate is determined by the temperature of the membrane surface, the operating pressure of the CVD reaction chamber and the composition and chemistry of the gas phase. Figure 1.24 shows the dependence of the film growth on the temperature.

The plot in Figure 1.24 is divided into three regions. At low reactor temperatures, the film growth rate is controlled by the kinetic of chemical reactions. It increases exponentially with temperature, following an Arrhenius relation:

$$\text{Growth rate} \approx e^{E_A/RT}, \quad (1.20)$$

where E_A is the activation energy, R is the gas constant and T is the temperature. The film thickness here is controlled by the reaction temperature and the contact time. A uniform film thickness can be achieved by thorough temperature control over the membrane surface [158].

An increase in the reaction chamber temperature shifts the control to the diffusion of reacted intermediate species to the membrane surface. The overall film growth rate becomes diffusion controlled under the assumption that there is a boundary layer of passive precursors and counter-diffusing by-products near the membrane surface. Similarly, overheating of the membrane surface results in a massive desorption of intermediate species from the membrane surface before they react and become a part of a solid film. The film growth rate is controlled by the desorption rate and is usually lower than in the previous two regions.

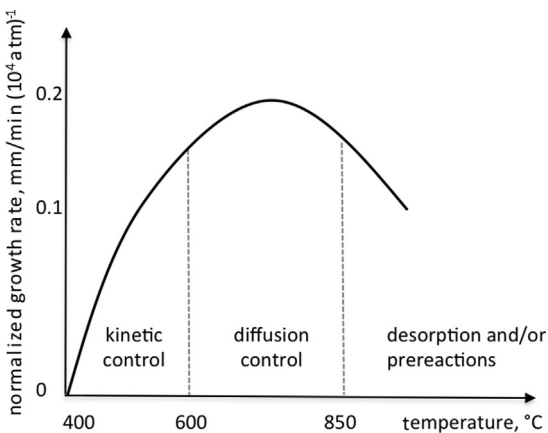


Figure 1.24 The dependence of the film growth on temperature. (Concept based on Ref. [160].)

The relative importance of each region is determined not only by the temperature but also by the pressure inside the chamber. Under APCVD, the gas-phase reactions are important and contribute to the formation of a significant boundary layer. The growth of a deposition film is controlled by both gas-phase reactions and diffusion through the boundary film. In low-pressure CVD (LPCVD), as the pressure falls below 1000 Pa, gas-phase reactions become less important. When the pressure is below 100 Pa, the reactions occur exclusively on the membrane surface. At very low pressures of 0.001 Pa, there is no mass transfer and the layer growth is controlled by the gas and substrate temperatures [158].

Many compounds can serve as CVD precursors. The following are the main requirements from these precursors [158]:

- 1) *Reactivity and thermal stability.* The precursor needs to react in a certain temperature window to give the desired intermediate. Not all precursors are volatile at ambient temperature, and some must be heated in a carrier before entering the reaction chamber. This can cause decomposition, generating particles that might contaminate the coating film [161]. Reactions at the membrane surface are especially vulnerable. A typical reaction at the membrane surface occurs at several hundred degrees, and yet the precursor should react at the membrane surface only. The precursor, therefore, should be reactive just in this narrow temperature range.
- 2) *Reasonable volatility at moderate evaporation temperatures, preferably well below the temperature of their thermal decomposition.* Some precursors are solids or liquids at room temperature, and boil/sublime at elevated temperatures. The volatility is affected by intermolecular forces such as van der Waals interactions, π -stacking and hydrogen bonds, and it increases with temperature.
- 3) *Thermal stability at evaporation temperatures.* Differential scanning calorimetry (DSC) is commonly used for determining the thermal stability of precursors by measuring the difference in heat flux between a precursor and a reference material as a function of temperature.
- 4) *High chemical purity.* A rather extreme example provided in Ref. [158] shows that the unintentional presence of 1 ppm of metal impurity makes a semiconductor unacceptable for most device applications. Carbon impurities might result in the thermal decomposition of either precursor or already formed film.
- 5) *Absence of or minimal side reactions and by-products.*
- 6) *Good adsorption* of reaction intermediates on the membrane surface.
- 7) *Long shelf life* under ambient conditions. The precursor should also be stable under misuse or a spilling accident to avoid massive losses at industrial conditions.
- 8) *Absence of or low toxicity* and no hazard risk. A low toxicity minimizes the expenses for storage and precautions during film formation. The environment-friendly precursors should preferably be recyclable.

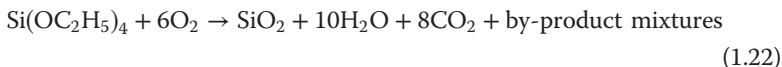
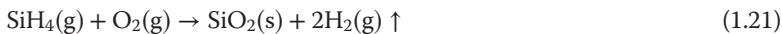
9) Competitive cost/performance ratio.

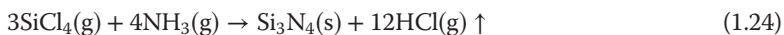
CVD is used in many industrial applications, including glass coating, silicon semiconductors, compound semiconductors, high-speed electronic devices, diode lasers and solar cells. According to a 2011 estimate, each of these has an annual turnover exceeding \$3 billion [162]. Industrial applications use a variety of precursors, including low-k silan-based precursors such as SiH(Me)₃, Si(Me)₄, and Si(Me)₂(OMe)₂, high k precursors such as Ta(OEt)₅, Al(Me)₃, HfCl₄, Hf(OtBu)₄, C₈H₁₈, C₆H₁₄, SiO₂ and SiN precursors such as Si₂Cl₆, Si(OMe)₄, SiCl₄, GeCl₄ and metal and nitride precursors such as TiCl₄, TaF₅, TaCl₅, Ru(EtCp)₂, and W(CO)₆.

In the ceramic membrane industry, CVD is considered a high-tech application that is relatively costly and difficult to scale up [157]. It is implemented when other options such as sol-gel are inapplicable or when the top layer should combine a very efficient precise separation with a high flux. Two of most popular implementations of CVD are coating of ceramic membranes with TiO₂ using PACVD and MOCVD [163], and silica membranes for hydrogen separation [155]. The latter application gains more interest due to its potential industrial use. The specific interest in inorganic membranes for that application is due to the possibility to create a thin yet defect-free top layer that will combine a high separation with high flux. This separation can be performed at elevated temperatures and under extreme chemical conditions.

In view of the thermostability demand, several silica precursors were used. These are SiH₄, SiCl₄, tetraethoxysilane (TEOS) and tetramethoxysilane (TMOS). These precursors react with an oxidizing agent, typically oxygen, water vapours or ozone. The reactants land on the support that can be either Vycor glass or alumina. Both materials are compatible with silica precursors and reactants. The initial work was reported on Vycor glass due to its small pores and intrinsic high uptake of hydrogen out of H₂-N₂ mixture. However, the limited permeance due to narrow pores in the glass shifted the attention towards the α-alumina and to γ-alumina coated on top of α-alumina despite their relatively large pore sizes between 110 and 180 nm [164]. In addition to a higher flux, alumina membranes are also cheaper and mechanically stronger than Vycor glass ones [155].

The CVD precursors form reactive intermediates in the vapour phase due to one of the following five reactions:

Oxidation*Reduction*

Nitridation*Hydrolysis*

Or else they are thermally decomposed (pyrolyzed) on the membrane support:



The first examples of using CVD for coating ceramic membranes with silica compounds were reported 40 years ago. Most of the initial work was performed in vapour phase using oxidation under atmospheric pressure CVD (APCVD). For example, the group of Gavalas used the oxidation of SiH_4 on the Vycor glass tubes with 4 nm pore sizes [165]. The reaction was run for 15 min until the pores were plugged. The H_2 - N_2 separation factor was as high as 3000 and H_2 permeance was $1.4 \times 10^{-8} \text{ mol}/(\text{m}^2 \text{ s Pa})$. These membranes, however, were not thermally stable at temperatures above 873 K and underwent ‘densification’, which is one of the most unpleasant surprises that accompany silicon coating ever since. The densification is attributed to a significant shrinkage of membrane pores in exposure to moisture. This shrinkage results in loss of up to 50% permeability during first 12 h of operation [166,167], preventing the industrial application of such membranes. Today, one of the central aspects in silica membrane studies is the development of silica-coated membranes that are stable at high temperatures in the presence of moisture. Several approaches were taken, including the incorporation of methyl groups into the silica microstructure [168], steam calcination [169] and Ni doping [170].

Vapour-phase reactions at elevated temperatures typically give high film growth rates of 200–300 nm/min. With typical film thickness of 0.5–1.0 μm , the entire top layer can be built in several minutes, although the usual step coverage is uneven. Such a ‘bread-loafing’ effect is often seen on the electron microscopy microfilms where SiO_2 loafs are separated by voids that are detrimental to both the separation and the permeation. One way of solving this problem is by using another precursor. Another way is by forming SiO_2 films on the membrane surface by thermal decomposition of precursors. A first attempt was done by Okubo and Inoue [171] who thermally decomposed tetraethoxysilane (TEOS) on a membrane surface heated up to 473 K. The experiment was also performed on a Vycor glass membrane, this time with 2 nm pores, and resulted in more efficient separation of helium and ozone. The He - O_3 separation factor however increased from 3 to 6 and was not considered a significant improvement in terms of gas separation. The second approach is realized via Eley–Rideal or Langmuir–Hinshelwood mechanism. In the former, a precursor A is adsorbed on the support surface and reacts with another precursor B that is in a gas phase. The growth rate is regulated by the covering of the support with molecules of A.

In the latter, molecules of both A and B are adsorbed on the support and react on the surface. The maximum growth rate is obtained when the support is covered equally [172].

Whether a reaction will run in the bulk or on the membrane surface is not only a question of precursors. The reactor geometry is also a factor. In one-side geometry, all reactants are introduced into the reaction chamber from the same side of the membrane surface. In counter-diffusion geometry, the precursors and oxidizers are supplied from the opposite side of the membrane surface. They counter-diffuse through the membrane and react inside or near membrane pores. Figure 1.25 shows the two types of CVD reactor configurations. The one-sided geometry is suitable for reactions in the vapour phase followed by chemisorption on the membrane support, and pyrolysis of precursors on the support. In hollow fibres and honeycomb geometries, pore plugging is avoided by sealing the permeate exits. This gives a relatively thick silica film.

Conversely, the counter-diffusion geometry yields a thin SiO_2 layer either on the membrane surface or within the pores. Several parameters influence the preferable location and the deposition rate: the molecular weight of a precursor, the membrane pore size and pore size distribution and the partial pressures of precursor and reactant [173]. The deposition rate slows down with time as the precursors and reactants diffuse not only through membrane pores but also through a previously deposited layer. Note that deposition inside the pores results in a pore narrowing and plugging. This plugging stops the reaction in a pore as the precursor and the reactant cannot meet [159].

In both one-sided and counter-diffusion geometries, precursors and reactants are introduced simultaneously. The reaction is fast, especially at temperatures above 600°C , and the limited control over the reaction rate creates a concentration gradient along the support surface. Alternatively, one can run the reaction in a one-sided geometry, where either the precursors or the reactants are supplied in oversaturation and the reaction proceeds until the concentration of the second compound drops to zero [174]. Then only the second compound is supplied to complete one reaction cycle. This introduction mode minimizes the

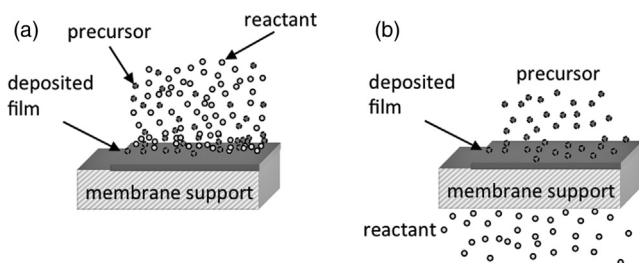


Figure 1.25 Schematic diagrams of precursor and reactant transport and reaction in one-sided (a) and counter-diffusion (b) processes in CVD. In the counter-diffusion geometry, the

size of a precursor might restrict its entrance into the pores, limiting the reaction to the outer part of the membrane support.

homogeneous particle formation limiting the reaction just to SiO_2 formation [159]. The film formation rate is slow as several reaction cycles are necessary to build a sufficiently thick coating layer.

There are many more studies on the formation and performance of silica-coated ceramic-based membranes [155]. Recent improvements raised the permeance to 10^{-7} mol/(m² s Pa) and the H_2/N_2 selectivity to ~ 1000 . This range is already of a commercial interest. Still the silica-coated ceramic-based membranes suffer from low hydrothermal stability. The CVD operation is still considered more expensive than sol-gel process, although the produced membranes possess a superior coverage [155]. One of the recent advances is the preparation of silica layers in non-oxide systems such as Si-C, Si-N, Si-C-N and Si-B-C-N. The latter approach resulted in a formed SiBCN-based layer with pores sizes of 0.6, 2.7 and 6 nm, and layer thickness of 1.75 μm [175]. The layer can withstand high temperatures and is therefore of interest for industrial applications. The silica stability in humid environments is increased by doping the membranes with alumina, zirconia or titania [176].

1.10.3

Sol-Gel Coating

In the sol-gel process, a colloidal or polymeric suspension is converted into a gelatinous network. The sol is a colloidal suspension of solid particles in a liquid, and gel is a porous solid 3D net. Colloids in a sol are metallic or metalloid elements surrounded by various ligands. The ligands do not include another metal or metalloid atom. For example, common colloids for aluminium oxide are inorganic salts such as $\text{Al}(\text{NO}_3)_3$ and metal alkoxide such as $\text{Al}(\text{OC}_4\text{H}_9)_3$. Silica gels are often made of tetraethoxysilane ($\text{Si}(\text{OC}_2\text{H}_5)_4$, abbreviated as TEOS) or tetramethoxysilane (TMOS). Metal alkoxides are metallo-organic compounds with a general formula $\text{M}(\text{OR})_m$, where M is Si, Sn, Ti, Zr, Al, Mo, W and Ce and alkoxide OR is $\text{OC}_n\text{H}_{2n+1}$. The reactivity of these precursors falls on an order of $\text{Si}(\text{OR})_4 \ll \text{Sn}(\text{OR})_4 = \text{Ti}(\text{OR})_4 < \text{Zr}(\text{OR})_4 = \text{Ce}(\text{OR})_4$ [177].

The sol-gel technology for coating ceramic membranes was first reported in the mid-1980s. Previously, ceramic membranes with pore sizes larger than 50 nm were used in coarse separation, competing with other separation technologies. The new layered structure of ceramic membranes opened new research opportunities. The pore sizes first narrowed towards 2–10 nm, yielding membranes that were suitable for liquid filtration. Since the 1990s, sol-gel-coated membranes have been considered a valid gas separation technology. This separation requires membranes with pores smaller than 1 nm. New horizons were set in the mid-1990s when tailor-made syntheses allowed controlled pore size and porosity, hydrophilic/hydrophobic membranes, catalytic activity and ionic conduction.

One striking example is the separation of nitrogen and oxygen based on their kinetic diameters. These two gases are nearly identical (kinetic diameters of 3.64 and 3.46 Å and molecular weights of 28 and 32 g/mol, respectively). Nevertheless, a properly designed ceramic membrane can separate them using

solution–diffusion and molecular sieving mechanisms. Another example is the generation of dense ceramic ion-conducting membranes for solid oxide fuel cells. These applications and other applications of membranes prepared using sol–gel technology are discussed in detail in Chapter 4. Here we will cover only the basics of the sol–gel operation and discuss the advantages and possible uses of this technology. Readers interested in more details of the fundamental sol–gel process should consult Ref. [178].

The sol–gel process is basically a sequence of chemical reactions starting from the dissolution of the precursor in polar or non-polar solvent such as water or organics. Depending on the chosen solvent, the reaction proceeds through either the gelation of separate colloids or the formation of polymer net. Water directs the sol–gel to the colloidal route. Alcohol as a solvent favours the polymer route. In the case of silicon alkoxide, the use of a base catalyst leads to the colloidal route, while adding an acid catalyst leads to open polymeric species [179]. Upon dissolution, the precursors are hydrolyzed as shown in Eq. (1.27), forming a colloidal sol that contains particles of sizes between 0.01 and 0.1 μm or linear organic–colloidal polymers.



The stability of colloids in the sol is maintained by electrostatic repulsion of charged particles or by steric interactions of surface-active or polymer substances. Here, R represents an alkyl group $\text{C}_n\text{H}_{2n+1}$, M–OR is the alkoxide and R–OH is the alcohol. The reaction replaces the alkoxide group OR with hydroxyl group OH. Depending on the amount of water and catalyst present, hydrolysis may go to completion (so that all of the OR groups are replaced by OH), or stop while the metal is only partially hydrolyzed M(OR)(OH)_n . The stability of colloidal sol is interrupted by changing its pH value so that two hydrolyzed colloids react with each other in an alcohol (alcoholysis) and water (hydrolysis) condensation reaction, resulting in the formation of a 3D gel laying on the membrane surface:



or



Polymers in the sol are intentionally unstable and form condensate spontaneously. The condensation reaction and self-polymerization produce metal–oxo-metal bonds and liberate small by-product molecules such as ethanol. Unlike the polymer gels, the formation of colloidal gels is reversible. Alcoholysis and hydrolysis are catalyzed by mineral acids, ammonia, acetic acid, KOH, amines, KF, HF and various oxides [180]. This colloidal route provides a possibility for forming both linear and cross-linked polymers. The degree of polymerization depends on the water:alkoxide ratio, as well as on the catalyst concentration.

Subsequently, the wet gel is transformed into a xerogel by removing the water in a series of heating steps. The water (or alcohol) is first evaporated at

100–200 °C. This process is similar to the initial stage of drying described earlier. Evaporation first occurs from the sol–gel surface, followed by solvent diffusion to the surface. The evaporation rate is high and uneven. One reason for this is that the interplay with the capillary forces results in a faster release of the solvent from larger pores, forming unintended U-shapes. Quick drying may cause cracking and even peeling off of the entire layer. Therefore, drying is done gradually, with 0.15–2.0 °C/min heating ramp targeting a temperature slightly above 100 °C for water and below 200 °C for organic solvents. This gradual regime also helps in minimizing the aggregation of particles in the sol, which results in unevenly distributed pores, high pore volume and low mechanical strength of the entire film. A good microporous membrane requires individual grains of 10 nm or less. The grains should be kept separated until the calcination stage. Ultimately, the separation is driven by strong electrostatic repulsions of colloids in a sol, or significant steric hindrance that prevents the formation of aggregates at the stage of gel formation. Dense microporous membranes are obtained from uniform grains that ensure the highest packing density of 0.74 (see Section 1.9) and low porosity of $\epsilon < 0.3$ [181].

In classical sol–gel applications, the porous bulk oxides are simply made by drying and calcination of separate gels in aqueous or organic solvents. But the formation of a multilayer ceramic membrane requires that the sol–gel layer be placed on top of a porous membrane support. The coating is performed in the form of dip coating or spin coating. Both methods use an already existing gel. This differs from liquid- and gas-phase impregnation, where the coating is done by the reacting several precursors, either on the surface, nearby or inside the membrane support. In dip coating, a porous support is dipped into a gel solution for few seconds. The coating film is formed by the capillary suction of the sol dispersant by the support pores. This is a slow process, and the thickness of the coating layer depends on suspension viscosity and dipping time. Conversely, film coating is fast and the viscosity of the suspension is high.

The final step in the formation of a top layer is the calcination, performed at 200–600 °C. This step (if done above 350 °C) yields a pure inorganic membrane. Any physically adsorbed water, residual organic solvents, hydroxides, nitrates or sulfates are decomposed. As in sintering, a continuous heating results in the formation of necks between the particles (calcining below 350 °C is used in the synthesis of hybrid membranes, yet leaves residual organics in the gel) [182]. The necks broaden, forming a 3D dense final metal oxide [183]. Figure 1.26 summarizes the various steps of the sol–gel routes.

The choice between the colloidal and polymer route depends on the intended membrane application. Through the colloidal route, the final net will be a series of interconnected colloids. These will be at a distance from each other and the final structure will be crystalline and mesoporous, containing pores in sizes of 2–10 nm at least. This pore size range is suitable for intermediate membrane layers and for liquid filtration. Conversely, gas separation membranes should have pores smaller than 1 nm and linear species with limited branching. These layers are produced by the polymeric route. The branched structure of the

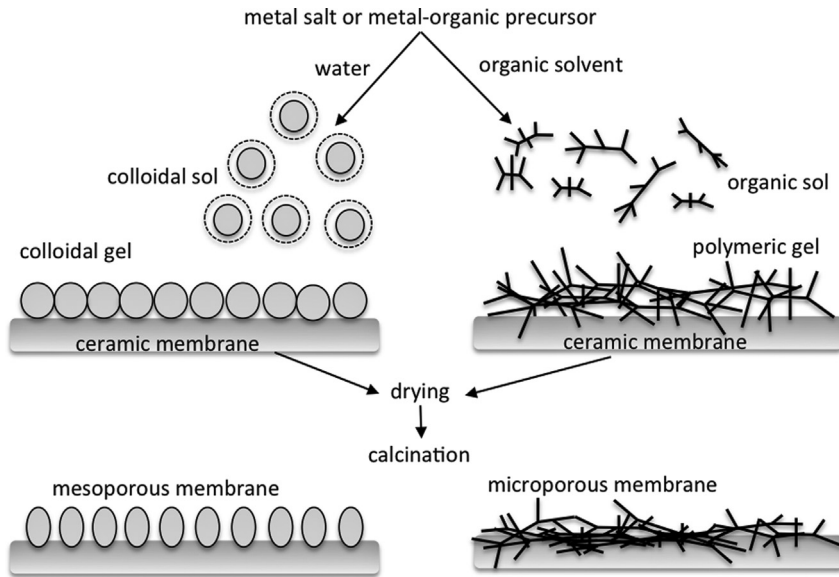


Figure 1.26 Diagram of colloidal and polymer routes in the preparation of sol-gel-coated ceramic membranes.

polymer intermediates is partially destroyed during calcination. This gives an amorphous microporous net with pores in an order of the spaces inside polymer chains that are considerably smaller than interpolymer distances.

1.10.4

Zeolite Coating

Zeolites are a special class of ceramic compounds that contain a uniform system of channels with a 0.3–2 nm diameter. That pore size is close to the size of single molecules and therefore zeolites are good molecular sieves. The separation requires uniformity in pore size and indeed zeolites possess a narrow pore size distribution. There are three options for zeolite membrane filtration: Zeolites can be used as self-standing membranes or coated on top of ceramic supports. An intermediate option is embedding zeolite crystals into a dense polymer membrane. All three options are used, although coating is the most popular. Self-standing zeolites are grown on a support such as mercury or Teflon that is easily separated from the zeolite crystal when the growth is complete. Such zeolites are interesting for modelling transport studies, but not for practical applications. This is because growing zeolite layers larger than few square centimetres is difficult, and the fragility of large zeolite structures prevents their industrial implementation. A proper zeolite type governs the membrane selectivity, and the content of embedded zeolite determines membrane permeability. At the moment however, the method suffers from technical difficulties in the formation of large

defect-free membrane surfaces. The inherent problem of embedded zeolites is the general zeolite selection mechanism. The preferable absorption might with time clog zeolite pores and discard the entire membrane. There is no regeneration option for zeolite-organic frameworks.

Conversely, zeolites coated on top of ceramic supports present many important advantages over sol-gel and CVD methods. Zeolites are crystals with a crystalline structure that determines the pore dimensions and uptake selectivity. Their crystallinity reduces the chances of inconsistency, layer breach or abnormal pores. The zeolite layer is thin yet strong.

There is an additional large group of materials that are not zeolites *per se*, but possess pores of the same size range. These are 'zeolite-like materials' or zeotypes, such as silicalites, aluminophosphates (AIPO) and silicoaluminophosphates (SAPO). The variety of zeotype structures increases the chance of finding a perfect separation layer with the right pore size, shape and density. There are more than 300 structures with pores in the range of 0.3–2 nm to choose from. Each structure contains pores of one size. The size is determined by the ring structure. Theoretical calculations showed that zeolites with 4, 6, 8, 10 or 12 oxygen anions in one ring have the maximum pore openings of 0.26, 0.34, 0.42, 0.63, and 0.74 nm, respectively [184].

The chemical composition (and therefore the properties) of a coated zeolite is changeable. Its Si/Al ratio determines the membrane hydrophilicity and the metal exchange capacity. Hydrophilic zeolites have a low Si/Al ratio. They can be used for separating organic-aqueous mixtures by selective uptake of water. The most successful (and currently, the only industrial) zeolite membrane separates water from water-organic mixtures [185]. This application is called *pervaporation* (for details on this and other membrane applications, see Chapter 4). Zeolites with a high silica level such as silicalite-1 are hydrophobic and can serve for a selective uptake of organics out of the same mixture. When a solution contains a cation different from that of the zeolite, the latter can serve as an ion exchanger. One of the known features of NaA zeolites is their capacity to release Na^+ cations, accumulating Ca^{++} and Mg^{++} from water. This operation is called *water softening* and it is efficient in reducing water hardness. NaA zeolites are typically arranged in a bed and can be easily regenerated when all sodium ions are replaced by the calcium and magnesium ions.

Several zeolites are used in chemistry and petrochemistry as catalysts. Thus, zeolite membranes can combine separation with catalytic activity (for details on such combined applications and zeolite membrane reactors, see Chapter 4). Zeolites can selectively uptake and transfer other than H_2 or O_2 molecules in dense high-temperature catalytic reactions. For example, a zeolite membrane was used for separating isooctene from hexadecene at temperatures $>25^\circ\text{C}$. Under optimal pressure of 15 bars and temperature higher than 70°C , using a catalytic zeolite reactor allowed increasing the yield of C_8 target fraction and depressing the further undesirable conversion to C_{12} and C_{16} fractions [186].

The zeolites are coated on top of different ceramic supports, including alumina, titanium dioxide, zirconia and mullite. Coating is performed by crystallization

followed by a substantial growth of the initial crystals on the membrane support. The crystallization goes via one of the following four routes [187]: (i) The nuclei can be generated in a bulk and attracted to the membrane support by collision or diffusion. (ii) They can be attached to the substrate surface before the crystallization. (iii) The nuclei-formed compounds can be transported to the substrate surface for the *in situ* generation of the initial nuclei (the so-called *in situ* nucleation). (iv) A dry gel that contains potential nucleus can be placed on the substrate surface and activated by vapour or steam (the so-called dry gel conversion method). Either route can occur on the support surface or within the pores.

The use of pre-nucleated seeds as the nucleation bases (route (i)) separates the stages of crystal nucleation and growth. Here, the initial step is the forming of a colloidal suspension that contains zeolite crystals smaller than 1 μm [188]. Then, the preformed zeolite crystals are attached to the support using dip coating, filtering, electrostatic attraction or rubbing. Dip coating is a simple process, but it needs to be repeated several times for a proper coverage of the support surface. It can be improved by modifying the surface charges of the support with a cationic electrolyte or by electrophoretic deposition [189]. For example, silicalite-1 seeds are negatively charged and a coating of a support surface with a positively charged polydiallyldimethylammonium (PDDA) chloride increases the electrostatic attraction [190].

Filtering can increase the surface coverage without electrostatic effects [191,192]. The secondary growth is performed at concentrations lower than those needed for the nucleation, formation of new nucleation centres is unlikely and the zeolite layer forms by growing of preformed crystal seeds. A more strict control over the formation and growth of zeolite crystals prevents the crystallization of undesired zeolite phases and the dissolution of support [193]. The additional advantage of the seeding is the possibility to control the crystal orientation. A passage of molecules through the membrane is possible only when interconnected zeolite channels are turned perpendicular to the support surface. For example, MFI zeolites have straight, sinusoidal and elliptic pores, and an unfavourable direction of the straight pores might result in low or no transmembrane flow. Usually, the initial orientation achieved during seeding remains after the calcination step [80].

Another method for attaching the zeolite powder to the support surface is by rubbing it with a small brush, followed by hydrothermal attack (route (ii)). This results in a partial dissolution of the zeolites and leaching of Si and Al ions. The dissolved ions serve as additional nucleation bases that encourage crystallization of zeolites, giving a continuous defect-free zeolite layer. The penetration of dissolved Al and Si ions into the support enhances the integrity of the entire construct and the mechanical strength of the separation layer. At a later stage, one can remove the zeolite powder from the support surface, as this gives a more homogeneous layer [194]. If the initial zeolite seeds are not removed, the zeolite layer grows preferentially in a close vicinity of the initial nucleus. The disadvantage of this process is its low reproducibility.

The *in situ* nucleation (route (iii)) often results in defect-free zeolite separation layer. Any defects are not much larger than the zeolite pores, so the transport of

fluids occurs only through the zeolite pores. The *in situ* nucleation is performed by covering a support with a gel that contains hydrated silica and alumina and organic template to form a zeolite structure. Typical zeolite supports are α -alumina and sintered stainless steel with pore sizes between 0.1 and 10 μm . Another option is coating on an α -alumina support that is itself coated with a γ -alumina intermediate layer. Using the intermediate layer enables the synthesis of membranes with 5 nm pores [195]. Other supports are seldom used, as this changes the mechanism of nucleation. For instance, the support itself may undergo dissolution in the synthesis gel and change its composition or provide nucleation sites with new elements [193].

Basically, the *in situ* nucleation route is a modified sol-gel process performed under controlled hydrothermal conditions, using crystalline zeolites instead of amorphous silica. The controlled conditions include temperature that can be between 90 °C (zeolite A) and 180 °C (silicalite A) and time that can range from hours to days [196]. Formation of a separation zeolite layer starts from the immersion of the support in a synthesis gel with a composition similar to that reported in the synthesis of self-standing crystals. The synthesis gel is prepared from a silica source (e.g. TEOS, sodium silicate or fumed silica), an aluminium source (e.g. sodium aluminate, aluminium sulfate or alumina), a mineralizing agent (e.g. NaOH, NaF or KOH) and a templating agent such as tetrapropylammonium hydroxide (TPAOH) or tetrapropylammonium bromide (TPABr) [197,198]. Using high concentrations of silicon and aluminium increases the chances of a defect-free layer.

The support is dipped into the gel solution in an autoclave, and the gel is crystallized under pressure at elevated temperatures for several days, and then calcined. For example, Matsukata and Kikuchi [184] performed calcination at 500 °C using a 0.1 °C/min heating rate in the temperature range between 100 and 500 °C. The number of synthesis cycles depends on the particular zeolite and intended depth of the coating layer. Vroon and coworkers [199] used two consecutive hydrothermal treatments at different temperatures of 371 and 459 K to prepare an MFI membrane on α -alumina support. One cycle was not enough for connecting the individual zeolite grains. Three cycles gave a thick layer that cracked after the template was removed. Technical difficulties in *in situ* nucleation arise at the nucleation stage [196]. Loose control over crystallization results in generation of zeolite layers with undesirable microstructure [200]. A better control over nucleation and crystal growth is obtained by acid treatment, deposition of metals and metal oxides, mechanical polishing, adsorption of surfactant molecules or seeding [200]. The forming of a zeolite layer by *in situ* nucleation is a question of trial and error, and depends on gel compositions, synthesis times, methods for wetting the support and even the rotation of autoclave [188].

The dry gel conversion method (route (iv)) uses a dry aluminosilicate gel (the so-called *parent gel*) [201,202] and different solvents such as ethylene glycol [203], ethylenediamine and triethylamine [204]. The gel is deposited on top of a membrane support and converted into a zeolite layer by vapour or steam. In this case, the vapour phase contains organic compounds that are needed for the formation of the initial crystals. The layer formation is performed in autoclaves.

For example, Cheng *et al.* [205] reported a formation of a uniform zeolite layer with $\alpha(\text{CO}_2/\text{N}_2)$ of 55 by covering the surface of alumina support with seeds of zeolite and then with aluminosilicate gel. The layer was exposed to water vapour in an autoclave for several days. In steam-assisted crystallization, the steam contains the solvent that prevents homogeneous nucleation and reduces the consumption of binders and other organic additives [206].

The problem of zeolite membranes is their transport mechanism. Materials pass through the pores by adsorption, making it difficult to maintain a steady state as the zeolite becomes saturated with adsorbate. That said, retention by adsorption can also be advantageous, as large-pore zeolites can combine high permeate fluxes with high selectivity. Thermal stability up to 400–500 °C and resistance to organic solvents are additional advantages of zeolites over polymer membranes with same pore widths, facilitating their implementation. Zeolite membranes are often used in gas separation and catalytic membrane reactors at elevated temperatures. More details on these applications are given in Chapter 4. Several companies such as GFT Membrane Systems GmbH (Germany), Mitsui Engineering & Shipbuilding Corp. (Japan) and Sulzer Chemtech Allschwil Ltd. (Switzerland) offer full-scale installation of zeolite ceramic membranes. Laboratory experiments develop new zeolite synthesis strategies such as dynamic hydrothermal process [207], microwave heating [208], pre-aging of support material in the synthesis gel [209] and pore-plugging method [210]. There is now an extensive knowledge on the synthesis procedures and formation mechanisms (nucleation and growth) of zeolite layers. The future of zeolite membrane layers is probably in the development and implementation of new zeolite materials and combination of zeolites and polymers in mixed matrix membranes (MMMs).

1.11

Industrial Applications of Ceramic Membranes

Finally, after lots of hard work, many trials and a bit of luck, you have made your first ceramic membrane. It might not be perfect, but surely good for something. We only have to understand how this membrane separates mixtures and what are its features. These subjects are covered in Chapters 2 and 3, respectively. Then, we can offer our membrane to one of the relevant industrial sectors: the food and beverages, biotechnology, chemicals, pharmaceuticals and recovery and recycling (see the summary in Table 1.9).

In general, ceramic membranes are applied in those areas where they can compete with polymer membranes in performance and economics, as well as in specific cases that require their unique features. In the latter, they compete with other separation technologies but not with other membranes. The advantages of ceramic membranes include a wide range of possibilities for physical and chemical cleaning, a high resistance to harsh operating conditions and superior mechanical, thermal and chemical stability. Ceramic membranes are a dynamically developing field. New applications include industrial wastewater

Table 1.9 Applications of ceramic membranes in liquid-phase separations.

Area	Membrane type	Application examples
Food and beverage industry	MF and UF	Concentration of milk, concentration of protein, clarification of fruit juice, clarification of beer and wine, removal of microorganisms at fermentation
Biotechnology and pharmaceutical industry	MF and UF	Microorganism separation and cell debris filtration, plasma separation
Chemical and industrial applications	MF and UF	Oil–water separation, purification of used oil, removal of precipitated heavy metals and solids
Recovery and recycling	UF and NF	Drinking water and wastewater treatment

treatment (including the retention of heavy metals and synthetic dyes [211–213]), separation of asphaltene from crude oil [214] and the separation and concentration of organic solvents such as ethanol and hexane [215–217]. The classical applications are in the food and beverage industry, in gas separation (especially O₂/N₂ separation), in the reduction of CO₂ in power plants and, of course, in high-temperature fuel cells. All these applications and more are discussed in detail in Chapter 4. The corresponding economic considerations are outlined in Chapter 5.

1.12

Further Reading

There are many books about membranes, if fewer about ceramic ones. Here is a selection of further reading. All of the books listed below were in print and commercially available in January 2016.

Basic Principles of Membrane Technology by Mulder [16] is a clear and well-written graduate-level textbook. It gives an excellent introduction to many aspects of membrane technology. A clear, concise and yet comprehensive coverage at the sufficient depth level makes the book valuable for both membrane experts and students. Unfortunately, it is outdated (the last edition of the book was printed in 1996, 20 years ago). The membrane field has expanded tremendously since then and in many places the text needs updating with new ideas and discoveries.

Membrane Technology and Applications by Baker [17] is a more updated introductory level book on the basics of the membrane technology. It gives a comprehensive overview of membrane-based separation processes. Although the book starts with a series of general chapters on membrane preparation, transport theory, membrane modules and concentration polarization phenomenon, it

places much emphasis on the application fields, with numerous examples and much practical advice.

Encyclopedia of Membrane Science and Technology, edited by Hoek and Tarabara [218], and *Advanced Membrane Technology and Applications*, edited by Li *et al.* [18], are two large collective volumes that serve as references for various aspects of membrane principles, operations, materials, processes and applications. These books are written by invited groups of experts and cover numerous aspects of synthetic membranes at the fundamental as well as practical levels. Both books can be viewed as a reference guide in a branched membrane field but not as introductory books. Their relatively high price implies that they are more suitable for institute or corporate libraries.

Inorganic Membranes, by Burggraaf [219], and *Fundamentals of Inorganic Membrane Science and Technology*, edited by Burggraaf and Cot [10], are two excellent books on the basics and applications of ceramic membranes, although both were published almost 20 years ago. They give good and clear introduction to many aspects of ceramic membranes. The fabrication, characterization, transport theory and applications of porous and dense ceramic membranes are covered in detail.

Several other books on inorganic membranes detail applications of inorganic membranes in different fields. The emerging field of inorganic membrane reactors has been discussed in the book *Inorganic Membranes for Separation and Reaction* published in 1996 by Hsieh [85]. Several books on different aspects of uses of ceramic membranes had been published since then. *Recent Advances in Gas Separation by Microporous Ceramic Membranes*, edited by Kanellopoulos [220], and *Ceramic Membranes for Separation and Reaction*, published by Li [26] discuss the gas separation with inorganic membranes. *Catalytic Membranes and Membrane Reactors* by Sánchez Marcano and Tsotsis [221], *Nonporous Inorganic Membranes: For Chemical Processing* by Sammells and Mundschau [222], *Membrane Technology: In the Chemical Industry* by Nunes and Peinemann [223], and *Inorganic Membranes: Synthesis, Characterization and Applications* edited by Mallada and Menendez [60] discuss aspects of implementation of ceramic membranes in chemical industry. *Inorganic Membrane Reactors: Fundamentals and Applications* by Tan and Li discusses advances in inorganic membrane reactors with extensive coverage of ceramic, silica and zeolite reactors [224].

Exercises

- 1.1. Draw a three-layered ceramic membrane and list and explain the depth range and pore size of each layer.
- 1.2. A ceramic membrane was used in the direct purification of organic waste of a pharmaceutical factory. Suggest the most likely type of fouling, as well as a

cleaning procedure that aims at restoring the initial flux. How would your answer change if a polymer membrane was used instead of a ceramic one?

- 1.3. Calculate the volume flux, in $\text{l}/(\text{m}^2 \text{ h})$, through a 0.5 m^2 of α -alumina membrane. The total flux is $20 \text{ cm}^3/\text{s}$ and the membrane works at 0.85 recovery ratio. What assumption do you have to make? Is the flux you found high or low? Explain your answer.
- 1.4. Which ceramic membrane would you choose for separating water from a water–benzene mixture? Give at least two advantages of the membrane of your choice compared to other ceramic or polymer membranes.
- 1.5. You are in charge of optimization of α -alumina membrane supports. Currently, the membrane is 2 mm thick, has a mechanical strength at break of 30 MPa and the volume flux of $40 \text{ l}/(\text{m}^2 \text{ h})$. Your task is to increase the flux, while keeping the mechanical strength. Discuss the anticipated change in membrane properties as a function of
 - grain size of the initial powder,
 - amount of plasticizer,
 - sintering temperature, and
 - drying/heating/cooling rate.
- 1.6. Explain the difference between a retention ratio and molar retention ratio, and how it affects the transmembrane flux. A manufacturer offers you two alumina-based membranes for separating organic mixtures. Membrane (i) has a retention ratio of 0.1 and a transmembrane flux of $150 \text{ l}/(\text{m}^2 \text{ h})$. Membrane (ii) has a molar retention ratio of 0.1 and transmembrane flux of $50 \text{ l}/(\text{m}^2 \text{ h})$. Which one do you prefer?
- 1.7. You and your colleague discuss different membrane supports. You claim that α -alumina is a well-known and generally accepted material that your factory uses for 50 years. Your colleague says that it is out of mode and the entire membrane field revolves around titanium dioxide. Is your colleague correct? How would you convince them to continue using alumina supports?
- 1.8. A support layer has a nitrogen flux of $0.02 \text{ cm}^3/(\text{cm}^2 \text{ s cmHg})$. Calculate the flux in $\text{l}/(\text{m}^2 \text{ h})$ and in $\text{gallons}/(\text{ft}^2 \text{ day})$.
- 1.9. Your site manager is considering changing several separation processes into membrane-based ones. What type of membrane would you recommend for:
 - Desalination of sea water
 - Separation of bacteria from surface water
 - Isolation of ethanol from a fermentation broth
 - Separation of CO_2 from flue gas
- 1.10. Figure 1.27 depicts two sintering protocols for membranes A and B. Assume that the green body of both membranes was made of exactly the

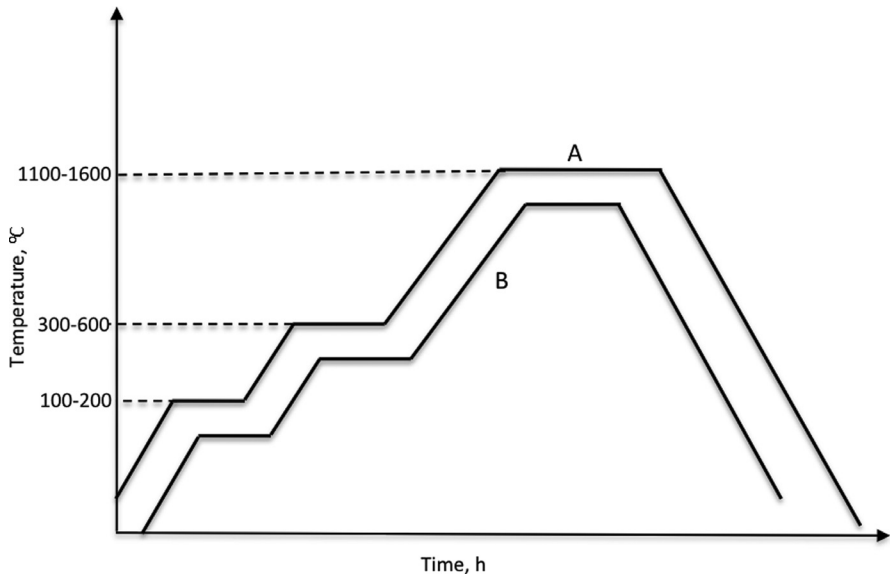


Figure 1.27 Stages of heating, thermolysis and sintering in the preparation of ceramic membranes A and B.

same materials and the only difference between two membranes is in the sintering protocol. Describe the anticipated difference in flux, retention ratio and mechanical strength of sintered A and B.

- 1.11.** Search the Internet and find the structures of zeolites A and Y. Assume that there are two ceramic membranes where each of these zeolites is coated on top of γ -alumina. Based on the structure of both zeolites, explain the difference in the retention ratio and transmembrane flux of these membranes.
- 1.12.** List the main foulant of ceramic membranes used in
- cheese production,
 - orange juice clarification,
 - surface water treatment,
 - wastewater treatment, and
 - gas separation

What type of cleaning protocol would you use in each case? Explain your answer.

- 1.13.** List three separation processes where ceramic membranes can successfully compete with polymer ones. How can you maximize the advantages of ceramic membranes in each case?
- 1.14.** A ceramic membrane is used for purifying surface water for drinking. The average transmembrane flow is $2 \text{ m}^3/\text{h}$, with a 0.95 recovery ratio. The

Filtration Mechanism

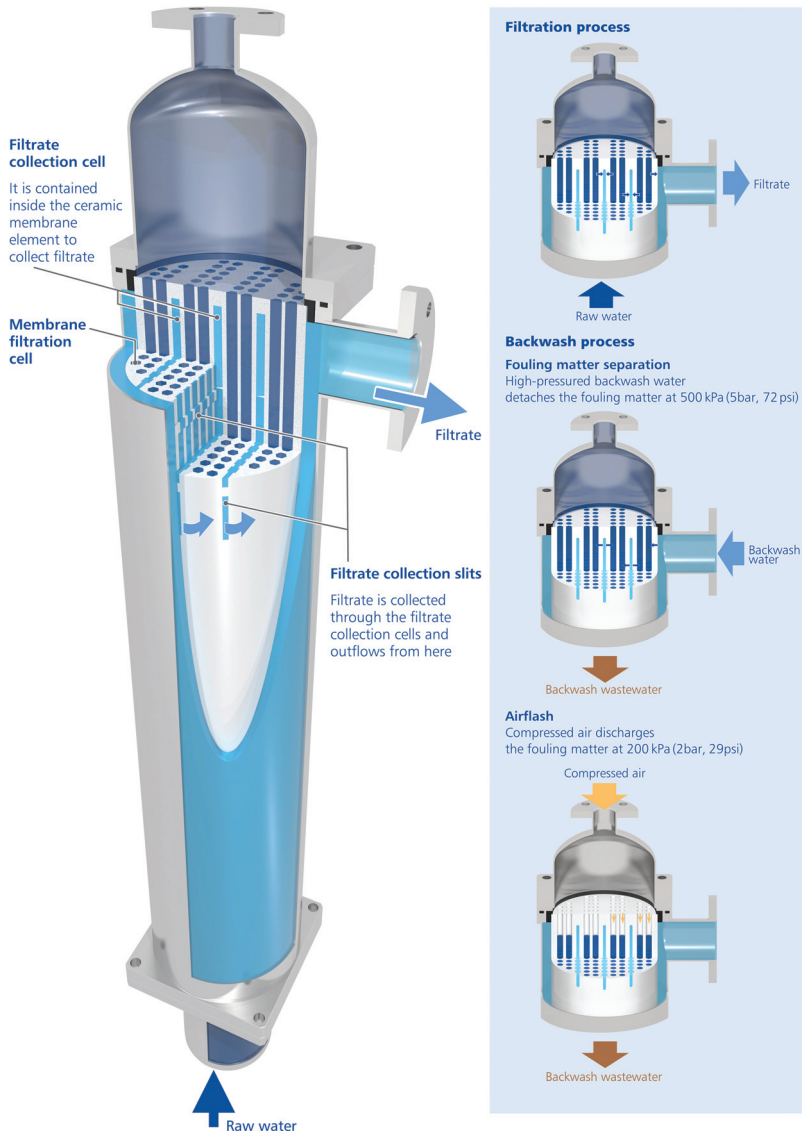


Figure 1.28 Schematic showing the filtration and backwash processes in a Metawater ceramic membrane element. (Image courtesy of Metawater Co., Japan.)

membrane is physically backwashed daily for 1 h (see Figure 1.28). Due to severe fouling, the site manager switches to two daily backwash cycles. How will this affect the recovery ratio? (You may assume that the recovery ratio is influenced only by the permeate losses due to hydraulic backwashes.)

References

- 1 Liu, D.M. (1996) *Porous Ceramic Materials: Fabrication, Characterization, Applications*, Trans Tech Publications Ltd., Zurich.
- 2 Owoeye, F.T., Olokode, O.S., Aiyedun, P.O., Balogun, H.O. and Anyanwu, B.U. (2012) Preparation and characterization of ceramic microfiltration membrane for water treatment. *The Pacific Journal of Science and Technology*, **13**, 28–38.
- 3 Harari, Y.N. (2012) *From Animals into Gods: A Brief History of Humankind*, CreateSpace, Charleston.
- 4 Fahlman, B.D. (2011) *Materials Chemistry*, Springer, Dordrecht.
- 5 Johnson, R.L. (2011) Ceramics in the classroom. Available at http://depts.washington.edu/matseed/mse_resources/Webpage/Ceramics/ceramics.htm (updated 18/7/2015).
- 6 Harris, R. (2003) *Pompeii*, Random House Paperbacks, New York.
- 7 Gillot, J. (1991) The developing use of inorganic membranes: a historical perspective, in *Inorganic Membranes: Synthesis, Characteristics and Application* (ed. R.R. Bhawe), Chapman & Hall, New York, pp. 1–9.
- 8 Bhawe, R.R. (1991) *Inorganic Membranes: Synthesis, Characteristics, and Applications*, Van Nostrand-Reinhold, New York.
- 9 Loeb, S. and Sourirajan, S. (1962) Sea water demineralization by means of an osmotic membrane. *Advances in Chemistry Series*, **38**, 117–132.
- 10 Burggraaf, A.J. and Cot, L. (1996) *Fundamentals of Inorganic Membrane Science and Technology*, Elsevier, Amsterdam, The Netherlands.
- 11 Vanderhorst, H.C. and Hanemaaijer, J.H. (1990) Cross-flow microfiltration in the food industry: state of the art. *Desalination*, **77** (1–3), 235–258.
- 12 Bolduan, P. and Latz, M. (2000) Ceramic membranes and their application in food and beverage processing. *Filtration+Separation*, **37** (3), 36–38.
- 13 de Vos, R.M. and Verweij, H. (1998) High-selectivity, high-flux silica membranes for gas separation. *Science*, **279** (5357), 1710–1711.
- 14 Aaron, D. and Tsouris, C. (2005) Separation of CO₂ from flue gas: a review. *Separation Science and Technology*, **40** (1–3), 321–348.
- 15 Shackleton, R. (1987) The application of ceramic membranes to the biological industries. *Journal of Chemical Technology and Biotechnology*, **37** (1), 67–69.
- 16 Mulder, M. (1996) *Basic Principles of Membrane Technology*, Kluwer, Dordrecht.
- 17 Baker, R. (2004) *Membrane Technology and Applications*, 2nd edn, John Wiley & Sons, Inc., Chichester.
- 18 Li, N.N., Fane, A.G., Ho, W.S.W. and Matsuura, T. (2011) *Advanced Membrane Technology and Applications*, John Wiley & Sons, Inc., Hoboken, NJ.
- 19 Arkhangelsky, E., Sefi, Y., Hajaj, B., Rothenberg, G. and Gitis, V. (2011) Kinetics and mechanism of plasmid DNA penetration through nanopores. *Journal of Membrane Science*, **371** (1–2), 45–51.
- 20 Burggraaf, A.J. (1996) Important characteristics of inorganic membranes, in *Fundamentals of Inorganic Membrane Science and Technology* (eds A.J. Burggraaf and L. Cot), Elsevier, Amsterdam.
- 21 Freger, V., Gilron, J. and Belfer, S. (2002) TFC polyamide membranes modified by grafting of hydrophilic polymers: an FT-IR/AFM/TEM study. *Journal of Membrane Science*, **209** (1), 283–292.
- 22 Herzberg, M., Sweity, A., Brami, M., Kaufman, Y., Freger, V., Oron, G. *et al.* (2011) Surface properties and reduced biofouling of graft-copolymers that possess oppositely charged groups. *Biomacromolecules*, **12** (4), 1169–1177.
- 23 Apel, P. (2001) Track etching technique in membrane technology. *Radiation Measurements*, **34** (1–6), 559–566.
- 24 Riscanu, D., Favis, B.D., Feng, C.Y. and Matsuura, T. (2004) Thin-film membranes derived from co-continuous polymer blends: preparation and performance. *Polymer*, **45** (16), 5597–5609.
- 25 Rouquerol, J., Avnir, D., Fairbridge, C.W., Everett, D.H., Haynes, J.H.,

- Pernicone, N. *et al.* (1994) Recommendations for the characterization of porous solids. *Pure and Applied Chemistry*, **66** (8), 1739–1758.
- 26 Li, K. (2007) *Ceramic Membranes for Separation and Reaction*, John Wiley & Sons, Inc., Chichester.
- 27 Zsigmondy, R. and Bachmann, W. (1918) Über neue Filter. *Zeitschrift für Anorganische und Allgemeine Chemie*, **103**, 119–128.
- 28 Gaikwad, A.V., Boffa, V., ten Elshof, J.E. and Rothenberg, G. (2008) Cat-in-a-cup: facile separation of large homogeneous catalysts. *Angewandte Chemie, International Edition*, **47** (29), 5407–5410.
- 29 Biesheuvel, P.M. and Verweij, H. (1999) Design of ceramic membrane supports: permeability, tensile strength and stress. *Journal of Membrane Science*, **156** (1), 141–152.
- 30 Bonekamp, B.C. (1996) Preparation of asymmetric ceramic membrane supports by dip-coating, in *Fundamentals of Inorganic Membrane Science and Technology* (eds A.J. Burggraaf and L. Cot), Elsevier, Amsterdam.
- 31 Sah, A., Castricum, H.L., Blik, A., Blank, D.H.A. and ten Elshof, J.E. (2004) Hydrophobic modification of gamma-alumina membranes with organochlorosilanes. *Journal of Membrane Science*, **243** (1–2), 125–132.
- 32 EPA (2001) Low-pressure membrane filtration for pathogen removal: application, implementation, and regulatory issues. US Environmental Protection Agency Office of Water 2001, EPA 815-C-01-001.
- 33 Stern, S.A., Sinclair, T.F., Gareis, P.J., Vahldieck, N.P. and Mohr, P.E. (1965) Helium recovery by permeation. *Industrial and Engineering Chemistry*, **57**, 49–60.
- 34 Hsieh, H.P., Bhawe, R.R. and Fleming, H.L. (1988) Microporous alumina membranes. *Journal of Membrane Science*, **39** (3), 221–241.
- 35 Dyer, P.N., Richards, R.E., Russek, S.L. and Taylor, D.M. (2000) Ion transport membrane technology for oxygen separation and syngas production. *Solid State Ionics*, **134** (1–2), 21–33.
- 36 Bray, T.D. (inventor) (1968) Reverse osmosis purification apparatus. U.S. Patent US3,417,870 (Gulf General Atomic Inc., assignee).
- 37 Westmoreland, J.C. (inventor) (1968) Spiral wrapped reverse osmosis membrane cell. US Patent US3,367,504 (Gulf General Atomic Inc., assignee).
- 38 Mahon, H.I. (inventor) (1966) Permeability separatory apparatus, permeability separatory membrane element, method of making the same and process utilizing the same. US Patent US3,228,876 (Dow Chemical Co., assignee).
- 39 Liu, S.M. and Gavalas, G.R. (2005) Oxygen selective ceramic hollow fiber membranes. *Journal of Membrane Science*, **246** (1), 103–108.
- 40 Charcosset, C. (2012) *Membrane Processes in Biotechnology and Pharmaceuticals*, Elsevier, Amsterdam.
- 41 EPA (2003) Membrane filtration guidance manual. US Environmental Protection Agency, Contract No. EPA 815-D-03-008.
- 42 Pierre, A. and Christian, G. (2008) Current status and prospects for ceramic membrane applications, in *Handbook of Membrane Separations*, CRC, Boca Raton, FL, pp. 139–179.
- 43 Porter, M.C. (1990) Ultrafiltration, in *Handbook of Industrial Membrane Technology* (ed. M.C.E. Porter), Noyes Publications, Westwood, CA.
- 44 Lipnizki, F. and Dupuy, A. (2013) Food industry applications, in *Encyclopedia of Membrane Science and Technology*, John Wiley & Sons, Inc., Hoboken, NJ.
- 45 McNaught, A.D. and Wilkinson, A. (eds) (1997) *International Union for Pure and Applied Chemistry: Compendium of Chemical Terminology*, 2nd edn (the Gold Book), Blackwell Scientific Publications, Oxford.
- 46 Field, R. (2010) Fundamentals of fouling, in *Membrane Technology, Volume 4: Membranes for Water Treatment* (eds K.V. Peinemann and S. Pereira Nunes), Wiley-VCH Verlag GmbH, Weinheim.
- 47 Shi, X., Tal, G., Hankins, N.P. and Gitis, V. (2014) Fouling and cleaning of ultrafiltration membranes: a review.

- Journal of Water Process Engineering*, **1** (0), 121–138.
- 48 Liu, C., Caothien, S., Hayes, J., Caothuy, T., Otoy, T. and Ogawa, T. (2006) Membrane chemical cleaning: from art to science. Pall Corporation, New York. Available at <http://www.pall.com/pdfs/Water-Treatment/mtcpaper.pdf> (updated 18/7/2015).
- 49 Scott, K. (1995) *Handbook of Industrial Membranes*, Elsevier, Amsterdam.
- 50 Faibish, R.S. and Cohen, Y. (2001) Fouling-resistant ceramic-supported polymer membranes for ultrafiltration of oil-in-water microemulsions. *Journal of Membrane Science*, **185** (2), 129–143.
- 51 Tragardh, G. (1989) Membrane cleaning. *Desalination*, **71** (3), 325–335.
- 52 Le-Clech, P., Chen, V. and Fane, T.A.G. (2006) Fouling in membrane bioreactors used in wastewater treatment. *Journal of Membrane Science*, **284** (1–2), 17–53.
- 53 Hong, S.K. and Elimelech, M. (1997) Chemical and physical aspects of natural organic matter (NOM) fouling of nanofiltration membranes. *Journal of Membrane Science*, **132** (2), 159–181.
- 54 Naim, R., Levitsky, I. and Gitis, V. (2012) Surfactant cleaning of UF membranes fouled by proteins. *Separation and Purification Technology*, **94**, 39–43.
- 55 Levitsky, I., Duek, A., Arkhangelsky, E., Pinchev, D., Kadoshian, T., Shetrit, H. *et al.* (2011) Understanding the oxidative cleaning of UF membranes. *Journal of Membrane Science*, **377** (1–2), 206–213.
- 56 Arkhangelsky, E., Kuzmenko, D. and Gitis, V. (2007) Impact of chemical cleaning on properties and functioning of polyethersulfone membranes. *Journal of Membrane Science*, **305** (1–2), 176–184.
- 57 Yacou, C., Wang, D., Motuzas, J., Zhang, X., Smart, S. and Diniz da Costa, J.C. (2013) Thin-film ceramic membranes, in *Encyclopedia of Membrane Science and Technology*, John Wiley & Sons, Inc., Hoboken, NJ.
- 58 Schwob, Y. (1949) *Sur l'hémi-perméabilité à l'eau des membranes de cellulose régénérée*. E. Privat, Toulouse, France.
- 59 Furukawa, D.H. (1999) New developments in desalination, in *Providing Safe Drinking Water in Small Systems: Technology, Operations, and Economics* (eds J.A. Cotruvo, G.F. Craun and N. Hearne), CRC Press, Boca Raton, FL, pp. 257–263.
- 60 Mallada, R. and Menéndez, M. (2008) *Inorganic Membranes: Synthesis, Characterization and Applications*, Elsevier, Amsterdam.
- 61 Robeson, L.M. (1991) Correlation of separation factor versus permeability for polymeric membranes. *Journal of Membrane Science*, **62** (2), 165–185.
- 62 Uhlhorn, R.J.R., Zaspalis, V.T., Keizer, K. and Burggraaf, A.J. (1992) Synthesis of ceramic membranes. 2. Modification of alumina thin-films: reservoir method. *Journal of Materials Science*, **27** (2), 538–552.
- 63 Kucera, J. (2013) Membrane materials and module development: historical perspective, in *Encyclopedia of Membrane Science and Technology* (eds E.V. Hoek and V.V. Tarabara), John Wiley & Sons, Inc., Hoboken, NJ.
- 64 Charpin, J., Bergez, P., Valin, F., Barnier, H., Maurel, A. and Martinier, J.M. (1987) Inorganic membranes: preparation, characterization, specific applications. *Material Science Monograph*, **38**, 2211–2235.
- 65 Louwerse, M.J. and Rothenberg, G. (2013) Modeling catalyst preparation: the structure of impregnated–dried copper chloride on γ -alumina at low loadings. *ACS Catalysis*, **3** (7), 1545–1554.
- 66 Wefers, K. and Bell, G.M. (1972) Oxides and hydroxides of aluminum. Alcoa Research Laboratories. Available at https://www.alcoa.com/global/en/innovation/papers_patents/pdf/TP19_Wefers.pdf.
- 67 Holleman, A.F., Wiberg, E. and Wiberg, N. (2001) *Holleman–Wiberg's Inorganic Chemistry*, Academic Press, San Diego, CA.
- 68 de Vos, R.M. and Verweij, H. (1998) Improved performance of silica membranes for gas separation. *Journal of Membrane Science*, **143** (1–2), 37–51.
- 69 Xu, R., Wang, J.H., Kaneshashi, M., Yoshioka, T. and Tsuru, T. (2013) Reverse osmosis performance of organosilica membranes and comparison

- with the pervaporation and gas permeation properties. *AIChE Journal*, **59** (4), 1298–1307.
- 70 Castricum, H.L., Kreiter, R., van Veen, H.M., Blank, D.H.A., Vente, J.F. and ten Elshof, J.E. (2008) High-performance hybrid pervaporation membranes with superior hydrothermal and acid stability. *Journal of Membrane Science*, **324** (1–2), 111–118.
- 71 Baerlocher, C. and McCusker, L.B. (2001) Database of zeolite structures. Available at <http://www.iza-structure.org/databases/> (cited and updated 9/08/2013).
- 72 Zakersalehi, A., Choi, H., Andersen, J. and Dionysiou, D.D. (2013) Photocatalytic ceramic membranes, in *Encyclopedia of Membrane Science and Technology* (eds E.M.V. Hoek and V.V. Tarabara) John Wiley & Sons, Inc., Hoboken, NJ.
- 73 Nair, P., Mizukami, F., Okubo, T., Nair, J., Keizer, K. and Burggraaf, A.J. (1997) High-temperature catalyst supports and ceramics membranes: metastability and particle packing. *AIChE Journal*, **43** (11), 2710–2714.
- 74 Kritikaki, A. and Tsetsekou, A. (2009) Fabrication of porous alumina ceramics from powder mixtures with sol–gel derived nanometer alumina: effect of mixing method. *Journal of the European Ceramic Society*, **29** (9), 1603–1611.
- 75 Tsapovski, L. (2013) *Ceramic Catalytic Membranes for Tertiary Wastewater Treatment*, Ben Gurion University of the Negev.
- 76 Phonthammachai, N., Gulari, E., Jamieson, A.M. and Wongkasemjit, S. (2006) Photocatalytic membrane of a novel high surface area TiO₂ synthesized from titanium triisopropanolamine precursor. *Applied Organometallic Chemistry*, **20** (8), 499–504.
- 77 Kulprathipanja, S. (2010) *Zeolites in Industrial Separation and Catalysis*, Wiley-VCH Verlag GmbH, Weinheim.
- 78 Siebdrath, N., Ziskind, G. and Gitis, V. (2012) Cleaning secondary effluents with organoclays and activated carbon. *Journal of Chemical Technology and Biotechnology*, **87** (1), 51–57.
- 79 Baerlocher, C., McCusker, L.B. and Olson, D.H. (2007) *Atlas of Zeolite Framework Types*, Elsevier, Amsterdam.
- 80 Lai, Z.P., Bonilla, G., Diaz, I., Nery, J.G., Sujaoti, K., Amat, M.A. *et al.* (2003) Microstructural optimization of a zeolite membrane for organic vapor separation. *Science*, **300** (5618), 456–460.
- 81 Komolikov, Y.I. and Blaginina, L.A. (2002) Technology of ceramic micro and ultrafiltration membranes (review). *Refractories and Industrial Ceramics*, **43** (5–6), 181–187.
- 82 Lin, Y.S., Chang, C.H. and Gopalan, R. (1994) Improvement of thermal stability of porous nanostructured ceramic membranes. *Industrial and Engineering Chemistry Research*, **33** (4), 860–870.
- 83 Delange, R.S.A., Keizer, K. and Burggraaf, A.J. (1995) Aging and stability of microporous sol–gel-modified ceramic membranes. *Industrial and Engineering Chemistry Research*, **34** (11), 3838–3847.
- 84 Chang, C.H., Gopalan, R. and Lin, Y.S. (1994) A comparative study on thermal and hydrothermal stability of alumina, titania and zirconia membranes. *Journal of Membrane Science*, **91** (1–2), 27–45.
- 85 Hsieh, H.P. (1996) *Inorganic Membranes for Separation and Reaction*, Elsevier, Amsterdam.
- 86 Sekulic, J., Luiten, M.W.J., ten Elshof, J.E., Benes, N.E. and Keizer, K. (2002) Microporous silica and doped silica membrane for alcohol dehydration by pervaporation. *Desalination*, **148** (1–3), 19–23.
- 87 Van Gestel, T., Vandecasteele, C., Buekenhoudt, A., Dotremont, C., Luyten, J., Leysen, R. *et al.* (2002) Alumina and titania multilayer membranes for nanofiltration: preparation, characterization and chemical stability. *Journal of Membrane Science*, **207** (1), 73–89.
- 88 Chang, Y., Ling, Z.Y., Liu, Y.S., Hu, X. and Li, Y. (2012) A simple method for fabrication of highly ordered porous alpha-alumina ceramic membranes. *Journal of Materials Chemistry*, **22** (15), 7445–7448.
- 89 Byrappa, K. and Yoshimura, M. (2001) *Handbook of Hydrothermal Technology*:

- A Technology for Crystal Growth and Materials Processing*, Noyes Publications, Norwich.
- 90 Larbot, A. (1996) Ceramic processing techniques of support systems for membranes synthesis, in *Fundamentals of Inorganic Membrane Science and Technology* (eds A.J. Burggraaf and L. Cot), Elsevier, Amsterdam.
 - 91 Aste, T. (2005) Variations around disordered close packings. *Journal of Physics: Condensed Matter*, **17**, S2361–S2390.
 - 92 Bideau, D. and Troadec, J.P. (1984) Compacity and mean coordination number of dense packings of hard disks. *Journal of Physics C: Solid State Physics*, **17** (28), L731–L740.
 - 93 Visscher, W.M. and Bolsterl, M. (1972) Random packing of equal and unequal spheres in 2 and 3 dimensions. *Nature*, **239** (5374), 504–507.
 - 94 Zhang, Y.H., Qin, C.W. and Binner, J. (2006) Processing multi-channel alumina membranes by tape casting latex-based suspensions. *Ceramics International*, **32** (7), 811–818.
 - 95 Shanefield, D.J. (1996) *Organic Additives and Ceramic Processing, Second Edition: With Applications in Powder Metallurgy, Ink, and Paint*, Kluwer Academic Publishers, Dordrecht.
 - 96 Shan, M., Mao, X.J., Zhang, J. and Wang, S.W. (2009) Electrophoretic shaping of sub-micron alumina in ethanol. *Ceramics International*, **35** (5), 1855–1861.
 - 97 Das, N., Bandyopadhyay, S., Chattopadhyay, D. and Maiti, H.S. (1996) Tape-cast ceramic membranes for microfiltration application. *Journal of Materials Science*, **31** (19), 5221–5225.
 - 98 Sarraf, H. and Havrda, J. (2007) Rheological behavior of concentrated alumina suspension: effect of electrosteric stabilization. *Ceramics-Silikaty*, **51** (3), 147–152.
 - 99 Lewis, J.A. (1997) Binder removal from ceramics. *Annual Review of Materials Science*, **27**, 147–173.
 - 100 Onoda, G.Y. (1976) Theoretical strength of dried green bodies with organic binders. *Journal of the American Ceramic Society*, **59** (5–6), 236–239.
 - 101 Bayliss, R.W. (1986) *The Sintering, Microstructural Analysis and Mechanical Properties of Two Beta MgSiAlON Ceramics*. Department of Physics, University of Warwick.
 - 102 Lindqvist, K. and Liden, E. (1997) Preparation of alumina membranes by tape casting and dip coating. *Journal of the European Ceramic Society*, **17** (2–3), 359–366.
 - 103 Das, N. and Maiti, H.S. (1998) Formation of pore structure in tape-cast alumina membranes: effects of binder content and firing temperature. *Journal of Membrane Science*, **140** (2), 205–212.
 - 104 Yang, W.P., Shyu, S.S., Lee, E.S. and Chao, A.C. (1996) Effects of PVA content and calcination temperature on the properties of PVA/boehmite composite film. *Materials Chemistry and Physics*, **45** (2), 108–113.
 - 105 Pierre, A.C. (1997) Porous sol–gel ceramics. *Ceramics International*, **23** (3), 229–238.
 - 106 Lyckfeldt, O. and Ferreira, J.M.F. (1998) Processing of porous ceramics by ‘starch consolidation’. *Journal of the European Ceramic Society*, **18** (2), 131–140.
 - 107 Kristoffersson, A., Roncari, E. and Galassi, C. (1998) Comparison of different binders for water-based tape casting of alumina. *Journal of the European Ceramic Society*, **18** (14), 2123–2131.
 - 108 Zhang, Y.G. and Binner, J. (2002) Tape casting aqueous alumina suspensions containing a latex binder. *Journal of Materials Science*, **37** (9), 1831–1837.
 - 109 Saggiowoyansky, J., Scott, C.E. and Minnear, W.P. (1992) Processing of porous ceramics. *American Ceramic Society Bulletin*, **71** (11), 1674–1682.
 - 110 Othman, M.R. and Mukhtar, H. (2000) Review on development of ceramic membrane from sol–gel route: parameters affecting characteristics of the membrane. *International Islamic University Malaysia Engineering Journal*, **1** (2), 29–34.
 - 111 Lambert, C.K. and Gonzalez, R.D. (1999) Effect of binder addition on the properties of unsupported gamma-Al₂O₃ membranes. *Materials Letters*, **38** (2), 145–149.

- 112 Hutchison, R.B., Curryhyde, H.E. and Raper, J.A. (1994) Preparation of composite ceramic membrane from titania powders. *Powder Technology*, **81** (3), 249–257.
- 113 Lin, B., Zhang, S.Q., Zhang, L.C., Bi, L., Ding, H.P., Liu, X.Q. *et al.* (2008) Prontonic ceramic membrane fuel cells with layered $\text{GdBaCO}_2\text{O}_{5+x}$ cathode prepared by gel-casting and suspension spray. *Journal of Power Sources*, **177** (2), 330–333.
- 114 Ding, X.B., Fan, Y.Q. and Xu, N.P. (2006) A new route for the fabrication of TiO_2 ultrafiltration membranes with suspension derived from a wet chemical synthesis. *Journal of Membrane Science*, **270** (1–2), 179–186.
- 115 Wang, Y.H., Zhang, Y., Liu, X.Q. and Meng, G.Y. (2007) Sol-coated preparation and characterization of macroporous $\alpha\text{-Al}_2\text{O}_3$ membrane support. *Journal of Sol-Gel Science and Technology*, **41** (3), 267–275.
- 116 Kim, D.J., Park, I.S., Choi, H.J., Lee, D.Y. and Han, J.S. (2004) Aqueous-based alumina tape casting for 3-dimensional forming. *Key Engineering Materials*, **264–268**, 173–176.
- 117 Sepulveda, P. and Binner, J.G.P. (1999) Processing of cellular ceramics by foaming and *in situ* polymerisation of organic monomers. *Journal of the European Ceramic Society*, **19** (12), 2059–2066.
- 118 Dörre, E. and Hübner, H. (1984) *Alumina: Processing, Properties, and Applications*, Springer, Berlin.
- 119 Hotza, D. and Greil, P. (1995) Aqueous tape casting of ceramic powders. *Materials Science and Engineering A*, **202** (1–2), 206–217.
- 120 Pincus, A.G. and Shipley, L.E. (1969) The role of organic binders in ceramic processing. *Ceramic Industry*, **92** (4), 106–109.
- 121 Barmala, M., Moheb, A. and Emadi, R. (2009) Applying Taguchi method for optimization of the synthesis condition of nano-porous alumina membrane by slip casting method. *Journal of Alloys and Compounds*, **485** (1–2), 778–782.
- 122 Li, N., Wen, Z.Y., Liu, Y., Xu, X.G., Lin, J. and Gu, Z.H. (2009) Preparation of Na-beta-alumina film by tape casting process. *Journal of the European Ceramic Society*, **29** (14), 3031–3037.
- 123 Leenaars, A.F.M. and Burggraaf, A.J. (1985) The preparation and characterization of alumina membranes with ultrafine pores. 2. The formation of supported membranes. *Journal of Colloid and Interface Science*, **105** (1), 27–40.
- 124 Nishio, H., Sato, M. and Watanabe, K. (inventors) (1993) Method of producing ceramic sintered body having dense ceramic membrane. US Patent US5,250,242A (Nkk Corporation, assignee).
- 125 Wu, Z., Wang, B. and Li, K. (2010) A novel dual-layer ceramic hollow fibre membrane reactor for methane conversion. *Journal of Membrane Science*, **352** (1–2), 63–70.
- 126 Steenkamp, G.C., Keizer, K., Neomagus, H.W.J.P. and Krieg, H.M. (2002) Copper (II) removal from polluted water with alumina/chitosan composite membranes. *Journal of Membrane Science*, **197** (1–2), 147–156.
- 127 Qiu, M., Feng, J., Fan, Y. and Xu, N. (2009) Pore evolution model of ceramic membrane during constrained sintering. *Journal of Materials Science*, **44** (3), 689–699.
- 128 Jedidi, I., Khemakhem, S., Saïdi, S., Larbot, A., Elloumi-Ammar, N., Fourati, A. *et al.* (2011) Preparation of a new ceramic microfiltration membrane from mineral coal fly ash: application to the treatment of the textile dyeing effluents. *Powder Technology*, **208** (2), 427–432.
- 129 Xia, C.R. and Liu, M.L. (2001) A simple and cost-effective approach to fabrication of dense ceramic membranes on porous substrates. *Journal of the American Ceramic Society*, **84** (8), 1903–1905.
- 130 Bouzerara, F., Harabi, A., Achour, S. and Larbot, A. (2006) Porous ceramic supports for membranes prepared from kaolin and doloma mixtures. *Journal of the European Ceramic Society*, **26** (9), 1663–1671.
- 131 Falamaki, C., Afarani, M.S. and Aghaie, A. (2004) Initial sintering stage pore growth mechanism applied to the manufacture of ceramic membrane

- supports. *Journal of the European Ceramic Society*, **24** (8), 2285–2292.
- 132 Aranzabal, A., Iturbe, D., Romero-Sáez, M., González-Marcos, M.P., González-Velasco, J.R. and González-Marcos, J.A. (2010) Optimization of process parameters on the extrusion of honeycomb shaped monolith of H-ZSM-5 zeolite. *Chemical Engineering Journal*, **162** (1), 415–423.
- 133 Isobe, T., Kameshima, Y., Nakajima, A., Okada, K. and Hotta, Y. (2006) Extrusion method using nylon 66 fibers for the preparation of porous alumina ceramics with oriented pores. *Journal of the European Ceramic Society*, **26** (12), 2213–2217.
- 134 Dong, C. (1990) *Binder Removal in Ceramics: Department of Materials Science and Engineering*, Massachusetts Institute of Technology.
- 135 Schnabel, W. (1981) *Polymer Degradation: Principles and Practical Applications*, Hanser International, Munich.
- 136 Higgins, R.J. (1989) The chemistry of carbon retention during non-oxidative binder removal from ceramic greenware. Ph.D. thesis, Department of Materials Science and Engineering, Massachusetts Institute of Technology.
- 137 Onoda, G.Y. and Hench, L.L. (1978) *Ceramic Processing before Firing*, Wiley-Interscience, New York.
- 138 Rahaman, N. (2007) *Sintering of Ceramics*, CRC Press, Boca Raton, FL.
- 139 Mehrer, H. (2007) *Diffusion in Solids: Fundamentals, Methods, Materials, Diffusion-Controlled Processes*, Springer, Berlin.
- 140 Kang, S.J.L. (2005) *Sintering: Densification, Grain Growth and Microstructure*, Elsevier, Amsterdam.
- 141 Ashby, M.F. (1972) A first report on deformation-mechanism maps. *Acta Metallurgica*, **20** (7), 887–897.
- 142 Shi, J.L., Deguchi, Y. and Sakabe, Y. (2005) Relation between grain growth, densification and surface diffusion in solid state sintering: a direct observation. *Journal of Materials Science*, **40** (21), 5711–5719.
- 143 Shi, J.L. (1999) Relations between coarsening and densification and mass transport path in solid-state sintering of ceramics: model analysis. *Journal of Materials Research*, **14** (4), 1378–1388.
- 144 Levanen, E. and Mantyla, T. (2002) Effect of sintering temperature on functional properties of alumina membranes. *Journal of the European Ceramic Society*, **22** (5), 613–623.
- 145 Brook, R.J. (1985) Processing technology for high-performance ceramics. *Materials Science and Engineering*, **71** (1–2), 305–312.
- 146 Chaim, R., Levin, M., Shlayer, A. and Estournes, C. (2008) Sintering and densification of nanocrystalline ceramic oxide powders: a review. *Advances in Applied Ceramics*, **107** (3), 159–169.
- 147 Balachandran, U., Dusek, J.T., Mieville, R.L., Poeppel, R.B., Kleefisch, M.S., Pei, S. et al. (1995) Dense ceramic membranes for partial oxidation of methane to syngas. *Applied Catalysis A: General*, **133** (1), 19–29.
- 148 Kleinogel, C. and Gauckler, L.J. (2000) Sintering and properties of nanosized ceria solid solutions. *Solid State Ionics*, **135** (1–4), 567–573.
- 149 Nandi, B.K., Uppaluri, R. and Purkait, M.K. (2008) Preparation and characterization of low cost ceramic membranes for micro-filtration applications. *Applied Clay Science*, **42** (1–2), 102–110.
- 150 Riedel, R. and Chen, I.W. (2008) *Ceramics Science and Technology, Volume 1, Structures*, Wiley-VCH Verlag GmbH, Weinheim.
- 151 Gu, Y.F. and Oyama, S.T. (2007) Ultrathin, hydrogen-selective silica membranes deposited on alumina-graded structures prepared from size-controlled boehmite sols. *Journal of Membrane Science*, **306** (1–2), 216–227.
- 152 Gu, Y.F. and Oyama, S.T. (2007) High molecular permeance in a poreless ceramic membrane. *Advanced Materials*, **19** (12), 1636–1640.
- 153 Gu, Y.F., Hacırlıoglu, P. and Oyama, S.T. (2008) Hydrothermally stable silica–alumina composite membranes for hydrogen separation. *Journal of Membrane Science*, **310** (1–2), 28–37.
- 154 Bayati, B., Bayat, Y., Charchi, N., Ejtemaei, M., Babaluo, A.A., Haghghi, M.

- et al.* (2013) Preparation of crack-free nanocomposite ceramic membrane intermediate layers on alumina tubular supports. *Separation Science and Technology*, **48** (13), 1930–1940.
- 155 Khatib, S.J. and Oyama, S.T. (2013) Silica membranes for hydrogen separation prepared by chemical vapor deposition (CVD). *Separation and Purification Technology*, **111**, 20–42.
- 156 Galuszka, J. and Giddings, T. (2011) Silica membranes: preparation by chemical vapour deposition and characteristics, in *Membranes for Membrane Reactors: Preparation, Optimization and Selection*, John Wiley & Sons, Inc., Chichester.
- 157 Yacou, C., Wang, D., Motuzas, J., Zhang, X., Smart, S. and da Costa, J.C.D. (2013) Thin-film ceramic membranes. *Encyclopedia of Membrane Science and Technology*, John Wiley & Sons, Inc., Hoboken, NJ.
- 158 Jones, A.C. and O'Brien, P. (1997) *CVD of Compound Semiconductors: Precursor Synthesis, Development and Applications*, Wiley-VCH Verlag GmbH, Weinheim.
- 159 Khatib, S.J., Oyama, S.T., de Souza, K. and Noronha, F.B. (2011) Review of silica membranes for hydrogen separation prepared by chemical vapor deposition, in *Inorganic Polymeric and Composite Membranes, Volume 14: Structure, Function and Other Correlations*, Elsevier, Amsterdam.
- 160 Leys, M.R. (1987) Metal organic vapour phase epitaxy. *Chemtronics*, **2** (4), 155–164.
- 161 Malik, M.A. and O'Brien, P. (1997) Basic chemistry of CVD and ALD precursors, in *CVD of Compound Semiconductors: Precursor Synthesis, Development and Applications*, Wiley-VCH Verlag GmbH, Weinheim.
- 162 Leese, A.B. and Mills, A.R. (1997) Commercial aspects of CVD, in *CVD of Compound Semiconductors: Precursor Synthesis, Development and Applications*, Wiley-VCH Verlag GmbH, Weinheim.
- 163 Puma, G.L., Bono, A., Krishnaiah, D. and Collin, J.G. (2008) Preparation of titanium dioxide photocatalyst loaded onto activated carbon support using chemical vapor deposition: a review paper. *Journal of Hazardous Materials*, **157** (2–3), 209–219.
- 164 Sea, B.K., Soewito, E., Watanabe, M., Kusakabe, K., Morooka, S. and Kim, S.S. (1998) Hydrogen recovery from a H₂–H₂O–HBr mixture utilizing silica-based membranes at elevated temperatures. 1. Preparation of H₂O- and H₂-selective membranes. *Industrial & Chemical Engineering Research*, **37**, 2502–2508.
- 165 Gavalas, G.R., Megiris, C.E. and Nam, S.W. (1989) Deposition of H₂-permselective SiO₂ films. *Chemical Engineering Science*, **44** (9), 1829–1835.
- 166 Wu, J.C.S., Sabol, H., Smith, G.W., Flowers, D.L. and Liu, P.K.T. (1994) Characterization of hydrogen-permselective microporous ceramic membranes. *Journal of Membrane Science*, **96** (3), 275–287.
- 167 Sea, B.K., Kusakabe, K. and Morooka, S. (1998) Hydrogen recovery from a H₂–H₂O–HBr mixture utilizing silica-based membranes at elevated temperatures. 2. Calculation of exergy losses in H₂ separation using inorganic membranes. *Industrial and Engineering Chemistry Research*, **37** (6), 2509–2515.
- 168 de Vos, R.M., Maier, W.F. and Verweij, H. (1999) Hydrophobic silica membranes for gas separation. *Journal of Membrane Science*, **158** (1–2), 277–288.
- 169 Gu, Y., Hacıoğlu, P. and Oyama, S.T. (2008) Hydrothermally stable silica–alumina composite membranes for hydrogen separation. *Journal of Membrane Science*, **310** (1–2), 28–37.
- 170 Kanezashi, M. and Asaeda, M. (2006) Hydrogen permeation characteristics and stability of Ni-doped silica membranes insteam at high temperature. **271** (1–2), 86–93.
- 171 Okubo, T. and Inoue, H. (1989) Introduction of specific gas selectivity to porous-glass membranes by treatment with tetraethoxysilane. *Journal of Membrane Science*, **42** (1–2), 109–117.
- 172 Lin, Y.S. and Burggraaf, A.J. (1992) CVD of solid oxides in porous substrates for ceramic membrane modification. *Aiche Journal*, **38** (3), 445–454.
- 173 Labropoulos, A.I., Romanos, G.E., Karanikolos, G.N., Katsaros, F.K., Kakizis,

- N.K. and Kanellopoulos, N.K. (2009) Comparative study of the rate and locality of silica deposition during the CVD treatment of porous membranes with TEOS and TMOS. *Microporous and Mesoporous Materials*, **120**, 177–185.
- 174 Kim, S. and Gavalas, G.R. (1995) Preparation of H₂ permselective silica membranes by alternating reactant vapor deposition. *Industrial & Engineering Chemistry Research*, **34** (1), 168–176.
- 175 Voelger, K.W., Hauser, R., Kroke, E., Riedel, R., Ikuhara, Y.H. and Iwamoto, Y. (2006) Synthesis and characterization of novel non-oxide sol-gel derived mesoporous amorphous Si–C–N membranes. *Journal of the Ceramic Society of Japan*, **114** (1330), 567–570.
- 176 Morooka, S. and Kusakabe, K. (1999) Microporous inorganic membranes for gas separation. *MRS Bulletin*, **24** (3), 25–29.
- 177 Novak, B.M. (1993) Hybrid nanocomposite materials: between inorganic glasses and organic polymers. *Advanced Materials*, **5** (6), 422–433.
- 178 Sakka, S. (2005) *Handbook of Sol–Gel Science and Technology. 1. Sol–Gel Processing*, Kluwer Academic Publishers.
- 179 Bonekamp, B.C., Kreoter, R. and Vente, J.F. (2008) Sol–gel approaches in the synthesis of membrane materials for nanofiltration and pervaporation, in *Sol–Gel Methods for Materials Processing: Focusing on Materials for Pollution Control, Water Purification, and Soil Remediation*, Nato Science for Peace and Security Series C: Environmental Security (eds P. Innocenzi, Y.L. Zub and V.G. Kessler), Springer, pp. 47–65.
- 180 Voronkov, M.G., Mileshkevich, V.P. and Yuzhelevskii, Y.A. (1978) *Siloxane Bond: Physical Properties and Chemical Transformations*, Studies in Soviet Science, Springer, New York.
- 181 Guizard, C., Ayrat, A., Barboiu, M. and Julbe, A. Sol–gel processed membranes, in *Handbook of Sol–Gel Science and Technology: Processing, Characterization and Applications*, Kluwer Academic Publishers, Dordrecht.
- 182 Guizard, C. (1996) Sol-gel chemistry and its application to porous membrane processing. *Fundamentals of Inorganic Membrane Science and Technology*, Elsevier, Amsterdam.
- 183 Riedel, R., Ionescu, E. and Chen, I.W. (2008) Modern trends in advanced ceramics. *Ceramics Science and Technology. Vol. 1: Structures*, Wiley-VCH Verlag GmbH, Weinheim.
- 184 Matsukata, M. and Kikuchi, E. (1997) Zeolitic membranes: synthesis, properties, and prospects. *Bulletin of the Chemical Society of Japan*, **70** (10), 2341–2356.
- 185 Morigami, Y., Kondo, M., Abe, J., Kita, H. and Okamoto, K. (2001) The first large-scale pervaporation plant using tubular-type module with zeolite NaA membrane. *Separation and Purification Technology*, **25** (1–3), 251–260.
- 186 Piera, E., Tellez, C., Coronas, J., Menendez, M. and SaIntamaria, J. (2001) Use of zeolite membrane reactors for selectivity enhancement: application to the liquid-phase oligomerization of i-butene. *Catalysis Today*, **67** (1–3), 127–138.
- 187 Myatt, G.J., Budd, P.M., Price, C. and Carr, S.W. (1992) Synthesis of a zeolite NaA membrane. *Journal of Materials Chemistry*, **2** (10), 1103–1104.
- 188 Fedosov, D.A., Smirnov, A.V., Knyazeva, E.E. and Ivanova, I.I. (2011) Zeolite membranes: synthesis, properties, and application. *Petroleum Chemistry*, **51** (8), 657–667.
- 189 Seike, T., Matsuda, M. and Miyake, M. (2002) Preparation of FAU type zeolite membranes by electrophoretic deposition and their separation properties. *Journal of Materials Chemistry*, **12** (2), 366–368.
- 190 Navascues, N., Tellez, C. and Coronas, J. (2008) Synthesis and adsorption properties of hollow silicalite-1 spheres. *Microporous and Mesoporous Materials*, **112** (1–3), 561–572.
- 191 Algieri, C., Bernardo, P., Barbieri, G. and Drioli, E. (2009) A novel seeding procedure for preparing tubular NaY zeolite membranes. *Microporous and Mesoporous Materials*, **119** (1–3), 129–136.
- 192 Pera-Titus, M., Llorens, J., Cunill, F., Mallada, R. and Santamaria, J. (2005)

- Preparation of zeolite NaA membranes on the inner side of tubular supports by means of a controlled seeding technique. *Catalysis Today*, **104** (2–4), 281–287.
- 193 Coronas, J. and Santamaria, J. (1999) Separations using zeolite membranes. *Separation and Purification Methods*, **28** (2), 127–177.
- 194 Wang, Z., Ge, Q., Shao, J. and Yan, Y. (2009) High performance zeolite LTA pervaporation membranes on ceramic hollow fibers by dipcoating–wiping seed deposition. *Journal of the American Chemical Society*, **131** (20), 6910–6911.
- 195 Jia, M.D., Chen, B.S., Noble, R.D. and Falconer, J.L. (1994) Ceramic–zeolite composite membranes and their application for separation of vapor/gas mixtures. *Journal of Membrane Science*, **90** (1–2), 1–10.
- 196 Tellez, C. and Menendez, M. (2011) Zeolite membrane reactors. *Membranes for Membrane Reactors: Preparation, Optimization and Selection*, John Wiley & Sons, Inc., Chichester.
- 197 Au, L.T.Y., Mui, W.Y., Lau, P.S., Ariso, C.T. and Yeung, K.L. (2001) Engineering the shape of zeolite crystal grain in MFI membranes and their effects on the gas permeation properties. *Microporous and Mesoporous Materials*, **47** (2–3), 203–216.
- 198 Burkett, S.L. and Davis, M.E. (1995) Mechanisms of structure direction in the synthesis of pure-silica zeolites. 1. Synthesis OF TPA/SI-ZSM-5. *Chemistry of Materials*, **7** (5), 920–928.
- 199 Burggraaf, A.J., Vroon, Z., Keizer, K. and Verweij, H. (1998) Permeation of single gases in thin zeolite MFI membranes. *Journal of Membrane Science*, **144** (1–2), 77–86.
- 200 Chau, J.L.H., Tellez, C., Yeung, K.L. and Ho, K.C. (2000) The role of surface chemistry in zeolite membrane formation. *Journal of Membrane Science*, **164** (1–2), 257–275.
- 201 Xu, W.Y., Dong, J.X., Li, J.P., Li, J.Q. and Wu, F. (1990) A novel method for the preparation of zeolite ZSM-5. *Journal of the Chemical Society, Chemical Communications*, (10), 755–756.
- 202 Matsukata, M., Nishiyama, N. and Ueyama, K. (1994) Zeolitic membrane synthesized on a porous alumina support. *Journal of the Chemical Society, Chemical Communications*, (3), 339–340.
- 203 Bibby, D.M. and Dale, M.P. (1985) Synthesis of silica-sodalite from non-aqueous systems. *Nature*, **317** (6033), 157–158.
- 204 Xu, W., Dong, J. and Li, J. (1990) Simultaneous crystallization of two dissimilar zeolites from the system ethylenediamine-Na₂O-Al₂O₃-SiO₂-H₂O-triethylamine. *Journal of the Chemical Society, Chemical Communications*, (2), 131–132.
- 205 Cheng, Z.L., Gao, E.Q. and Wan, H.L. (2004) Novel synthesis of FAU-type zeolite membrane with high performance. *Chemical Communications*, (15), 1718–1719.
- 206 Alfaro, S., Arruebo, M., Coronas, J., Menendez, M. and Santamaria, J. (2001) Preparation of MFI type tubular membranes by steam-assisted crystallization. *Microporous and Mesoporous Materials*, **50** (2–3), 195–200.
- 207 Aoki, K., Kusakabe, K. and Morooka, S. (2000) Separation of gases with an A-type zeolite membrane. *Industrial and Engineering Chemistry Research*, **39** (7), 2245–2251.
- 208 Xu, X.C., Yang, W.S., Liu, J. and Lin, L.W. (2000) Synthesis of a high-permeance NaA zeolite membrane by microwave heating. *Advanced Materials*, **12** (3), 195–198.
- 209 Yan, Y.G., Chaudhuri, S.R. and Sarkar, A. (1996) Synthesis of oriented zeolite molecular sieve films with controlled morphologies. *Chemistry of Materials*, **8** (2), 473–479.
- 210 Miachon, S., Ciavarella, P., van Dyk, L., Kumakiri, I., Fiaty, K., Schuurman, Y. et al. (2007) Nanocomposite MFI-alumina membranes via pore-plugging synthesis: specific transport and separation properties. *Journal of Membrane Science*, **298** (1–2), 71–79.
- 211 Finley, J. (2005) Ceramic membranes: a robust filtration alternative. *Filtration+Separation*, **42** (9), 34–37.
- 212 Cheryan, M. (1998) *Ultrafiltration and Microfiltration Handbook*, CRC Press, Boca Raton, FL.

- 213 Sondhi, R., Bhave, R. and Jung, G. (2003) Applications and benefits of ceramic membranes. *Membrane Technology*, **2003** (11), 5–8.
- 214 Guizard, C., Rambault, D., Urhing, D., Dufour, J. and Cot, L. (1993) *Deasphalting of a Long Residue Using Ultrafiltration Inorganic Membranes*. Worcester Polytechnic Institute, Worcester, MA, pp. 345–354.
- 215 Marchetti, P., Solomon, M.F.J., Szekely, G. and Livingston, A.G. (2014) Molecular separation with organic solvent nanofiltration: a critical review. *Chemical Reviews*, **114** (21), 10735–10806.
- 216 Tsuru, T., Miyawaki, M., Kondo, H., Yoshioka, T. and Asaeda, M. (2003) Inorganic porous membranes for nanofiltration of nonaqueous solutions. *Separation and Purification Technology*, **32** (1–3), 105–109.
- 217 Tsuru, T., Narita, M., Shinagawa, R. and Yoshioka, T. (2008) Nanoporous titania membranes for permeation and filtration of organic solutions. *Desalination*, **233** (1–3), 1–9.
- 218 Hoek, E.V. and Tarabara, V.V. (eds) (2013) *Encyclopedia of Membrane Science and Technology*, John Wiley & Sons, Inc., Hoboken, NJ.
- 219 Burggraaf, A.J. (1992) *Inorganic Membranes*, Trans Tech Publications Ltd., Pfaffikon, Zürich.
- 220 Kanellopoulos, N. (2000) *Recent Advances in Gas Separation by Microporous Ceramic Membranes*, 1st edn, Elsevier, Amsterdam.
- 221 Sánchez Marcano, J.G. and Tsotsis, T.T. (2004) *Catalytic Membranes and Membrane Reactors*, Wiley-VCH Verlag GmbH, Weinheim.
- 222 Sammells, A.F. and Mundscha, M.V. (2006) *Nonporous Inorganic Membranes: For Chemical Processing*, Wiley-VCH Verlag GmbH, Weinheim.
- 223 Nunes, S.P. and Peinemann, K.V. (2001) *Membrane Technology: In the Chemical Industry*, Wiley-VCH Verlag GmbH, Weinheim.
- 224 Tan, X. and Li, K. (2015) *Inorganic Membrane Reactors: Fundamentals and Applications*, John Wiley & Sons, Inc., Hoboken, NJ.

